Department of Geomatics Engineering

Development of Map Aided GPS Algorithms for Vehicle Navigation in Urban Canyons
(URL: http://www.geomatics.ucalgary.ca/links/GradTheses.html)

by

Salman Syed

June 2005

UNIVERSITY OF
CALGARY

UNIVERSITY OF CALGARY

Development of Map Aided GPS Algorithms for Vehicle Navigation in Urban Canyons

by

Salman Syed

A THESIS

SUBMITTED TO THE FACULTY OF GRADUATE STUDIES

IN PARTIAL FULFILMENT OF THE REQUIREMENTS FOR THE

DEGREE OF MASTER OF SCIENCE

DEPARTMENT OF GEOMATICS ENGINEERING

CALGARY, ALBERTA

JUNE, 2005

ABSTRACT

A major portion of the Location-Based Services (LBS) market deals with applications involving in-car navigation systems. The Global Positioning System (GPS) is the most popular choice for positioning in such applications. Many LBS applications involve positioning in urban areas having high rise buildings. Although GPS has good positioning accuracy in open sky conditions, it suffers from line-of-sight issues in urban canyons.

This thesis formulates some new methods for aiding GPS using maps for vehicle navigation in urban canyons. GPS satellite availability in urban canyons can be improved by using a High Sensitivity GPS (HS GPS) receiver which can track weak signals. However, this introduces large errors and noise in measurements. Thus, reliability monitoring becomes necessary with such receivers in signal degraded environments. Maps and Digital Elevation Models (DEM) provide effective constraints to compute an outlier-free solution. In this research, a robust fuzzy logic-based approach is developed for road segment identification. This identified road segment is then used in a GPS computation model and is referred to as Map Aided GPS (MAGPS). The performances of different map matching approaches are analyzed and results show that the proposed algorithms can be effectively used to navigate the vehicle in urban canyons as compared to the conventional GPS-based approaches. The input to the system comes from a low cost gyro (Murata ENV-05), a HS GPS receiver (SiRF XTrac) and a map database. The effect of height aiding from Digital Elevation Model (DEM) is also analyzed.

ACKNOWLEDGEMENTS

DEDICATION

To Prophet Muhammad (peace be upon him), his life and his mission

TABLE OF CONTENTS

LIST OF TABLES

LIST OF FIGURES AND ILLUSTRATIONS

LIST OF ABBREVIATIONS

ANFIS	Adaptive-Network-Based Fuzzy Inference System
BLUUE	Best Linearly Uniform Unbiased Estimate
C/A	Coarse-Acquisition
C/No	Carrier-to-Noise ratio
dB	deciBel
dBW	deciBel per Watt
DEM	Digital Elevation Model
DGPS	Differential GPS
DLL	Delay Lock Loop
DoD	Department of Defense
DOM	Degree of Membership
DR	Dead Reckoning
E911	Enhanced 911
EKF	Extended Kalman Filter
FCC	Federal Communications Commissions
FIS	Fuzzy Inference System
GDOP	Geometric Dilution of Precision
GPS	Global Positioning System
GIS	Geographic Information System
HPE	Horizontal Positioning Error
HS GPS	High Sensitivity GPS

IAEKF	Iterative Adaptive Extended Kalman Filter
ICD	Interface Control Document
JPO	Joint Program Office
LBS	Location-Based Services
LKF	Linearized Kalman Filter
LOS	Line-Of-Sight
MAGPS	Map Aided GPS
MDB	Marginally Detectable Blunder
MEMS	Micro Electro-Mechanical Systems
MF	Membership Function
NAVSTAR	NAVigation Satellite Timing And Ranging
PDF	Probability Density Function
PLL	Phase Lock Loop
PPS	Precise Positioning Service
PRN	Pseudo Random Noise
RAIM	Receiver Autonomous Integrity Monitoring
RMS	Root Mean Square
SA	Selective Availability
SNR	Signal-to-Noise Ratio
SPS	Standard Positioning Service
TTFF	Time-To-First-Fix

LIST OF SYMBOLS

$E[\ ]$ — Expected value of random variable

φ — Latitude of the position solution

λ — Longitude of the position solution

v_n — Velocity in the north direction

v_e — Velocity in the east direction

v_u — Velocity in the vertical direction

$\vec{V}$ — Velocity vector

$R_M(\varphi, \lambda)$ — Meridian radius of curvature of earth at position (φ, λ),

$R_T(\varphi, \lambda)$ — Transverse radius of curvature of earth at position (φ, λ)

α — Probability of Type-I errors (Rejection of null hypothesis when it is true)

β — Probability of Type-II errors (Acceptance of null hypothesis when it is false)

γ — Residue-in-abstentia

$\delta(\alpha, \beta)$ — Non-centrality parameter corresponding to given Type-I error probability of α and Type-II error probability of β

ρ — Pseudorange measurement

$\dot{\rho}$ — Pseudorange-rate measurement

Δt — Receiver clock bias

Δt_1	Navigation solution computation interval
$\Delta \dot{t}$	Receiver clock drift in m/s
$\mathbf{H}(\varphi, \lambda, h)$	Design matrix corresponding to a given position solution (φ, λ, h)
$\mathbf{H}_{doppler}$	Design matrix relating pseudorange-rate measurements to velocity components
$\mathbf{P}$	Covariance of state vector
$\mathbf{R}$	Covariance of measurement noise
$\mathbf{Q}$	Covariance of transition noise
$\vec{\eta}_m$	Measurement noise vector
$\vec{\eta}_{k+1/k}$	Process noise for the transition of state vector from k to $(k+1)^{th}$ epoch
$\vec{P}_{k,GPS}$	Position solution vector obtained from pseudorange computation at k^{th} epoch
$\vec{P}_{k,final}$	Map matched position solution vector obtained at k^{th} epoch
$pr()$	Projection of position solution on identified road segment
W	Weight of the projected pseudorange-derived position solution in the final map matched position solution
C/N_0	Carrier to noise ratio
$|L_0|$	Length of road segment
$\hat{L}_0$	Vector along the road segment in 2-D coordinate system

$f_{DEM}(\varphi,\lambda)$	DEM mapping from the two dimensional coordinates (φ,λ) to the height at that point.
$\vec{\Omega}$	Angular velocity vector
$\vec{\vartheta}$	Innovation sequence
$\mathbf{C}_{\tilde{r}}$	Covariance of residuals
$\mathbf{E}$	Redundancy matrix
ξ	Covariance of innovation sequence

CHAPTER 1: INTRODUCTION

The Global Positioning System (GPS) is being increasingly used for vehicle navigation to provide users with location-specific information. The primary motivation behind using GPS for such applications is its capability to autonomously locate the vehicle with good accuracy. The output from GPS is then map matched to the road network in order to give the drivers information about their location on the map. In this thesis, some novel methods of combining GPS with map information for enhanced vehicle navigation are presented.

1.1 Background

The confluence of wireless technology and GPS has led to the development of a new set of applications to serve the location-based needs of users. These applications are popularly known as Location-Based Services (LBS). The intent of LBS is to use accurate real-time user position information to connect them to nearby points of interest (such as retail businesses, public facilities or travel destinations), to advise them of current conditions (such as traffic and weather), or to provide routing and tracking services (Liu, 2000). The numerous applications for LBS include logistics, vehicle automation, real estate, field services, travel services and E911 (Gao et al., 2001). About one billion people around the world are expected to use LBS by 2005 (Astroth, 2001). For operators, location-based advertising is expected to be a great source of revenue (Kyriazykos et al., 2000). The commercial aspect of geography-based information (better known as g-

commerce) is still in an early and evolving stage and is one of the major driving forces for the development of LBS. Progressive industry leaders are building solid foundations today to support well-conceived solutions for new location applications and value-added services. The other strong impetus for the development of LBS came from the US Federal Communication Commission (FCC), which has set a wireless mandate requiring that all mobile phones be located for 67% of calls with an accuracy of 100 metres for network-based technologies and 50 metres for handset-based technologies (FCC, 2000).

LBS applications require a positioning system along with a Geographic Information System (GIS) (Virrantaus et al., 2001). The basic steps involved in a typical LBS application are:

1) To obtain the output from the positioning sensor and suitably geo-reference it on map.

2) To do a location-based query with the output (from step 1) in order to obtain the relevant information.

LBS applications are broadly classified as:

1) Applications for vehicle navigation.

2) Applications for pedestrian/personal navigation.

The scope of this thesis is restricted to the vehicle navigation using GPS. Vehicle navigation systems are being installed in cars by almost all leading manufacturers.

Examples of such systems include GM's Onstar system, Mercedes's Teleaid system, BMW's BMW-Assist system, and the ETAK systems (Etak, 2000; Laplin, 1999).

LBS applications based on in-car vehicle navigation systems essentially consist of:

1) A positioning system

2) A map to geo-reference the output from (1)

There are, in essence, three different ways to determine the user's location (Bernstein and Kornhauser, 1996). The first is to use some form of dead reckoning (DR) in which the user's speed of movement, direction of movement, etc is continuously used to update her/his location (Collier, 1990). The second is to use a ground-based beacon that broadcasts its location to nearby users (Iwaki et al., 1989). The third is to use some form of radio/satellite positioning system that transmits information that the user can use to determine his/her location. This last approach is by far the most popular and a great many users employ GPS to determine their location (Hofmann-Wellenhof et al., 1994).

The output obtained from the positioning techniques described above is independent of any map information. The process of mapping the output from the positioning system onto the road network is called *map matching*. This is an essential step for providing user with any location-specific information (Tsakiri, 1996).

Many LBS applications require positioning in downtown urban environments which are characterized by high rise buildings. This can create Line of Sight (LOS) issues for GPS.

The vehicle navigation system performance can be improved if a High Sensitivity GPS (HS GPS) receiver is used instead of a conventional GPS receiver (Chansarkar and Garin, 2000). By increasing the non-coherent integration period of the GPS signal up to 700 ms, the HS GPS receiver can acquire and track weak signals of strength up to 15 dB less then the tracking threshold of a conventional GPS receiver (MacGougan, 2003). By tracking weak signals, the problem of satellite availability is alleviated.

1.2 Problem Statement and Objectives of Thesis

An ideal vehicle navigation system has the following characteristics:

1) *Affordable cost*: The cost of a navigation system should be economical in order to be installed in a car. Costly, high accuracy navigation systems may never find a place in the car navigation market.

2) *Prescribed accuracy requirements*: The system accuracy for effective vehicle navigation should be of the order of about 20 m for 95% of time (ACN, 2000).

3) *Automatic initialization*: The system should initialize itself on a user's request and should not require calibration or other inputs from the user for initialization.

4) *Effective display of information*: The navigation output should convey information in an appropriate form to the user. For example it makes no sense if a

user is informed that his/her current position is 51.3645° latitude and -114.2346° longitude, instead of the street on which he/she is traveling.

As stated in the previous section, a vehicle navigation system consists of a positioning sub-system and a map database. In general, vehicles mostly travel on the road network and this condition gives special constraints to the vehicle navigation problem (Scott, 1994). If both the map and positioning system were to be ideal then the output from the positioning sensor will indeed lie accurately on the correct road segment. But in real life, the various noise sources affecting the signals and the instrumentation used by the positioning system, along with the map inaccuracies, result in the estimated position not necessarily being overlaid onto the road network (Taylor and Blewitt, 1999; Quddus et al., 2003). The problem of map matching can be stated as the identification of correct road segment followed by the determination of position on it. If the position output is accurate, as in the case of GPS position in open area conditions, then geometric mapping of the point to the closest road segment will be accurate and reliable (Zhao et al., 2002).

GPS has been increasingly used for vehicle navigation systems because of its 24 hours a day, free of charge, availability (Harvey, 1998). In addition it does not suffer from initialization problems as in the case of DR systems. The additional advantage of using GPS for navigation is its long term accuracy unlike the DR sensors which have large error growth over time (Jekeli, 2000). However, GPS suffers from LOS issues which make it less effective in situations like urban canyons where there is low satellite availability due to signal blocking from high rise buildings. In addition, multipath signals

arising from building reflections introduce large errors in the navigation solution (Lachapelle et al., 2003). HS GPS receiver technology can alleviate the problem of availability by tracking weak signals. However this is not always beneficial because of incorrect acquisition due to cross correlation effects and the tracking of echo-only multipath signals (MacGougan et al., 2002). Thus the accuracy of every low-cost positioning system is limited in urban canyons. In addition to the limited positioning accuracy of the sensors, the task of vehicle tracking is further complicated in urban canyons by the increase in the road network density.

One way of solving this problem is to combine GPS with DR sensors (Nayak, 2000). A better way of aiding GPS is to provide information from map or Digital Elevation Model (DEM). The following are the advantages of integrating GPS with map/DEM information as compared to aiding from DR sensors:

1) Reduction in uncertainty as the level of randomness associated with the map/DEM information is generally bounded as compared to the output from a low cost DR sensor, whose level of uncertainty changes with temperature/vibration, etc.

2) The tight integration of GPS with a map and DEM provides a better way of detecting outliers in GPS measurements. The DR sensors may themselves have outliers which are not useful for reliability testing.

3) In the scenario where three satellites are available, a GPS receiver either fixes the height to the last computed height or employs a predictive model to smooth the height. But before a GPS receiver switches into this mode due to signal masking, the position is already degraded by multipath, and height prediction (from DR sensors or mathematical models) does not benefit the computation. On the other hand, DEM provides outlier-free height information as it is independent of GPS errors.

The aim of this thesis is to develop vehicle navigation algorithms using an HS GPS receiver, a digital map, a DEM, and a low cost gyro to provide reliable navigation in urban canyon conditions with low satellite availability.

The objectives of this thesis are to:

1) Develop a map matching framework for road segment identification.

2) Develop navigation algorithms using map information to aid GPS in computation of navigation solution in low satellite availability conditions.

3) Use the map information to monitor the integrity of GPS measurements.

4) Analyze the results obtained from different navigation approaches.

The details of these objectives are discussed in Section 1.5 after presenting the related past research.

1.3 Related Research

A number of map matching algorithms have been proposed and implemented, and it is not possible to discuss all of them in this thesis. However, a few selected map matching approaches are presented in this section.

Map matching can be done using either GPS or DR sensors or a combination of both. Map matching with DR sensors is dealt in Zhao (1997). The main idea is to compensate the growing DR errors by detecting vehicle turns on a map. The problem with this approach is that it requires external initialization of position. Also, there is an ambiguity in the selection of the correct road segment after traversing a long distance without a turn.

Most of the GPS-based map matching algorithms work well on open highways and have limitations when there are LOS issues. Map matching techniques vary from those using simple GPS point data, integrated with optical gyro and velocity sensors (Kim et al., 1996), to those using more complex mathematical techniques such as Kalman filtering (Taylor et al., 2001). The most complex approach is the generalized map matching algorithm that does not assume any knowledge or any other information regarding the expected location of the vehicle (Bernstein and Kornhauser, 1996).

Map matching algorithms usually adopt one of the following three approaches:

1) *Pure geometric approach*: This essentially involves only arc (road link) to point (position output) mapping and arc (formed from position outputs) to arc (road link) matching. The geometric approach works well in the absence of large positioning system errors and high noise. Algorithms using high quality sensors may work well with this approach.

2) *Statistical approach/Conditional probability*: This approach involves probabilistic estimation of the correct road link given a set of measurements and history of vehicle motion. The algorithm is more robust than the geometric method, and can recover from false positioning quickly as it takes into account the history. However, it requires more computation time and more memory to store the car trajectory. Also, it is very difficult to model the vehicular motion dictated by a complex road network.

3) *Algorithms based on information theory*: These approaches involve the assignment of weights to different measurements followed by either geometric or probabilistic matching. The weights are assigned using a soft computation approach like fuzzy logic.

The common steps in most of the map matching algorithms are:

1) Identification of the correct road link.

2) Determination of the vehicle position on the road link identified in step 1.

3) Tracking the vehicle as long as it is moving on that road link.

4) Searching for the correct link at road intersections or other junctions and repeating steps 2 and 3.

Many of the map matching algorithms are restricted to identification of the correct road segment without determining the accurate position of vehicle on it, and many others do not carry forward the history of vehicle motion after initialization. A description of many algorithms can be found in Bernstein and Kornhauser (1996) and Quddus et al. (2003). Some of the algorithms reviewed are:

1) Algorithms based on Geometric approaches:

- Taylor and Blewitt (1999) proposed a Road Reduction Filter (RRF) algorithm based on the concept of virtual differential GPS. This algorithm, based on autonomous GPS, applies pseudorange corrections computed at a previous epoch in the current epoch. A filtering method based on shape correlation is employed to remove incorrect road links. The approach helps in reducing time correlated errors caused by atmospheric effects and Selective Availability (SA) (when it was on). However, errors arising from multipath and other interference effects cannot be tackled by this approach.

- Greenfeld (2002) proposed an algorithm based on curve-to-curve matching, taking into account the weighted topology algorithm. This algorithm assumes a high quality GPS measurement to employ shape/topology correlation. The

similarity criteria fails when there is an array of similar road segments in close vicinity which is typically found in many urban areas.

- Bernstein and Kornhauser (1996) proposed an algorithm that does curve matching. The method for matching the two arcs is to use the distance between them. The problem with this algorithm is that it will reliably detect only the best match for arcs of the same length. This limits its ability to identify the correct arc in certain circumstances, such as slow moving vehicles. In addition, this system is unstable as it completely relies on geometric information and cannot sustain high measurement noise and errors.

- Joshi (2001) proposed a rotational variation metric approach for comparing vehicular and map paths for map matching. This method is purely geometrical and assumes an outlier-free navigation solution.

- Taylor et al. (2001) proposed another algorithm which uses road network connectivity information along with the drive restrictions to map the vehicle onto the road network. These additional conditions provide vital information to filter out the incorrect road segments.

- Zhao et al. (2002) proposed an algorithm by assigning weights to different geometric properties. The algorithm uses DR sensors in addition to DGPS. This

approach assigns empirical weights to different parameters and does not employ any learning procedure.

- French (1997) proposed a map matching algorithm which determines where the vehicle is on the road network using odometer and heading measurements. This approach requires external initialization. In addition, odometers suffer from issues such as fluctuations of the tire radius and variations of the road profile which leads to tire slippages and loss of wheel pulse counts.

2) Algorithms based on statistical approaches:

- Krakiwsky et al. (1988) proposed an algorithm involving statistical estimation of the curve and constraining the curves to match with the road network. Although approach works well for simple trajectories, it is very difficult to model real-life trajectories which are governed by complex road networks.

- Lamb and Threbaux (2000) proposed a Markov model for map matching to handle the topological aspects of a map. The algorithm relies heavily on the assumption that the initialization is very accurate, and fails if the previous few epochs have consistent blunders.

- Scott (1994) proposed a map aided positioning (MAP) estimator to determine the location of the vehicle on a road network. The MAP estimator is an effective

approach for simple trajectories. However, complex trajectories are not dealt by this approach. In addition, it assumes plenty of GPS measurements.

3) An algorithm based on a fuzzy logic approach:

- Kim and Kim (1999) proposed an adaptive fuzzy network approach to identify the correct link. This method uses fuzzy logic to identify the road segment. However, the approach is limited to the identification of the road segment followed by geometric snapping of the GPS position solution onto road segment.

In addition to the above mentioned map matching algorithms, Stephen (2000) proposed a loosely coupled GPS/odometer/gyro integration scheme for vehicle navigation in urban canyons. Harvey (1998) proposed a dual antenna system integrated with a multi-sensor system for land vehicle attitude application.

1.4 Limitations of Past Research

While GPS/INS integration provides a good accuracy navigation solution (of less than 10 m) for GPS data outages of up to one minute using navigation grade IMU (eg. El-Sheimy et al., 1995; Grejner-Brzezinska et al., 1998), the cost of these systems places a severe restriction for their use in land vehicle navigation (Petovello, 2003). Low cost DR sensors and GPS cannot generally provide the accuracy to meet the requirements of navigation in urban canyons (as discussed in the previous section).

The use of map matching is an effective and economical way to improve the navigation solution as compared to low cost GPS/DR integration. In addition, map matching is essential for route guidance as the driver needs to know his/her current position on a road map instead of only coordinates. Most of the map matching algorithms based on dead reckoning use the road turns to recalibrate the sensors while those based on GPS identify the road segment by comparing the road shape with the GPS position output trend.

Although most of the GPS-based map matching algorithms (discussed in the previous section) work well in open area conditions with a sparse road network, none of them are specifically designed to face the challenges of navigation in urban canyons.

The drawbacks of previous research work in map matching techniques include:

1) *Non optimality in navigation solution computation*: Most of the algorithms discussed above do not deal with GPS computations and take the navigation solution from external GPS software without attempting to improve it with map information. This type of map matching is not the best way of obtaining a navigation solution in urban canyons because of the GPS LOS issues. Since the accuracy of GPS coupled with a low cost DR sensor is limited in urban canyons, the navigation solution is already corrupted before mapping it on the correct road. This leads to the incorporation of many sensor errors into the map matched solution and may lead to the location of the vehicle on an incorrect road link.

2) *Lack of robustness in identifying correct road segment*: Map matching with a noisy navigation solution (after removing the blunders) in a complex road network is difficult unless a robust road identification technique is used. Many of the algorithms reviewed above lose track of the correct road link when the sensor noise increases.

3) *Lack of navigational integrity monitoring*: For successful navigation of vehicles, especially in urban canyons, the measurement outliers need to be removed before computing a navigation solution. This can be achieved by monitoring individual pseudorange measurements for "large" multipath and incorrect acquisition effects. The navigation solution should then be computed after excluding the faulty measurements. None of the map matching algorithms have the provision of GPS reliability monitoring incorporated in them.

1.5 Present Research

Given the limitations of past research in vehicle navigation and map matching, the present research addresses the problem of vehicle positioning in urban canyons using a low cost gyro and a digital map. The purpose of this research is not to locate the vehicle with a very high accuracy (sub-metre level), but to provide an accuracy sufficient to identify the correct road segment. For this purpose, a fuzzy logic framework for road link identification is devised upon which three sets of algorithms were developed. The three approaches are:

1) *Position domain approach*: In this approach, the GPS navigation solution is computed independently by an external GPS processing algorithm. A fuzzy logic framework is then used for map matching the GPS output. This is primarily done to demonstrate the effectiveness of the proposed map matching framework.

2) *Map-aided least squares approach*: In this approach, the conditions imposed by the map information are used as constraints in the GPS least squares model. This approach will be referred to as Map-Aided GPS (MAGPS).

3) *Map-aided filtering approach:* In this approach, a Kalman filter is developed for processing the GPS measurements along with the constraints from identified road segment. The map aiding is used to filter both the pseudorange and Doppler measurements. This approach will be referred to as the MAGPS filtering algorithm.

The MAGPS approaches were then tested to see the effect of height augmentation. The aiding was provided from a Digital Elevation Model (DEM).

The salient features of the present work are:

- *Tight integration of map information with GPS:* One of the novelties of this research is to implement the map constraints in the GPS measurement model

(involving pseudorange and Doppler measurements) as opposed to the other algorithms (which compute the GPS solution independent of the map information).

- *The use of fuzzy logic in the algorithm for correct road identification*: Fuzzy logic is a soft computational technique developed by Zadeh (1965). The advantages of using fuzzy logic are the simplicity in the computation model and increased tolerance to high noise and contradictory information. When suitably used, fuzzy logic generates precise information from noisy and contradictory input. The algorithm develops a simple but effective model for determining the road link on which the vehicle is traveling.

- *The development of a map-based integrity monitoring of GPS measurements*: The algorithms use the map information to remove the GPS measurements having large errors due to multipath and cross correlation effects (which are frequently encountered while using HS GPS). This type of integrity monitoring is attempted for the first time in this research. A new multiple outlier detection technique was developed based on a separation of solution approach, the details of which will be discussed in Chapter 5.

By incorporating all these features in the MAGPS (filtering) algorithm, seamless navigation is possible in urban canyon conditions. Field data collected in an urban environment is used to compare the performances of different map matching approaches.

1.6 Thesis Outline

This thesis consists of seven chapters which are organized as follows:

Chapter 2 deals with the background information on GPS, DR sensors, maps and DEMs. The chapter briefly explains the HS GPS receiver concept and its expected performance.

Chapter 3 introduces the concept of fuzzy logic. This chapter describes the theory of fuzzy sets, degree of membership, logical operators and the Fuzzy Inference System.

Chapter 4 presents the estimation techniques. This chapter covers least squares estimator and adaptive Kalman filtering techniques. In addition, the concept of reliability testing in navigation is also discussed.

Chapter 5 discusses the proposed algorithm based on the estimation techniques presented in Chapter 4. The fuzzy logic framework for road link identification is presented followed by the MAGPS computation model. The map aided integrity monitoring of GPS measurements is also presented in this chapter.

Chapter 6 discusses the results obtained by using the proposed algorithms. The effect of height information on the solution is also analyzed. The performances of proposed algorithms are compared with a geometric map matching algorithm.

Chapter 7 presents the conclusions of the study and suggests recommendations for future work.

Appendix A presents an introduction to random processes/variables and their characteristics.

CHAPTER 2: SYSTEM OVERVIEW

This chapter first describes GPS and its error sources followed by an introduction to HS GPS. The latter half of the chapter deals with dead reckoning, maps and DEMs.

2.1 GPS Overview

GPS is a satellite-based navigation system which was originally developed as a military force enhancement system in 1973 (GPSSPSD, 2001). GPS has the ability to provide position and velocity information anywhere on Earth, 24 hours a day, regardless of weather. Position determination is based on measurements of the transit time of radio signals from at least four satellites, whereas velocity determination is based on Doppler measurements (Axelrad and Brown, 1994). The GPS system consists of three segments: space, control and user segments (Spilker and Parkinson, 1994). The space segment consists of 29 satellites transmitting range information on earth. The control segment deals with monitoring the health of satellites, and updating satellite clock and orbit corrections (Misra and Enge, 2001).

The user segment is the largest and the most dynamic of the three segments. It mainly consists of GPS receivers and related systems. These receivers use the satellite range information to determine their position and time with the single point accuracy specified by the Joint Program Office (JPO). The user segment consists of applications intended for

either military or for civilians (Langley, 1991). Military users have exclusive access to the high accuracy encrypted Precise code (P(Y)-code), whereas the civilian users can only use the less precise Coarse/Acquisition (C/A) code (Hofmann-Wellenhof et al., 1994). Civilian users constitute a major portion of the user segment market and the estimated number of users in this segment is approximately a few million and is growing every year (Lachapelle, 1995). The GPS market in the user segment is expected to be about $30 billion/year by 2005 (Cannon, 2001).

A GPS receiver computes the range by measuring the transit time of the signal from the satellite to the receiver antenna. To compute position and time, the receiver performs triangulation using range measurements from at least 3 satellites. However, since the receiver local clock is not in synchronisation with satellite clocks, an additional measurement is required to solve for this clock offset (Langley, 1993). The quality of the resulting position estimate ranges from several metres to the centimetre level (Petovello, 2003), depending on the measurements and methods employed. GPS measurements are of two types:

1) Code (pseudorange) measurements
2) Doppler/incremental phase measurements

To this end, the carrier phase observable is the most precise measurement available to GPS users with a resolution of 0.2–1 m (Cannon et al., 2001; Cannon et al., 2003). This precision, combined with differential GPS (DGPS) techniques involving two (or more) GPS receivers, is what allows for centimetre-level positioning (Syed and Kulkarni, 2002).

However, this level of positioning is only possible using GPS if the carrier phase ambiguities are resolved to their true integer values (Hans and Rizos, 1997). For this reason, many applications requiring accuracy of the order of few metres use code measurements augmented with Doppler measurements.

2.1.1 GPS Pseudorange Measurements

A GPS pseudorange measurement is the apparent distance between receiver and satellite obtained as a difference between transmission and reception time (Leick, 1995). The term *pseudo* comes from the fact that the measured range has an unknown clock bias which has to be estimated (Misra and Enge, 2001). GPS measurements suffer from various errors arising out of clock and other propagation errors as shown in Equation 2.1.

$$p(t) = \rho(t) + d_{orb} + d_{trop}(t) + d_{iono}(t) + c(dt(t) - dT(t)) + \varepsilon_p \qquad (2.1)$$

where

$p(t)$ is the pseudorange measurement at time t,

$\rho(t)$ is the true range between satellite and receiver at time t,

$d_{orb}(t)$ is the orbital error at time t,

$d_{trop}(t)$ is the tropospheric error at time t,

$d_{iono}(t)$ is the ionospheric error at time t,

$dt(t)$ is the satellite clock error at time t,

$dT(t)$ is the receiver clock error at time t, and

ε_p is the combined error due to multipath and receiver noise.

Table 2.1 shows the GPS range error budget in single point and differential mode. DGPS can be used to minimize the errors of single-point GPS by cancelling the parts of the error that are common to receivers in close proximity (Langley, 1993). DGPS is normally implemented by differencing the ranges to common satellites from two receivers. If the coordinates of one station are known, an accurate position of the second station can be determined (Misra and Enge, 2001). Alternatively, a coordinate difference between stations can be computed using approximate coordinates for one of the stations. DGPS reduces or eliminates errors caused by satellite clock and orbital errors, and atmospheric propagation (Grewal et al., 2001). It does not reduce multipath, and the noise of a differenced observation is larger than that of an individual measurement by a factor of $\sqrt{2}$ (Hofmann-Wellenhof et al., 1994).

For vehicle navigation in DGPS mode, the dominant source of error is multipath (Phatak et al., 1999). Multipath is a highly variable error source that refers to the reception of a signal through any path other than the minimum travel time path (Braasch 1996). Multipath is caused either by reflections or diffractions, or a combination of both (Ray, 2001). Multipath is not correlated spatially, but sometimes loosely correlated in time when the receiver is static (Kelly and Braasch, 2001). The temporal correlation is highly unpredictable for a moving GPS receiver.

Table 2.1: GPS Pseudorange Error Sources (Misra and Enge, 2001)

Error source	Single point (m)	Differential errors (ppm)
Orbit	3-8	0.1-0.5
Clock	10	-
Ionosphere	2-50	0.5-2
Troposphere	2-30	0.1-1
Code multipath	0.2-3	-
Code noise	0.1-3	-
Carrier Multipath	0.001-0.03	-
Carrier noise	0.0002-0.002	-

Multipath can cause errors in ranging which are both positive and negative, depending on the strength, phase and delay of the multipath signal. An approximate envelope that contains the entire range of errors for a 1 chip spacing early-late C/A-code discriminator with a multipath to signal ratio of -20 dB is shown in Figure 2.1. If the multipath and direct signals are in phase, a maximum positive range error will occur, while if the signals are 180° out of phase, a maximum negative range error will occur. If the two are separated by a phase angle of 90°, no error is induced. Improved discriminators can reduce the error envelope, but receivers with better discriminators are generally more expensive. Unlike code multipath, carrier phase multipath can cause an error up to one

quarter of a wavelength, due to the nature of the Phase Lock Loop (PLL) (Misra and Enge, 2001).

A derivation for carrier phase error due to multipath and experimental results can be found in Ray (2000). Typical values for carrier phase multipath seldom exceeds 1-2 cm. Since Doppler measurements are derived from the rate of phase change, the effect of multipath on GPS velocity measurements is very small.
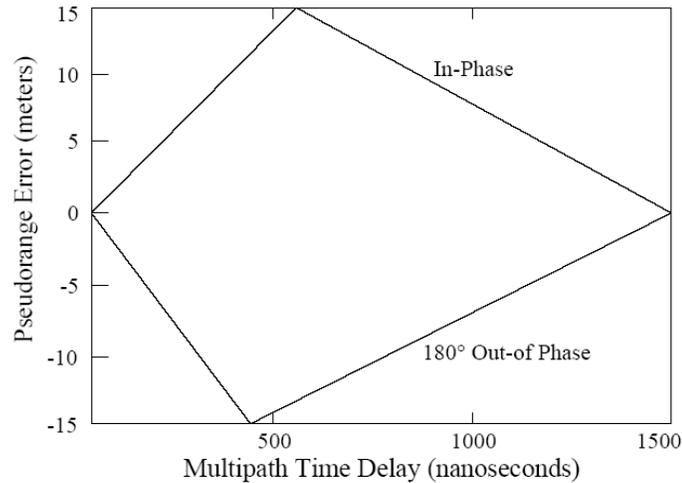
Figure 2.1: Error Envelope for a 1 Chip Spacing Early-Late C/A Delay Lock Loop (DLL) (Braasch, 1996)

Since the accuracy requirements of vehicle navigation are of the order of about 20 metres (Stephen, 2000), GPS code measurements coupled with Doppler measurements can provide adequate accuracy.

2.1.2 GPS Doppler Measurements

The Doppler effect is the change in reception frequency due to the relative motion of the transmitter and receiver (Ashjaee, 1985) and is a direct measure of the rate of change of range between the two points. Thus Doppler measurement can be used to calculate the velocity between transmitter and receiver. In GPS, Doppler is a measure of the instantaneous phase rate of a tracked satellite's signal (Ward, 1996). Hence, the velocity of the user with respect to a GPS satellite can be determined by the corresponding Doppler measurement. A GPS Doppler measurement not only includes effects due to motion but also has a contribution from the receiver clock drift (Lipp and Gu, 1994). Thus, a minimum of four Doppler measurements are needed to estimate the user velocity and receiver clock drift. Equation 2.2 describes the Doppler measurement error

$$\dot{\phi}(t) = \dot{\rho}(t) + \dot{d}_{orb}(t) + \dot{d}_{trop}(t) + \dot{d}_{iono}(t) + c(d\dot{t}(t) - d\dot{T}(t)) + \dot{\varepsilon}_p \tag{2.2}$$

where

$\dot{\phi}(t)$ is the observed range rate derived from Doppler measurements at time t,

$\dot{\rho}(t)$ is the true geometric range rate between satellite and receiver at time t,

$\dot{d}_{orb}(t)$ is the orbital drift error at time t,

$\dot{d}_{trop}(t)$ is the tropospheric delay drift error at time t,

$\dot{d}_{iono}(t)$ is the ionospheric delay drift error at time t,

$d\dot{t}(t)$ is the satellite clock drift at time t,

$d\dot{T}(t)$ is the receiver clock drift at time t, and

$\dot{\varepsilon}_p$ is the combined drift error due to multipath and receiver noise.

The effect of troposphere, ionosphere, orbital error and satellite clock drift is negligible and is often compensated by differencing or by the parameters in the navigation message (MacGougan, 2003). The effect of multipath on Doppler measurement is fairly small as it is derived from the phase range measurements (which are less effected by multipath than pseudorange measurements). However the effect of the receiver clock is variable and depends on the quality of the oscillator used in the GPS receiver. This effect is fairly large for low cost GPS receivers and is commonly estimated as an unknown parameter.

2.1.3 GPS Signal Power Budget

A conventional GPS receiver can give a navigation solution using unobstructed LOS signals of sufficient strength. Weak signals, whether they are attenuated LOS signals, diffracted signals, multipath signals or echo only signals were not desirable for use because they may have large noise and errors associated with them (MacGougan, 2003). The expansion of GPS for location-based services such as E911 is changing that paradigm (Ziedan and Garrison, 2004; Garin et al., 1996). Indoor positioning, navigation in foliage and in urban canyons is gaining importance in LBS applications (Choi and Tekinay, 1992). This led to the development of the HS GPS receiver.

The minimum specified signal strength received for the L1 C/A-code is -160 dBW (ICD200C, 2000). The minimum reception power for most of the satellites is 3 to 7 dB

(with an average of 5.4 dBW) higher than the specified level (Spilker, 1996). The signal power budget in Table 2.2 assumes an LOS signal. Signal attenuation due to propagation through various materials, multipath interference, and other interference effects are not considered. The amount of signal attenuation due to signal masking depends on the material, its density, and how much material the signal passes through. High sensitivity GPS receiver manufacturers are aiming for sensitivity levels in the range of -182 dBW to -188 dBW (Moeglein and Krasner, 1998). This will allow a receiver to function at attenuations of 27 to 33 dB with respect to the average typical received power of -154.6 dBW.

Table 2.2: GPS Signal Power Budget (Ray, 2000)

SV antenna power (dBW)	13.4
SV antenna gain (dBW)	13.4
User antenna gain (hemispherical) (dB)	3.0
Free space loss (L1) for R = 25092 km (dB)	-184.4
Atmospheric attenuation (dB)	-2.0
Depolarization loss (Db)	-3.4
User receiver power (dBW)	-160.0

GPS signal deterioration can occur due to signal masking caused by either natural (e.g. foliage) or man-made (e.g. buildings) obstructions, ionospheric scintillation, Doppler shift, multipath, jamming, evil waveforms, and receiver and antenna effects. These factors can lead to signal tracking errors, and in severe circumstances, may lead to total

loss of signal track (Kevin and Chansarkar, 1996). The partial loss of lock can lead to bad geometry and problem of availability, whereas undetected faulty tracking can lead to a large error in position. The processing task involved in obtaining weak signal measurements depends on the context. The acquisition of the signal is difficult relative to tracking, and signal reacquisition is somewhere in between the two processes (Lin and Tsui, 2001).

2.1.4 HS GPS Receiver

The theory of weak signal processing and HS GPS is discussed in detail in Peterson et al. (1997), Moeglein and Krasner (1998), Garin et al. (1999), Van Diggelen (2001), Chansarkar and Garin (2000), Shewfelt et al. (2001) and MacGougan (2003). For the sake of completeness, a brief overview is given in this section.

The GPS is a spread spectrum system. Each satellite has a distinct Pseudo Random Noise (PRN) sequence which is nearly uncorrelated with others. GPS signals are transmitted at two frequencies 1575.42 MHz (L1) and 1227.60 MHz (L2). While L1 is modulated with the C/A-code (in phase) and P(Y) code (in quadrature), L2 is only bi-phase modulated with the P(Y) code. Each C/A-code has a chipping rate of 1.023 Mchips/s and a PRN sequence length of 1023, resulting in a code repetition period of 1 ms. The relatively short periodic nature of the C/A-code produces a discrete spectrum with spectral lines spaced 1 KHz apart. Details of the GPS signal structure are discussed in Kaplan (1996).

The acquisition and tracking of a GPS signal can broadly be defined as the identification of code delay and corresponding carrier frequency offset. The power of a GPS signal is very low as compared to the noise floor (Aloi and Van Graas, 2004). The receiver usually integrates a signal for a fixed time to enhance the signal power to noise power ratio. However, the signal is also modulated by navigation data having a frequency of 20 ms (Spilker, 1996). Thus, in standalone (unaided) GPS mode the integration of signal can be performed coherently for up to 20 ms. In most of the conventional GPS receiver, this coherent integration time is limited up till 5 ms (Moeglein and Krasner, 1998). It is very difficult to acquire the weak signal by such a small integration time. The HS GPS receivers, on the other hand, integrate the signal for a longer period in non-coherent mode (which is basically the integration of the squared signal). By integrating the signal in non coherent mode, the effect of the bit boundary change due to the navigation message can be overcome at the cost of increased noise due to squaring. This increase in noise due to squaring is half as compared to the increase in signal power due to extended integration time, thereby facilitating weak signal acquisition. The problem is relatively easy for tracking and reacquisition where the navigation bit change is known before hand. Weak signal processing is further facilitated in assisted mode (often termed as hot start mode) (Feng and Law, 2002). The assistance is provided by Doppler aiding and/or other navigation data wipe off techniques. The details of assisted GPS can be found in Biacs et al. (2002) and Karunanayake et al. (2004).

2.2 DR Systems

DR is the technique of providing navigation information using an initial state plus relative positioning information (Bullock, 1995). It is different from GPS, which gives an absolute position fix in a known coordinate frame. DR and GPS have complementary characteristics which are in excellent synergy. GPS provides an absolute position that is of moderate accuracy, and DR provides highly accurate changes in position, but needs an absolute starting reference point (Salychev, 1998). It is often said that GPS provides the low frequency position information and DR provides the high frequency information in an integrated position solution. DR is not prone to signal masking or outages, but often requires strong external calibration, a great deal of redundancy, or the use of very stable and expensive sensors to function effectively.

Most DR sensors can be grouped into motion sensing and heading sensing categories (Borenstein, 1994). The former are termed as accelerometers, whereas the latter are called gyroscopes (gyros). In this research, only a gyro is used and will be the only DR sensor to be discussed further. A description of other DR sensors can be found in Stephen (2000).

A gyro is an instrument to measure the rate of rotation or integrated heading change of a platform (Savage, 1978). A gyro can only measure rotations in a single plane. A triad of gyros is often mounted orthogonally in a single enclosure to monitor the three possible rotations in 3-D space. In vehicle navigation, roll and pitch are generally negligible and only one gyro is needed to monitor the change in azimuth. There are many types of gyros

which can be broadly classified as gimbaled or strapdown (Jekeli, 2000). Gimbaled gyros maintain a fixed physical orientation in an inertial frame (relative to distant galaxies), whereas strapdown gyros maintain this orientation analytically.

Piezoelectric gyros are the most commonly used low cost strapdown gyros. Piezoelectric materials are those which exhibit the piezoelectric effect in which a vibration of crystal produces electric potential within the material (Yang, 1998). The gyro essentially utilizes a physical phenomenon called Coriolis force (Wang and Baigen, 2003). When a mass, m, vibrating with a velocity, $\vec{V}$, is revolved with angular velocity, $\vec{\Omega}$, then the resulting Coriolis force, $\vec{F}$, is given by Equation 2.3.

$$\vec{F} = -2m\ \vec{\Omega} \times \vec{V} \tag{2.3}$$

The Coriolis force operates in a direction perpendicular to the motion of the tuning bar vibrator and is proportional to its velocity (Konno and Sugawara, 1987). The piezoelectric vibrating gyroscope has its tuning bar vibrator made up of piezoelectric ceramic. If this vibrating system is given a revolving angular velocity, a Coriolis force is generated in a direction perpendicular to the original vibration. This in turn generates a fixed voltage. By knowing this voltage, the Coriolis force can be estimated leading to the estimation of angular velocity using Equation 2.3. The low cost Murata piezoelectric vibrating gyro (ENV-05) was used in this research whose specifications are given in Table 2.3.

Table 2.3: Murata Gyro (ENV-05) Specifications (Murata, 1999)

Characteristic	Symbol	Condition	Min	Std	Max	Unit
Supply voltage	Vcc		+4.5	+5.0	+5.5	VDC
Current consumption	Lcc	At Vcc=5VDC	-	-	15	mA
Max. angular velocity	Omax	AT -30 to 80	-60	-	60	Deg/s
Output					2.85	VDC
Scale factor	Vo	At -10 to 60	-	-	27.0	mV/deg/s
Assymetry CW & CCW	Sv		-	-	3	deg/s
Drift		At -30 to 80	-	-	9	deg/s
Start up		Vo after 5s	-	-	±1	Deg/s/10mi
Noise level		10 KHz noise	-	-	20	mVrms
Linearity		In the Omax	-	10	-	%Fs
Response		Phase delay: 90	-	10	-	Hz
Operation temp. range	Topr		-30	-	80	C
Storage temp. range	Tstg		-40	-	85	C
Weight			-	-	20	G
Dimensions			11.5 (D) × 19.6 (W) × 23.2 (H)			

2.3 Digital Maps and DEMs

A map can be defined simply as a graphic representation of real life geographic features (Thomas, 1998). The level and type of description depends on the specific user needs. In

vehicle navigation research, this information is generally limited to road information (Bullock, 1995). Further to this, since the research is not intended for vehicle safety applications, the lateral width of the road is not taken into account. Hence, this research deals with linear road segments, where any road curve is represented in two dimensions by a set of piecewise linear segments $\bar{l} \subset \Re^2$. Any road segment $l \subseteq \bar{l}$, is represented by the coordinates of the nodes. Figure 2.2 shows a sample representation of a road segment used in this research. The centre line accuracy of the road map used in this research is of the order of a few metres. This accuracy is sufficient to impose a constraint in computation model to monitor the integrity of GPS measurements.

A DEM is the mapping from the two dimensional horizontal coordinates to the height (elevation) at that point (Endreney et al., 2000). Such information is generally obtained through a photogrammetric survey with a particular contour interval. The contour interval determines the precision of the DEM (Audenino et al., 2001).
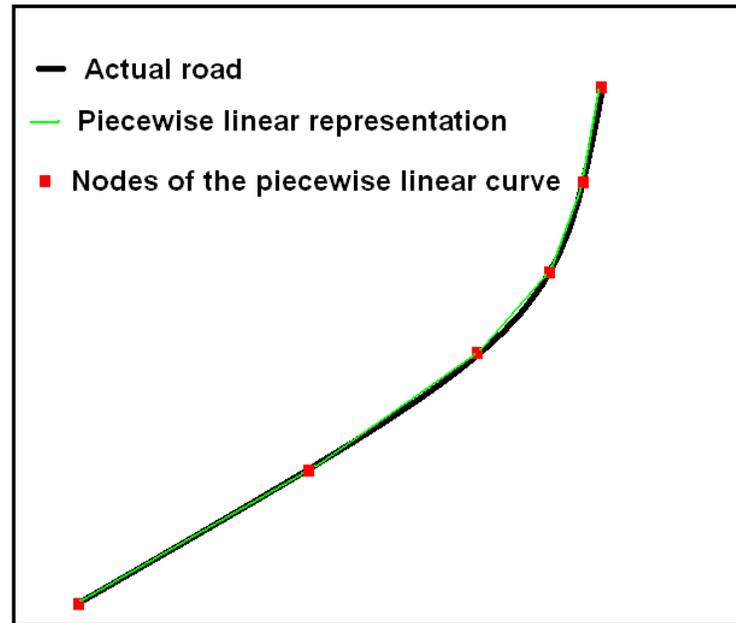
Figure 2.2: Piecewise Linear Representation of a Road Segment

The DEM is usually supplied in a grid format, which can be decoded to ASCII format using software such as PCI GEOMATICA (PCI Geomatics, 2004). The information obtained includes the number of rows and columns in the grid. This grid is defined by the coordinates of two reference vertices (like upper-left and lower-right vertices). Figure 2.3 describes the grid format of the DEM. The DEM provides height information corresponding to the centre of each rectangular segment. Any height information in between the midpoints can be obtained using linear interpolation along both the horizontal dimensions.
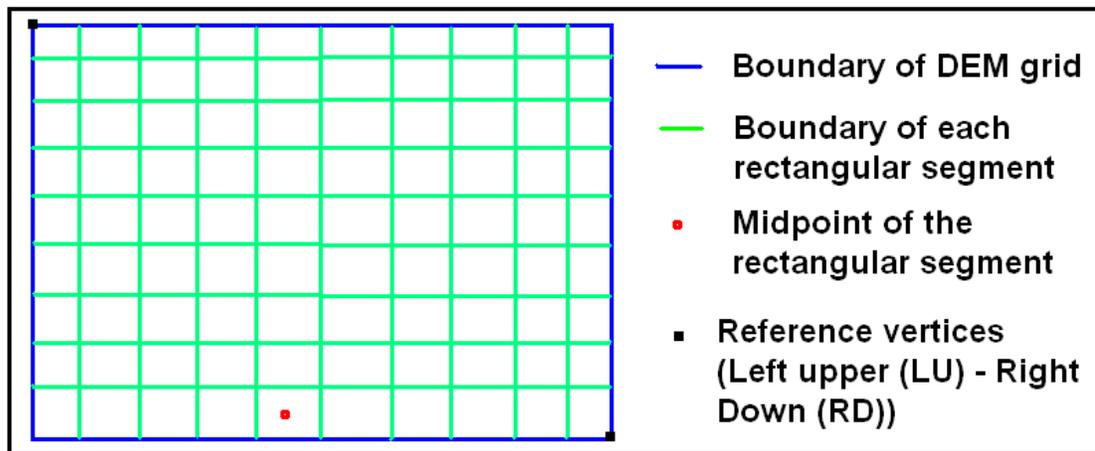
Figure 2.3: Grid Pattern of a DEM

CHAPTER 3: INTRODUCTION TO FUZZY LOGIC

Computational techniques can be broadly classified into two categories: (a) soft computation techniques and (b) classical computation techniques. Soft computation techniques such as Neural Networks, Fuzzy Logic, Genetic Algorithms has been gaining increased acceptance in the computation world (Dote, 1995). Fuzzy logic is a technique developed by Dr. Lotfi Zadeh, at the University of California at Berkley in the mid 1960's (Zadeh, 1995; Tanaka and Niimura, 1996). It is one of the most popular theories in control systems, and was originally developed in the context of data processing using fuzzy sets, as opposed to the classical computations involving classical (crisp) sets (Ross, 2004). This chapter first describes the concept of fuzzy logic, followed by an introduction to fuzzy sets, Degree of Membership (DOM), fuzzy rules, defuzzification and Fuzzy Inference System (FIS).

3.1 Fuzzy Logic

Fuzzy logic is a powerful problem-solving methodology, which has more stress on approximate but reliable information, as opposed to precision. This provides a remarkably simple way to draw definite conclusions from vague, ambiguous or imprecise information. In a sense, fuzzy logic resembles human decision making with its ability to work from approximate data and find precise solutions. It is very useful for solving problems involving decision making. In this research a fuzzy logic framework is

designed to decide if a particular road segment is the one on which the vehicle is traveling.

Unlike classical logic which requires a deep understanding of a system, exact equations, and precise numeric values, fuzzy logic incorporates an alternative way of thinking, which allows modeling complex systems using a higher level of abstraction originating from our knowledge and experience (Gibson et al., 1994).

Fuzzy logic has been gaining increasing acceptance during the past few years. There are thousands of commercially available products which use fuzzy logic, ranging from washing machines to high speed trains (Mendel, 1995). Nearly every application can potentially realize some of the benefits of fuzzy logic, such as performance, simplicity, lower cost, and productivity.

Other advantages of using fuzzy logic are:

1) Flexibility in computation, which is the ability to build a system over existing functionalities and algorithms. This flexibility eases the incorporation of fuzzy logic in an existing software/algorithm.

2) Tolerance to imprecise data and contradictory information due to fuzzy reasoning.

3) Ease of handling non-linear functions of arbitrary complexity which are difficult to deal with using classical computation techniques.

4) Ease of integration with conventional computational techniques to yield precise and robust results.

3.2 Fuzzy Set Theory

A key concept in computation is the definition of sets. Conventional sets (also known as crisp sets) follow Boolean logic in determining the belongingness or membership of a particular input. For example, the set of integers among all the real numbers is a Boolean set. The DOM of numbers like 1.34, 2.3, -2.6 etc. is 0 and those of integers such as -1, 0, 2000 is 1. There is no concept of intermediate DOM such as 0.5.

On the other hand, fuzzy sets do not have a clearly defined boundary. Fuzzy logic is primarily considered with quantifying and reasoning of linguistic and fuzzy sets which appears in our normal language (Zadeh, 1965). These terms are referred to as linguistic or fuzzy variables and the sets associated with them as fuzzy sets (Dote, 1995). Examples of such variables are high temperature, low pressure, etc. These sets have grey regions (i.e. partial DOM) as opposed to black and white conventional Boolean set theory.

The concept of DOM is closely associated with fuzzy sets. The DOM is defined as the extent to which the numerical inputs obtained from sensors belong to a fuzzy set

(Mendel, 1995). The DOM is determined by *Membership Function* (MF). The MF is a mapping between the input space and DOM of a fuzzy set. The input space is referred to as a *range* of inputs.

For example, if a "High temperature" fuzzy set is defined and associated with an exponential MF (as shown in Figure 3.1), then the numerical temperature, say 68 degrees Celsius, has a DOM of 0.135.
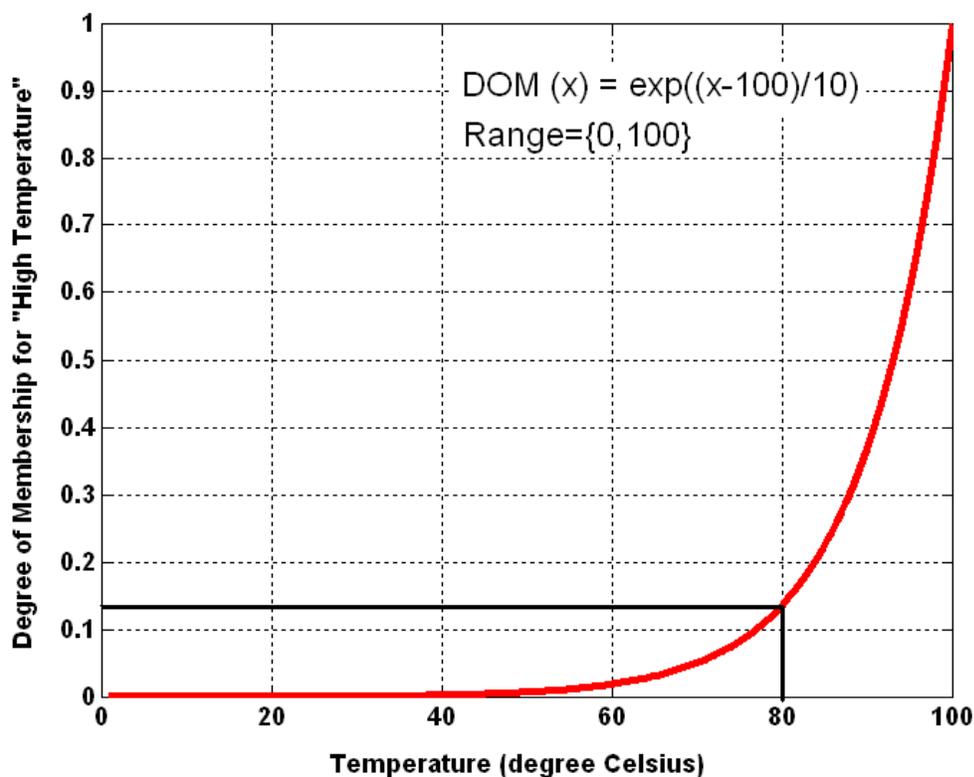
Figure 3.1: DOM for the Example Fuzzy Set: "High Temperature"

3.3 Logical Operations

Fuzzy logic involves a number of logical operations. The most important thing to realize about fuzzy reasoning is the fact that it is a superset of standard Boolean logic. In other words, if the fuzzy values are kept at their extremes of 1 (completely true), and 0 (completely false), standard Boolean logical operations should hold (Kauffman and Gupta, 1985).

The standard logical operations are: AND, OR, and NOT. These operations for conventional Boolean logic are shown in Figure 3.2.

A	B	A AND B
0	0	0
0	1	0
1	0	0
1	1	1

AND

A	B	A OR B
0	0	0
0	1	1
1	0	1
1	1	1

OR

A	NOT A
0	1
1	0

NOT

Figure 3.2: Operations in Conventional Boolean Logic

Now remembering that in fuzzy logic the truth of any statement is a matter of degree, these operations are modified to preserve the result of operations of the conventional Boolean logic and also extend to input values between 0 and 1. There are many ways in which these operations can be defined. One way is to use the *min-max* operation (Kickert, 1978). That is, resolve the statement *A* AND *B*, where *A* and *B* are limited to the range

(0,1), by using the function *min(A,B)*. Using the same reasoning, the OR operation can be replaced with the *max* function, so that *A* OR *B* becomes equivalent to *max(A,B)*. Finally, the operation NOT *A* becomes equivalent to $1-A$. While these operations are standard and hold well for control problems, a better way of dealing with sensor measurement is the use of the *normalized-multiplication-addition* approach.

The present research uses the multiplication-addition approach for fuzzy logic operations. That is, the statement A AND B is resolved by using the function $A \times B$. The OR operation can be performed by using A+B, and NOT A is same as defined above. Since this approach satisfies the basic equations of conventional Boolean logic, it can be appropriately used as a logical operation in fuzzy logic.

Additional operations, such as T-norms and S-norms, which are not dealt with here, are discussed in Jang and Sun (1997).

3.4 Fuzzy Rules

Fuzzy sets and fuzzy operators are the subjects and verbs of fuzzy logic. The if-then rule statements are then used to formulate the conditional statements that comprise fuzzy logic (Tong and Bonissone, 1984).

A single fuzzy if-then rule assumes the form: *If x is A then y is B*. Where *A* and *B* are the fuzzy sets on a given range of inputs and outputs, respectively. The if-part of the rule is called the *antecedent* or premise, while the then-part of the rule is called the *consequent* or conclusion. An example of such a rule might be: *If temperature is high then lower the heat.*

Thus a fuzzy rule connects input fuzzy sets to output fuzzy sets. This output fuzzified values are aggregated, and *defuzzified* later to obtain real world values. The concept of defuzzification is described in the next section.

Interpreting a fuzzy rule involves distinct parts: first evaluating the antecedent (which involves applying fuzzy operations on the input) and second applying that result to the consequent (known as *implication*). In the case of two-valued or binary logic, if-then rules are very straight forward and have the form: If the premise is true, then the conclusion is true or else the conclusion is false. If the restrictions of two-valued logic are relaxed, and the antecedent is a fuzzy statement, then the rules are of the form: if the antecedent is true to some degree, then the consequent is also true to the same extent (Mathwork, 2002). In other words:

In binary logic: $p \rightarrow q$ (*p* and *q* are either both true or both false.)

In fuzzy logic: $0.5\,p \rightarrow 0.5\,q$ (Partial antecedents provide partial implication.)

The antecedent of a rule can have multiple parts connected using logical operators like AND, OR and NOT. A generalized fuzzy rule assumes the form: *if x is A AND y is B OR z is C then Q is d.*

In such rules, all parts of the antecedent are calculated simultaneously and resolved to a single number using the logical operators described in the preceding section. The consequent of a rule usually has one part although in complex systems it may have multiple parts.

The *implication function* then modifies that fuzzy set to the degree specified by the antecedent (Bandemer and Nather, 1992). The most common ways to modify the output fuzzy set are truncation using the *min* function (where the fuzzy set is chopped off) or scaling using the *prod* function (where the output fuzzy set is squashed).

In general, one rule by itself does not do much good. The power of fuzzy logic can be harnessed effectively if there are multiple rules that interacts with each other (Chen and Hwang, 1992). The output fuzzy sets for each rule are then *aggregated* into a single output fuzzy set. Finally the resulting value is *defuzzified*, or resolved to a numerical output.

3.5 Defuzzification

Defuzzification is the process of obtaining an output for the real world from the aggregation of the fuzzy outputs from a set of rules. There are many ways of defuzzifying the aggregate fuzzy output. The most popular for the discrete decision making problem is the *max* function. For example, in this research the identification of correct road segment is based on defuzzification of output from a set of rules, and the road segment with highest aggregate fuzzy output is identified as the correct road segment. Figure 3.3 illustrates the process of defuzzification.
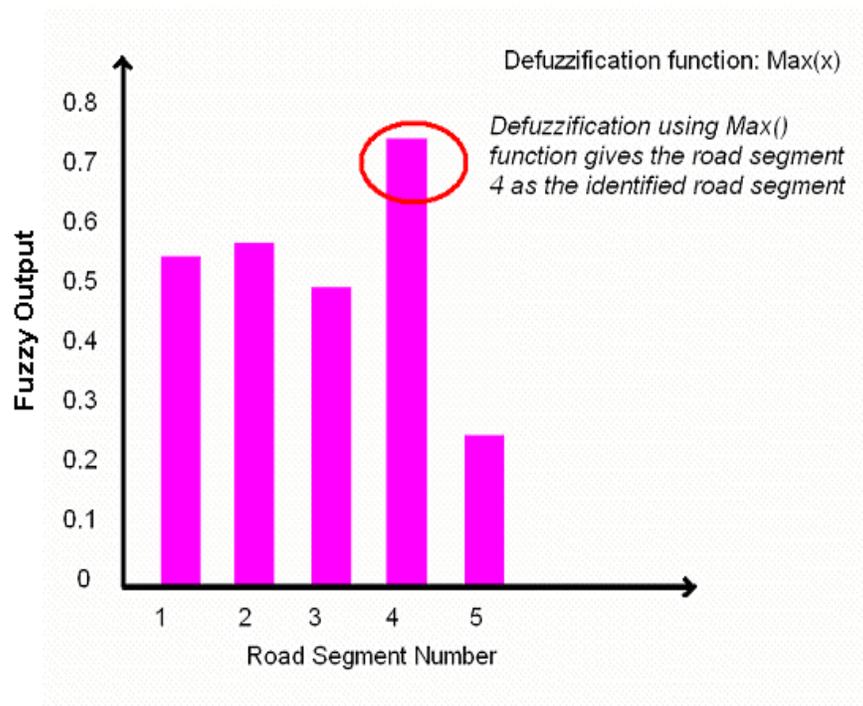
Figure 3.3: Example Showing the Defuzzification Process

3.6 Fuzzy Inference System

A Fuzzy Inference System (FIS) is the framework for systematically performing all the exercises discussed above to obtain a precise numerical output from a given input using fuzzy logic (Kauffman and Gupta, 1985). A schematic diagram of an FIS is shown in Figure 3.4. This is a mapping that provides a basis from which decisions can be made, or patterns discerned. There are many types of FISs, with the major two being Mamdani and Sugeno. The details of these FISs can be found in Jang and Sun (1997), Mamdani and Assilian (1975), and Sugeno (1985). The main difference between the two FISs is the way in which the output is determined.
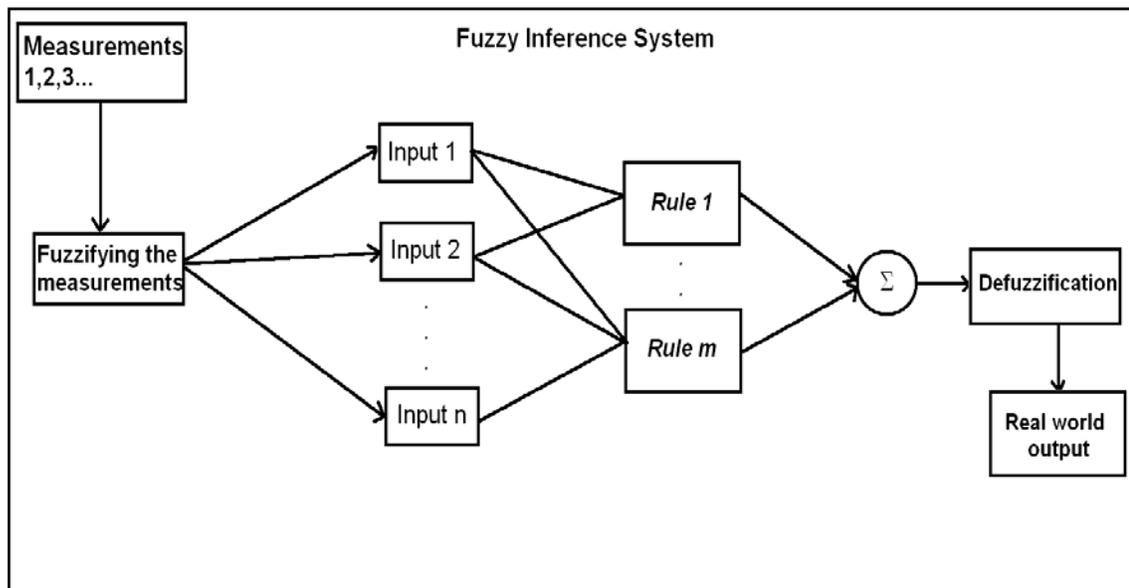
Figure 3.4: Schematic Representation of an FIS

In a Mamdani type FIS, the output MFs are contained in a fuzzy set obtained after the aggregation process. There is a fuzzy set for each output variable that needs defuzzification. The Sugeno-type FIS, on the other the hand, has output MF that is either linear or constant. A typical rule in a Sugeno fuzzy model then has the form:

If input $1 = x$ and input $2 = y$, then the output is $z = ax + by + c$

The order of equations used for evaluating z determines the order of the FIS (Dubois and Prade, 1979). The output from each rule is weighted, and the final output is determined as the weighted sum of the output from the individual rule. In this research a modified form of a first order Sugeno-Type FIS is used.

3.7 Adaptive Network-Based Fuzzy-Inference System

The success of any fuzzy logic algorithm depends on the effectiveness of the MF to fuzzify the input. The basic shape of an FIS is always intuitive (Grim, 1993). More than one shape can be used as a MF for fuzzification and defuzzification (e.g. Gaussian and Triangular shape). After deciding the basic shape of the input MF, the parameters used to describe the curve need to be determined and optimized. This is usually done by using a "training" data set. The parameters are empirically determined using techniques like back propagation and least squares. Matlab's fuzzy logic tool box provides a toolkit called the Adaptive Network-based Fuzzy Inference System (ANFIS) to model these parameters (Mathwork, 2002). The present research uses this tool kit to determine the MF.

CHAPTER 4: ESTIMATION THEORY

In this chapter, the estimation and filtering theory behind the proposed algorithm is discussed. A brief introduction to least squares and Kalman filtering techniques is provided. A discussion on reliability is presented at the end of the chapter. Much of the theory is taken from standard references such as Gelb (1974), Maybeck (1982), Brown and Hwang (1992). Appendix-A provides an introduction to random variables and their characteristics on which the estimation theory is built.

4.1 Estimators

The purpose of a parametric estimation model is to obtain a best estimate of the unknowns given a set of measurements and constraints. This "best" is defined with respect to a given set of criteria. A model for parametric estimation is usually represented by a set of unknown parameters $x_1,\ x_2,\ ......x_n$. The observations $y_1,\ y_1,\ .....,\ y_m$ are related to these parameters by a functional model F as:

$$(y_1,\ y_2,\ .....,\ y_m) = F(x_1,\ x_2,\ ......x_n), \quad \text{where } F : \mathfrak{R}^m \to \mathfrak{R}^n \tag{4.1}$$

The individual observation (which is either a measurement or a constraint) is related to the parameter as

$$y_i = F_i(x_1, \ x_2, \ ......x_n) \ \forall i \in \{1, \ 2, \ 3,...m\} \tag{4.2}$$

where F_i is the ith relation in the functional model F.

If each F_i is an explicit function then an inverse relation can be determined for parametric estimation as:

$$(x_1, \ x_2, \ ......x_n) = H(y_1, \ y_1, \ ....., \ y_m) \ , \quad \text{where } H : \Re^n \rightarrow \Re^m \tag{4.3}$$

The procedure used for parameter estimation is called an *estimator*. The following are the four ideal characteristics of an estimator (Wieser, 2002):

1) The estimator should be *unbiased*: The expectation or mean of the parameter(s) estimated by an estimator should be equal to the true value(s) of the parameter(s).

2) The estimator should be *consistent*: In other words, if the size of the sample which is selected from the population is increased, the estimator should yield a value which gets closer to the true value of the parameter being estimated.

3) The estimator should be *relatively efficient*: That is, of all possible statistics that could be used to estimate a particular parameter, the one having the smallest variance of the sampling distribution should be chosen.

4) The estimator should be *robust*: That is, it should be able to identify outliers and give a robust estimate.

A detailed discussion on estimation theory can be found in Beck and Arnold (1976), and Koch (1999). The theory of robust estimation can be found in Huber (1964) and Hampel et al. (1986).

4.2 Least Squares Estimation

The least squares method is an important class of estimator, which deals with a Gauss Markov model. This was developed by Gauss in 1809, and is very popular for geodetic applications. A Gauss Markov model is one in which the observables are related to parameter through a linear relationship.

$$\vec{Y}_{m\times1} = \mathbf{H}_{m\times n}\vec{X}_{n\times1} \tag{4.4}$$

where

$\vec{Y}_{m\times1}$ is a vector of observations,

$\mathbf{H}_{m\times n}$ is the matrix relating parameters to observation, and

$\vec{X}_{n\times1}$ is the vector of parameters.

The method is equivalent to solving a set of simple linear equations, if the number of observations, m, is equal to number of unknown parameters, n. However, when there are redundant observations, i.e. the number of observations is greater than the number of unknowns, then least squares gives a solution which minimizes squared sum of residuals. The squared sum of residuals is given by

$$\Theta = \vec{v}^{\,T}_{1\times m}\, \vec{v}_{m\times 1} \tag{4.5}$$

where

$\qquad \vec{v}_{m\times 1} \qquad$ is the vector of residuals, and

$\qquad \Theta \qquad$ is the squared sum of residuals.

Minimizing the squared sum of residual gives

$$\frac{d\Theta}{d\overline{\overline{X}}} = 0 \tag{4.6}$$

This condition after elementary matrix operations gives:

$$\vec{X}_{n\times 1} = (\mathbf{H}^{T}_{n\times m}\,\mathbf{H}_{m\times n})^{-1}\,\mathbf{H}^{T}_{n\times m}\,\vec{Y}_{m\times 1} \tag{4.7}$$

Least squares estimator does not make any assumptions about the error statistics. However, if it is assumed that the errors are normally distributed, then the least squares

estimate becomes the *maximum likelihood* estimate. Weighted least squares is based on the concept of minimizing the weighted sum of squared residuals. The weighted sum of squared residuals is given as:

$$\Theta = \vec{v}_{1\times m}^{T}\,\mathbf{P}_{m\times m}\,\vec{v}_{m\times 1} \tag{4.8}$$

where $\mathbf{P}_{m\times m}$ is the weight matrix of the observations.

Minimizing the squared sum of residual gives

$$\vec{X}_{n\times 1} = (\mathbf{H}_{n\times m}^{T}\,\mathbf{P}_{m\times m}\,\mathbf{H}_{m\times n})^{-1}\,\mathbf{H}_{n\times m}^{T}\,\mathbf{P}_{m\times m}\,\vec{Y}_{m\times 1} \tag{4.9}$$

If this $\mathbf{P}_{m\times m}$ is chosen to be the inverse of covariance matrix then the weighted least squares estimate will be the Best Linearly Uniform Unbiased Estimate (BLUUE) (Schaffrin, 1997). There is no assumption about the stationarity or ergodicity of the process in considering least squares estimate as a BLUUE. A detailed discussion on least squares estimation can be found in Wieser (2002).

The least squares method applies equally to non-linear functions which can be linearized about a fixed reference point, $\vec{X}^{0}$. This linearization method is effective only when the higher order terms have very small magnitude, which can be neglected on linearization. Thus, solving the non-linear function with small higher order terms is equivalent to solving the linear error equation given in Equation 4.13.

$$\vec{Y} = f(\vec{X})$$ (4.10)

$$\vec{X} = \vec{X}^0 + d\vec{X}$$ (4.11)

$$\vec{Y} = f(\vec{X}^0) + \frac{df}{d\vec{X}}\bigg|_{\vec{X}^0} d\vec{X} + higher \;\; order \;\; terms$$ (4.12)

$$d\vec{Y} = \vec{Y} - f(\vec{X}^0) \approx \frac{df}{d\vec{X}}\bigg|_{\vec{X}^0} d\vec{X}$$ (4.13)

4.3 Kalman Filtering

Kalman filter was first introduced by R.E. Kalman in 1960 for solving the linear filtering problem in a recursive way (Kalman, 1960). Since then, Kalman filter has been used extensively in the field of control systems and navigation (Greenspan, 1996). Kalman filtering offers flexibility such that it can be used either in a real-time or post-mission environment (Grewal and Andrews, 1993). Details of the Kalman filter and associated state space derivations can be found in many references such as Gelb (1974), Brown and Hwang (1996), Sorenson (1970), Lewis (1986) and Jacob (1993). For simplifying the notation, the order of matrices will be dropped in subsequent sections and subscripts will now represent time.

The Kalman filter for navigation applications attempts to estimate the discrete controllable state process, whose transition is given by the discrete difference:

$$\vec{X}_{k+1} = \mathbf{A}_{k+1/k}\vec{X}_k + \vec{\eta}_{k+1/k} \qquad (4.14)$$

where

$\vec{X}_k$ is the value of state vector at k^{th} epoch,

$\vec{\eta}_{k+1/k}$ is the transition noise, and

$\mathbf{A}_{k+1/k}$ is the transition matrix relating the state vectors between consecutive epochs.

In addition to the transition model, a measurement model is needed to estimate the state vector. The measurement model is given by:

$$\vec{Z}_k = \mathbf{H}_k\vec{X}_k + \vec{\eta}_{m,k} \qquad (4.15)$$

where

$\vec{Z}_k$ is the measurement vector at k^{th} epoch,

$\mathbf{H}_k$ is the design matrix at k^{th} epoch, and

$\vec{\eta}_{m,k}$ is the measurement noise at k^{th} epoch.

The matrix $\mathbf{A}_{k+1/k}$ is called the *transition matrix* and $\mathbf{H}_k$ is the *design matrix*. Either $\mathbf{A}_{k+1/k}$ or $\mathbf{H}_k$, or both, may vary with time in the non-stationary case. The random variables $\vec{\eta}_{k+1/k}$ and $\vec{\eta}_{m,k}$ are zero mean normally distributed vectors of random variables.

$$\vec{\eta}_{m,k} \sim (\vec{0}, \mathbf{R}_k) \tag{4.16}$$

$$\vec{\eta}_{k+1/k} \sim (\vec{0}, \mathbf{Q}_k) \tag{4.17}$$

If the process is stationary then covariance of $\vec{\eta}_{k+1/k}$, $\mathbf{Q}_k$, remains constant, otherwise it has to be adapted.

The basic steps involved in a Kalman filter are:

a) Prediction of the state vector given by Equation 4.18.

$$\vec{X}_{k+1/k} = \mathbf{A}_{k+1/k} \vec{X}_k \tag{4.18}$$

where $\vec{X}_{k+1/k}$ is the prediction of the state vector.

b) Prediction of the covariance matrix given by Equation 4.19.

$$\mathbf{P}_{k+1/k} = \mathbf{A}_{k+1/k} \mathbf{P}_k \mathbf{A}_{k+1/k}^T + \mathbf{Q}_{k+1} \tag{4.19}$$

where

$\mathbf{P}_{k+1/k}$ is the predicted Covariance of state vector, and

$\mathbf{P}_k$ is the Covariance of the state vector at k^{th} epoch.

c) The key concept behind Kalman filtering is to assign weights to predicted state relative to the state calculated from observations. This gain matrix, often referred to as Kalman gain, is calculated in order to minimize the variance of the state vector (see Jacob (1993) for a detailed derivation). The Kalman gain matrix, $\mathbf{K}_{k+1}$, is calculated using Equation 4.20.

$$\mathbf{K}_{k+1} = \mathbf{P}_{k+1/k} \mathbf{H}_{K+1}^T (\mathbf{H}_{k+1} \mathbf{P}_{k+1/k} \mathbf{H}_{k+1}^T + \mathbf{R}_{k+1})^{-1} \tag{4.20}$$

d) Computing the updated state vector by adding the product of Kalman gain and innovation sequence to the predicted value. The innovation sequence, $\vec{\vartheta}_k$, is defined as the difference between the actual and predicted measurements.

$$\vec{X}_{k+1} = \vec{X}_{k+1/K} + \mathbf{K}_{k+1} (\vec{Z}_{k+1} - \mathbf{H}_{k+1} \vec{X}_{k+1/k}) \tag{4.21}$$

e) Updating the covariance of the state vector.

$$\mathbf{P}_{k+1} = (\mathbf{I} - \mathbf{K}_{k+1}\mathbf{H}_{k+1})\mathbf{P}_{k+1/k} \qquad (4.22)$$

The above steps are valid when the measurement equation and difference equation (defining the transition of the state vector) are implicit and linear. GPS filtering involves non-linear measurement model. Hence the model has to be linearized before solving for the unknown parameters.

4.4 Extended Kalman Filtering

Non-linear Kalman filters are of two types:

a) Linearized Kalman filter (LKF): The trajectory along which linearization is done is predetermined.

b) Extended Kalman Filter (EKF): The point of linearization is derived from the last computed solution.

Brown and Hwang (1992) discussed the pros and cons of using each technique. In the present research, an EKF is used to tackle the non-linear relationship between GPS measurements and navigation parameters. An LKF is advantageous to use as compared to an EKF when the solution has large outliers and when $\mathbf{H}_k$ is too sensitive to the point of linearization. Since an LKF can only be used if an approximate trajectory is known in advance, it cannot be used for vehicle navigation problem as the approximate trajectory is

not predetermined. Also, since the proposed algorithm employs an effective outlier detection scheme, an EKF can be safely used for vehicle navigation.

In this section, a discussion on non-linear filtering is presented in the context of non-linearities in the measurement model. An important difference between linear and non-linear Kalman filtering is the state vector. In non-linear Kalman filtering, the errors in parameters are estimated instead of the parameters themselves. This follows from the non-linear least squares estimation problem discussed in Section 4.3 (see derivation of Equation 4.13).

If the measurement model is non-linear as in Equation 4.23, it can be linearized about a fixed point as given in Equation 4.24. Equation 4.24 serves as the measurement model for the Kalman filter.

$$\vec{Z} = f(\vec{X}) \tag{4.23}$$

$$d\vec{Z} = \vec{Z} - f(\vec{X}^{\,0}) \approx \left. \frac{df}{d\vec{X}} \right|_{\vec{X}^{\,0}} d\vec{X} \tag{4.24}$$

The transition matrix of the prediction model (Equation 4.25) remains the same for the error states.

$$d\vec{X}_{k+1} = \mathbf{A}_{k+1/k} d\vec{X}_k \tag{4.25}$$

The regular Kalman filtering algorithm (discussed in the previous section) is then implemented through Equations 4.24 and 4.25 as the measurement and transition equation, respectively. It is to be noted that the process noise and the measurement noise matrices remain unaffected in the EKF as the uncertainty in state is equal to uncertainty in the deviation of the error state from a zero value.

An improvement in the performance of non-linear Kalman filtering is obtained by implementing an *iterative* EKF (IEKF) instead of a normal EKF. In an IEKF, the point of linearization of $\mathbf{H}_k = \dfrac{df}{d\bar{X}}$ is updated for each iteration. In a normal EKF, there is no iteration and the linearization is about the predicted value of state vector $\overline{X}_{k/k-1}$. In addition, the performance can further be improved if the process noise is adapted instead of keeping it constant. This type of algorithm is referred as an Iterative Adaptive Extended Kalman Filter (IAEKF). Theory of covariance adaptation is discussed in Mehra (1970), Mehra (1972), Salychev (1998), Mohammed (1999) and Hu et al. (2003).

The scheme of an IAEKF is as follows:

1) An initial state $\vec{X}_0$ is first selected. $\vec{X}_{1/0}$ is obtained by applying the corrections obtained from Equation 4.25. If the transition model is linear then the predicted state vector can be directly calculated using Equation 4.18.

2) The process noise covariance is obtained by suitably assigning weights to the process noise covariance in the previous epoch, and the covariance derived from the current innovation sequence. The weight, w, depends on the stationarity of the process. The higher the stationarity of the process, the higher will be the weight. This value however, does not change with iterations and needs to be calculated only once during the first iteration.

$$\mathbf{Q}_k = w\mathbf{Q}_{k-1} + (1-w)\mathbf{K}_{k-1}\vec{\vartheta}_k\vec{\vartheta}_k^T\mathbf{K}_{k-1}^T \tag{4.26}$$

3) Linearize the design matrix $\mathbf{H}_k$ about the current state vector (see Equation 4.26). The value of current state vector in the first iteration is equal to the predicted value of state vector.

$$\mathbf{H}_k = \frac{df}{d\vec{X}}\bigg|_{\bar{X}_{k/k-1}} \tag{4.27}$$

4) The filtering algorithm uses the difference between the predicted state and the current state vector as the predicted error state vector for that iteration. In the first iteration, the value is a zero vector as the current value of the state vector is equal to the predicted state vector.

5) The difference between the actual measurements and the measurements derived from the current state vector serves as observations (see Equation 4.24).

6) The covariance matrix is propagated in space (Equation 4.19) using the covariance matrix of the previous epoch ($\mathbf{P}_k$).

7) The Kalman gain is calculated using Equation 4.20.

8) The error state vector for this iteration is obtained using Equation 4.21. The current state vector is obtained by applying these corrections to the previous state vector.

9) The covariance matrix is updated using Equation 4.22.

4.5 Analogy Between Least Squares Estimation and Kalman Filtering

An important difference between the least squares estimation and Kalman filtering is the prediction. While Kalman filter computes predicted value and then determines the weight that should be assigned to the predicted value relative to the value computed from the observation, least squares estimation gives a zero weight to prediction and relies completely on the value obtained using current observations. In other words, least squares estimator is a special form of Kalman filter with infinite process noise. This relation can be analytically expressed by Equation 4.28.

$$\mathbf{R}_k \mathbf{Q}_k^{-1} = \mathbf{0} \quad \forall k > 0 \tag{4.28}$$

The Kalman gain is then given as

$$\mathbf{K}_k = (\mathbf{H}_k^T \mathbf{P}_k \mathbf{H}_k)^{-1} \mathbf{H}_k^T \mathbf{P}_k \qquad (4.29)$$

The Kalman gain computed in Equation 4.29, when substituted in Equation 4.21, gives the weighted least squares estimate.

$$\vec{X}_k = (\mathbf{H}_k^T \mathbf{P}_k \mathbf{H}_k)^{-1} \mathbf{H}_k^T \mathbf{P}_k \vec{Z}_k \qquad (4.30)$$

4.6 Theory of Reliability

Reliability refers to the ability of detecting blunders in the measurements and estimating the effects of undetected blunders on the parameters (Ryan, 2002). Discussions on reliability can be divided into internal and external reliability. Internal reliability refers to the smallest outlier (blunder) that can be identified in an observation through statistical testing. External reliability, on the other hand, deals with the impact of the undetected outlier on the estimated parameters. A detailed discussion on reliability can be found in Baarda (1967; 1968) and Srikanthan (1961). This was further extended to dynamic models in Teunissen (1990). Since two estimation techniques (i.e. least squares and Kalman filter) are dealt with here, this section is sub-divided into two parts. The first part discusses outlier detection in the least squares method, whereas the second part deals with outlier detection in the Kalman filtering approach.

The effect of blunders can be reduced in two ways:

1) Elimination of blunders: This involves the detection of blunders in the solution followed by identification and isolation of the measurements having outliers.

2) Variance inflation method: This method changes the variance of measurements depending on a statistical test, thereby reducing the effect of measurements having outliers by increasing its variance.

In this research, the first method is used to remove the effect of outliers.

4.6.1 Outlier Detection in the Least Squares Approach

Least squares blunder detection is a snapshot way to determine the presence of an outlier as it does not take into account the history. The essential condition to detect a blunder is the existence of redundancy. The symbols used in this discussion are the same as those defined in Section 4.3.

If there are more observations than unknowns, the least squares solution is *over-determined* and a solution is obtained by minimizing the sum of squared residuals. The residual vector is then related to the bias in the observations as:

$$\vec{\hat{r}} = -\mathbf{C}_{\vec{\hat{r}}}\mathbf{P}\vec{\mathbf{V}} = -\mathbf{E}\vec{\mathbf{V}} \qquad (4.31)$$

$$\mathbf{C}_{\hat{\vec{r}}} = \mathbf{P}^{-1} - \mathbf{H}(\mathbf{H}^T\mathbf{P}\mathbf{H})^{-1}\mathbf{H}^T \qquad (4.32)$$

where

$\hat{\vec{r}}$ is the vector of residuals,

$\vec{\nabla}$ is the vector of bias in measurements,

$\mathbf{C}_{\hat{\vec{r}}}$ is the covariance matrix of the residuals, and

$\mathbf{E} = \mathbf{C}_{\hat{r}}\mathbf{P}$ is the redundancy matrix.

The trace of the idempotent matrix, $\mathbf{E}$, is equal to the redundancy in the observations. Each diagonal element of $\mathbf{E}$ corresponds to that observation's contribution to the overall redundancy. If the observations are uncorrelated, then the diagonal element $\mathbf{E}_{ii} \in [0,1]$. If $\mathbf{E}_{ii}$ is close to zero then that observation has no effect on redundancy, whereas $\mathbf{E}_{ii}$ close to unity implies large effect on redundancy. A balanced solution would have all of the diagonal elements approximately equal and there would be no weaknesses in the solution.

If one blunder is present, then the vector $\vec{\nabla}$ will only contain one non-zero term. Standardized residual testing involves checking the condition given by Equation 4.33.

$$\frac{\hat{r}_i}{\sqrt{(\mathbf{C}_{\hat{\vec{r}}})_{ii}}} \sim \mathbf{N}(0,\mathbf{I}) \qquad (4.33)$$

The assumption in this type of testing is that the residuals are normally distributed, and that a blunder while biasing the residual does not change its variance. Two types of errors can be made whenever a statistical test is performed:

a) A Type-I error occurs whenever a good observation is rejected. The probability associated with a Type-I error is denoted by α.

b) A Type-II error occurs whenever a bad observation is accepted. The probability associated with a Type-II error is denoted by β.

Figure 4.1 shows a graphical representation of the relationship between the Type-I/II errors and the corresponding bias in the standardized residual called the non centrality parameter, δ. By appropriately selecting the confidence probability α and β, a non-centrality parameter can be obtained for outlier testing. A non-centrality table can be found in Leick (1995).
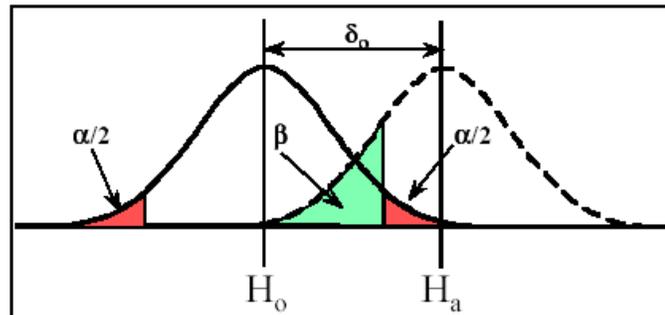
Figure 4.1: Type-I, Type-II Errors and Non-Centrality Parameter

The standardized residual test for uncorrelated observations is given by Equation 4.34.

$$\left| \frac{\hat{r}_i}{\sqrt{(\mathbf{C}_{\hat{r}})_{ii}}} \right| \leq \delta(\alpha, \beta) \qquad (4.34)$$

The smallest blunder that can be detected using this type of testing (often referred as the Maximum Detectable Blunder (MDB)) is given as

$$\left| \vec{\nabla} \right| \geq \delta(\alpha, \beta) \sqrt{\frac{(\mathbf{C}_{\hat{r}})_{ii}}{\mathbf{E}_{ii}}} \qquad (4.35)$$

Each observation has a different MDB which depends on its redundancy number. The lower the redundancy number, the higher the MDB. The impact of each MDB on the estimated parameter is given by Equation 4.36.

$$\vec{\hat{\delta}} = -(\mathbf{H}^T \mathbf{P} \mathbf{H})^{-1} \mathbf{H}^T \mathbf{P} \vec{\nabla}_0 \qquad (4.36)$$

where

$\vec{\hat{\delta}}$ is a column of errors in estimated parameters, and

$\vec{\nabla}_0$ is a column vector with all zeroes except 1 in the ith position.

The maximum horizontal positioning error (HPE) due to a blunder in the ith measurement is given as

$$(HPE)_i = \sqrt{(\Delta\varphi_i^2 + \Delta\lambda_i^2)} \qquad (4.37)$$

where

$\Delta\varphi_i$ is the error in latitude due to the ith blunder, and

$\Delta\lambda_i$ is the error in longitude due to the ith blunder.

Both $\Delta\varphi_i$ and $\Delta\lambda_i$ are the elements of the $\hat{\delta}$ vector. The standardized residual test is computationally expensive, and an efficient way of detecting outlier(s) in solution is to perform a *global test* before checking the standardized residuals. This global test follows from the fact that if individual random variables are normally distributed then their squared sum should satisfy a Chi-square distribution with a degree of freedom equal to the redundancy (Gelb, 1974). This condition can be expressed by Equation 4.38 which, on simplification, can be expressed in the form of Equation 4.39.

$$\vec{r}\mathbf{C}_{\vec{r}}\vec{r}^T \leq \chi^2_{n,1-\alpha} \qquad (4.38)$$

$$\vec{r}\mathbf{P}\vec{r}^T \leq \chi^2_{n-4,1-\alpha} \qquad (4.39)$$

where $\chi^2_{n-4,1-\alpha}$ is the value corresponding to a Chi-squared distribution function with $n-4$ degrees of freedom and a confidence probability of α.

The corresponding test for multiple blunders is given by Equation 4.40.

$$\left| \mathbf{E}_{ki} \vec{\nabla}_i + \mathbf{E}_{kj} \vec{\nabla}_j \right| \le \delta_0 \sqrt{(\mathbf{C}_{\hat{r}})_{kk}} \qquad (4.40)$$

The above equation tests the effect of blunders in the ith and j^{th} measurements on the kth residual. The theory of multiple blunder detection and the corresponding external reliability is dealt in with Kok (1984), Leick (1995) and Krakiwsky et al. (1999). One of the drawbacks of this approach is that if the signs of the outliers ∇_i and ∇_j are opposite, then the detection of the outlier pair becomes difficult. A more robust way to deal with outlier detection is the separation of solution (or measurement) approach.

The separation of solution is based on the assumption that the number of outlier measurements is less than the number of true measurements, and that the number of outlier-free measurements and constraints is one greater than number of unknowns. The separation of measurements is derived from separation of solutions method that was first introduced by Brown and McBurney (1987). It is probably the most heuristic of all the failure detection schemes (Brown, 1993). Subsets of available measurements are formed and tested for the presence of outliers. The measurement set without an outlier will satisfy the global test discussed in the previous section.

The following steps are involved in the least squares outlier detection scheme developed in this research:

1) A global test is performed using all the available measurements. If the global test is satisfied, the standardized residuals are also tested for the presence of outliers. If either of the tests fails then the algorithm proceeds further, otherwise an outlier-free solution is declared.

2) Subsets of available measurements are formed by eliminating one measurement at a time. It is to be noted that eliminated measurements are replaced before carrying out subsequent eliminations.

3) If an outlier-free solution is not obtained for any subset formed after elimination of one satellite at a time, then a similar procedure is carried out by eliminating two satellites at a time, and subsequent eliminations are carried out until an outlier-free combination is obtained.

4.6.2 Outlier Detection in the Kalman Filtering Approach

The presence of an outlier in Kalman filtering approach is detected by testing the innovation sequence. An innovation is defined as the difference between the actual and predicted measurements. The testing of innovations is based on the fact that they are zero mean, normally distributed, with a variance ξ_k (at k^{th} epoch) and is given by Equation 4.41.

$$\xi_k = \mathbf{R}_k + \mathbf{A}_{k/k-1}\mathbf{P}_k\mathbf{A}_{k/k-1}^T \qquad (4.41)$$

The global test for detecting blunders in Kalman filtering, often referred as a Chi-Square test, is given by Equation 4.42. It is based on the fact that the innovation sequence is normally distributed, and hence their sum of weighted squared value should follow a Chi-Square distribution.

$$\vec{\vartheta}_k \xi_k \vec{\vartheta}_k^T \leq \chi^2_{n,1-\alpha} \qquad (4.42)$$

where

$\vec{\vartheta}_k$ is the innovation sequence at k^{th} epoch, and

$\chi^2_{n,1-\alpha}$ is the value corresponding to a Chi-squared distribution with n degrees of freedom and confidence probability of α.

If an outlier is detected by a global test, a local test is performed to identify the measurement having outlier. This local test for detecting blunder in the ith measurement is based on the theory developed by Teunisson (1990) and is given by Equation 4.43.

$$\frac{\vec{\nabla}_i \xi_k \vec{\vartheta}_k^T}{\vec{\vartheta}_k \xi_k \vec{\vartheta}_k^T} \leq \delta(\alpha, \beta) \qquad (4.43)$$

where $\vec{\nabla}_i$ is the column vector with one at i^{th} position and zero else where.

The outliers can be sequentially eliminated based on the value of standardized residuals as opposed to the least squares outlier elimination technique based on separation of measurements approach. This is due to the fact that the value of the state vector in the next epoch is known with an uncertainty given by the ξ_k. Such predicted estimate of the state vector does is not available in least squares method due to which separation of measurements method has to be employed for multiple blunder detection.

4.7 Reliability Monitoring of GPS Measurements

GPS derives range and Doppler measurements from four or more satellites to calculate a navigation solution without any aiding. Integrity monitoring refers to the detection of faults in the measurements and subsequent exclusion of faulty measurements. Traditionally, Receiver Autonomous Integrity Monitoring (RAIM) was used in the aviation field to identify (and if possible isolate) faulty GPS measurements. The RAIM algorithm is contained in the receiver and hence the term "Autonomous" monitoring (Kaplan, 1996). The most commonly used RAIM algorithms are the Range Comparison method, the Least squares Residual method, the Parity method, the Constant-Detection-Rate method and the Maximum Separation of Solutions method. Details of these algorithms can be found in Brown (1993). In addition, Gao (1993) has devised a GPS integrity test procedure with reliability assurance to offer real-time precision and reliability checks on navigation solutions. Walter and Enge (1995) presented a versatile weighted form of RAIM where measurement sources are weighted based on a priori information or broadcast weighting information.

The integrity of range measurements can be monitored more effectively if the statistical tests are aided by some external means. A lot of work has been done on RAIM aided with the Russian GLONASS system and high accuracy inertial systems (Hewitson, 2003). More recently, Romay et al. (2001) investigated the availability of RAIM computed for GPS, Galileo and combined GPS/Galileo constellations through simulations. Integrity monitoring using an INS can be found in Brenner (1996). Lee (1993) demonstrated integrity monitoring using altitude aiding from a barometer. These algorithms, which use an external means to monitor GPS measurements, are referred as *Aided RAIM*.

Maps can be effectively used for monitoring GPS measurements in the land application case. The road segment on which the vehicle is travelling needs to be identified first before using the map constraints on position solution. In essence, the maps provide one extra and strong redundancy for the reliability assessment. The word "strong" implies that unlike an extra pseudorange measurement, which itself may be an outliers and which cannot be "trusted" without testing; this constraint remains blunder-free and trustworthy to the pre-stated level of uncertainty. One of the novel features of this research is the use of map for integrity monitoring of GPS measurements.

CHAPTER 5: PROPOSED ALGORITHM

Three sets of algorithms were developed during this research. They are: (a) a fuzzy logic-based position domain algorithm, (b) a fuzzy logic-based least squares algorithm, which is referred to as the MAGPS approach, and (c) a fuzzy logic-based Kalman filtering algorithm, which is referred to as the MAGPS filtering approach.

The three algorithms use a common road segment identification technique based on fuzzy logic. They however differ in the computation of navigation solution. The position domain approach matches the output from GPS solution and gyro using the fuzzy logic technique. The GPS solution in this case, is computed by an "external" algorithm, which does not use map information. The MAGPS and MAGPS filtering algorithms, on the other hand, use the map information for computing the GPS navigation solution using least squares method and Kalman filtering respectively. The role of gyro in all three approaches is restricted to the determination of a significant heading change, which is used to identify turns. The gyro measurements in this research are given as an input to the map matching FIS to determine the change in road segment. It is never used directly in the computation of the navigation solution. The architectures of the proposed algorithms are shown in Figure 5.1.
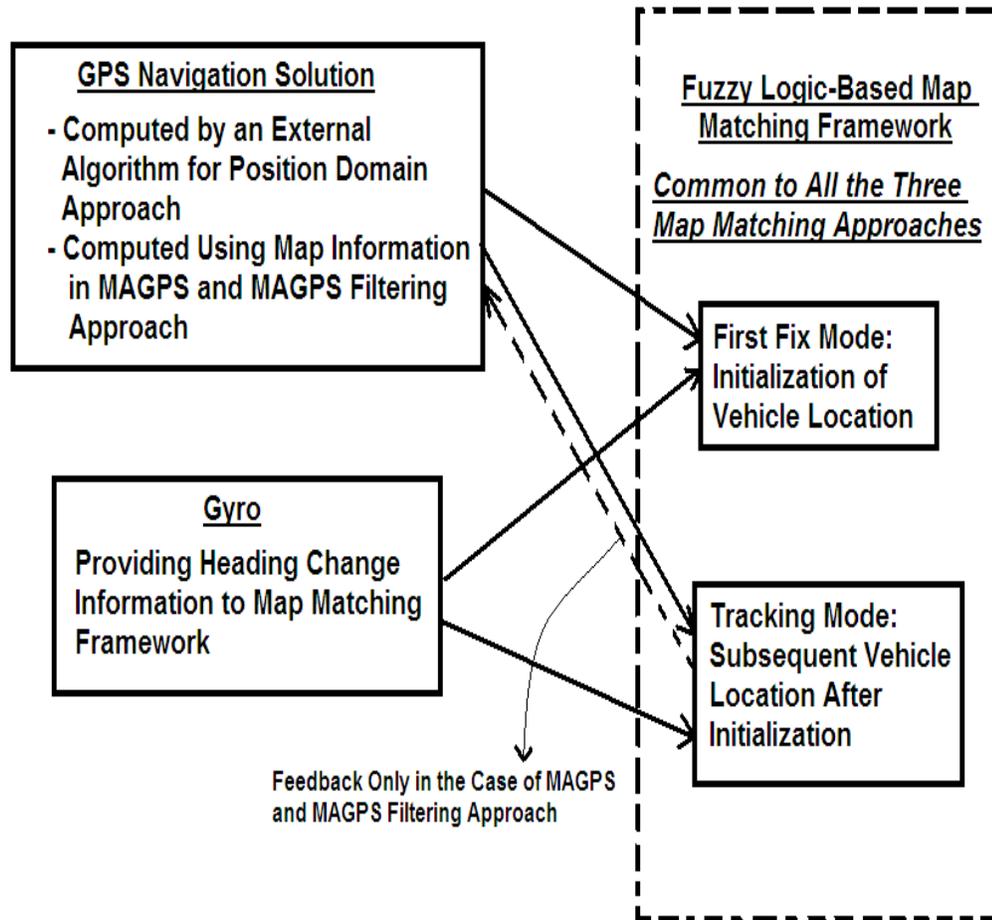
Figure 5.1: Architectures of the Proposed Algorithms

Section 5.1 describes the pre-processing of the map data to increase computational efficiency. Section 5.2 discusses the geometric concepts involved in map matching followed by Section 5.3, which describes the fuzzy logic-based position domain algorithm. Since the fuzzy logic-based position domain algorithm does not involve any interference with the GPS navigation solution computation, its discussion provides a

description of the map matching framework common to all three approaches. After describing this map matching framework, which is equivalent to a description of the fuzzy logic-based position domain approach, Section 5.4 focuses on the use of map information in the GPS measurement model. This measurement model will be used by both the MAGPS and MAGPS filtering approaches. The latter two sections describe the MAGPS and MAGPS filtering approaches, respectively. The concepts discussed in the preceding chapters will be frequently referred to in this chapter.

5.1 Pre-Processing Step

The City of Calgary has about 500,000 road segments as shown in Figure 5.2 (a). Computation over all these road segments becomes cumbersome, and hence the algorithm first extracts the road segment lying within 2 km from the first GPS position solution. This process, which is referred to as the *road refining process*, reduces the number of prospective road segments for evaluation to about 6000 as shown in Figure 5.2 (b). The 2 km distance is a balance between the frequency of the computationally intensive road refining process, and the number of prospective candidate road segments over which the map matching computations are performed.
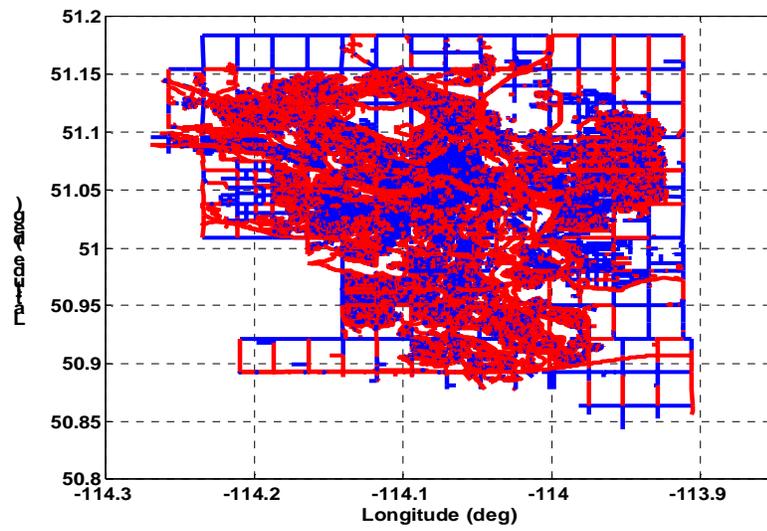
(a)
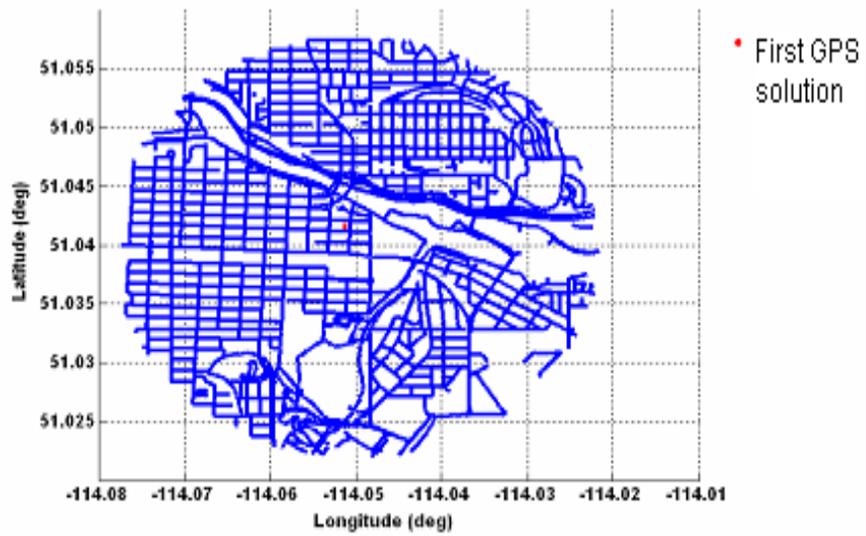
(b)

Figure 5.2: (a) Road Network of City of Calgary (b) Refined Road Network about the First GPS Position Fix

5.2 Computation of the Geometrical Attributes for Map Matching

This section briefly describes the methods used for calculating the geometrical properties involved in map matching. The road segments are considered as piecewise linear for computational purposes.

The length, $|L_0|$, of a two dimensional road segment having coordinates (N_1, E_1) and (N_2, E_2) is defined as:

$$|L_0| = \sqrt{(N_1 - N_2)^2 + (E_1 - E_2)^2} \tag{5.1}$$

The vector along the road segment, $\hat{L}_0$, is defined as

$$\hat{L}_0 = (N_1 - N_2)\hat{i} + (E_1 - E_2)\hat{j} \tag{5.2}$$

The angle, θ, between the two road segments, $\hat{L}_0$ and $\hat{L}_0'$, is defined as

$$\theta = \sin^{-1}\left(\frac{\hat{L}_0 \times \hat{L}_0'}{|\hat{L}_0||\hat{L}_0'|}\right) \tag{5.3}$$

The projection of a point on a road segment is defined as the perpendicular projection of that point on a road segment if the point is contained in the road segment; otherwise it is

considered to be the nearest end point (node) of the road segment. Figure 5.3 shows the projection of points on a road segment.
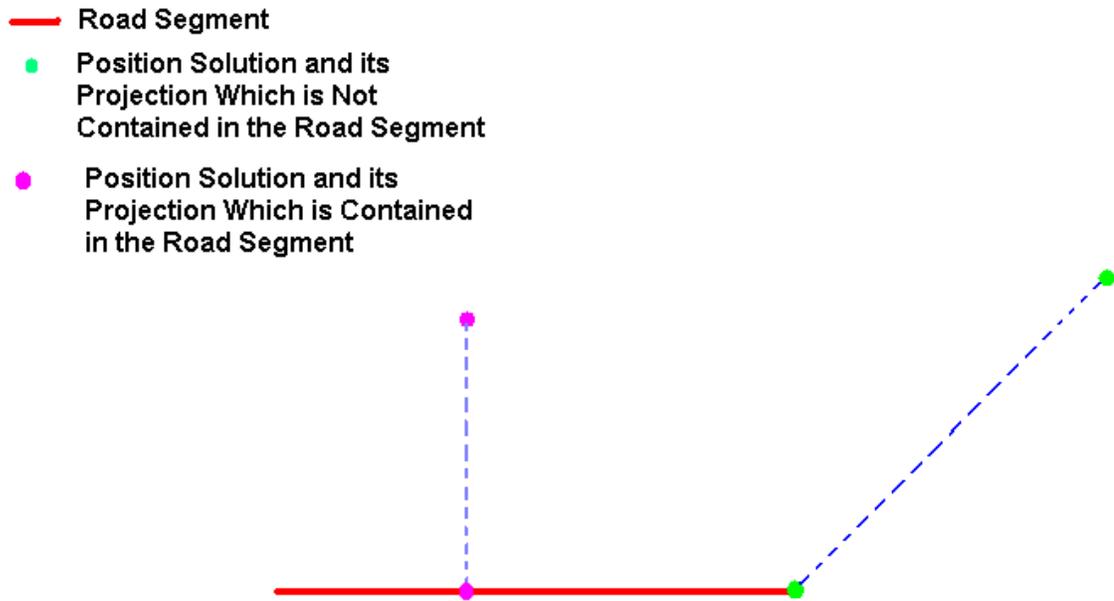
Figure 5.3: Projection of Position Solution onto a Road Segment

The distance of a position solution, $\vec{P}$, from a road segment, l, is defined as the distance between $\vec{P}$, and its projection on l, $pr(\vec{P})$.

5.3 Fuzzy Logic-Based Position Domain Algorithm: A Common Fuzzy Logic-Based Map Matching Framework

The proposed position domain algorithm is designed to identify both the correct link and the position on the identified link using the navigation solution obtained from an external

GPS navigation algorithm (e.g. the GPS receiver's internal solution algorithm, C^3NAVG^{2TM} algorithm, etc.). The description of the position domain algorithm is equivalent to the description of the fuzzy logic-based map matching framework which will be used in all three approaches. The basic steps in the proposed map matching framework are to:

1) Identify the first road link and determine the position of the vehicle on it,

2) Track the correct road link on the map, and

3) Determine the position on the road link tracked in Step 2.

5.3.1 First Fix Mode Sub-Algorithm

The most crucial step in map matching is the identification of the first correct road link (Scott, 1994). The success of subsequent vehicle tracking depends on this step. Considering this importance, the proposed algorithm in the position domain takes a minute or two (depending on the GPS availability conditions) to robustly identify the first road link. The corresponding time for the measurement domain approaches is less as they involve removal of outliers before initialization.

After initialization of the GPS receiver and the gyro, matching is done for 30 time epochs (e.g. 30 seconds with 1 Hz data). This matching is based on fuzzy logic giving high weights to the direction of motion determined from the GPS velocity estimates followed by the proximity of the point to the road link. A modified form of a Sugeno-type FIS is used for this sub-algorithm. The role of the gyro is to make sure that there is no

significant change in heading during this time. This sub-algorithm will be referred as *first fix* mode.

The following terms are used in this discussion (and are graphically shown in Figure 5.3):

- A *Close link set* for a given position output is a set of links, which are in a vicinity of empirically chosen value of 50 metres from the position output.

- The end point of a road segment, in the direction that the vehicle is heading, will be referred as the *destination point*.

- Two or more links are *concurrent* to each other if they share a common node.
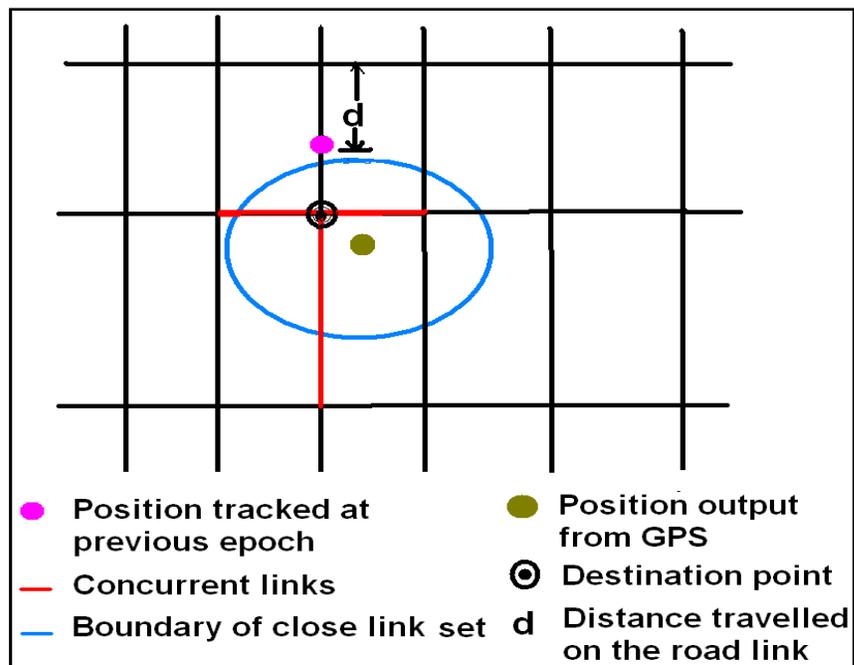
Figure 5.4: Graphical Description of Terms Used in the Discussion

Figure 5.5 shows the FIS diagram for this sub-algorithm. The fuzzy inputs to this FIS are:

1) Distance of the position output from the road links (obtained from the GPS),

2) Velocity direction with respect to the road links (obtained from the GPS),

3) Heading change (obtained from the gyro), and

4) Time.

The fuzzy sets used are the:

1) Nominal heading change,

2) Belongingness to a close link set,

3) Similarity of velocity direction and link orientation, and

4) Large number of epochs.

The MFs corresponding to the fuzzy inputs are shown in Figure 5.6. All MFs used in the above FIS are optimized using the ANFIS toolbox of Matlab. ANFIS uses techniques like least squares and back propagation for optimization (Mathwork, 1995). A trial data set was used to come up with a coarse estimate of the parameters using ANFIS. These parameters were then tweaked suitably to determine the final MFs. The fuzzy output is the *Resemblance*, which determines the similarity of a particular segment with the navigation solution.
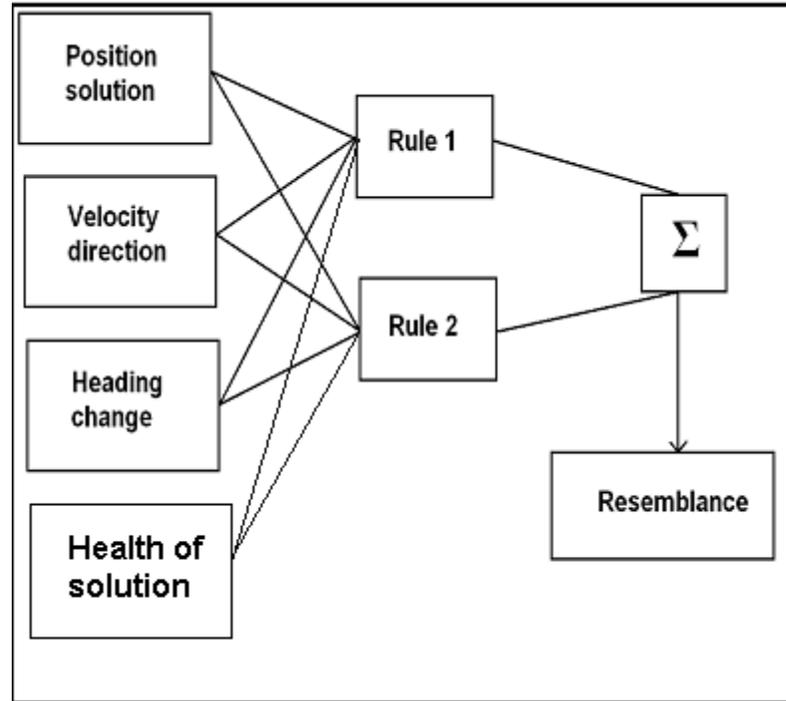
Figure 5.5: FIS for the First Fix Sub-Algorithm

The fuzzy rules for the FIS are:

Rule 1: If the <u>heading change</u> is nominal and a particular link belongs to a <u>close link set</u>

for a larger number of <u>epochs</u>, and the <u>magnitude of velocity</u> is high and the

<u>velocity direction</u> is the same as the road link orientation, then the <u>resemblance</u>, Z,

of that link is high. The resemblance, Z, is computed empirically as:

$$Z = MF1 \times MF2 \times MF3 \times MF4 \qquad (5.4)$$

where

    MF1   is the DOM of nominal heading change,

    MF2   is the DOM of belongingness to close link set,

MF3   is the DOM for large number of epochs, and

MF4   is the DOM for magnitude of velocity.

Rule 2: If the <u>heading change</u> is nominal and the <u>health of solution</u> is good and a particular link is <u>close to the road segment</u> for a larger number of <u>epochs,</u> then the <u>resemblance,</u> Z, of that link is high. The <u>resemblance,</u> Z, is computed empirically as

$$Z = MF1 \times \frac{1.5}{(1 + \frac{1}{1 + 0.1 \times MF2})} \times MF3 \times MF4 \qquad (5.5)$$

where

MF1   is the DOM of a nominal heading change,

MF2   is the DOM of closeness to the road link,

MF3   is the DOM for large number of epochs, and

MF4   is the DOM for the health of a solution.

$$MF4 = MF5 \times MF6 \times MF7 \qquad (5.6)$$

where

MF5   is the DOM for a good HDOP,

MF6   is the DOM for large number of satellites, and

MF7   is the DOM for good signal strength.

A factor of 0.1 is multiplied with MF2 in Equation 5.5 to reduce the weight of position proximity. Rule 3 will be evaluated if the output from this rule exceeds an empirically-

derived threshold value of 0.7; otherwise this step is repeated until the resemblance exceeds the threshold value. In case of measurement domain approaches, the MF for large number of epochs is changed. The new MF assumes a value of unity after 2 seconds of initialization.

Rule 3: If the <u>heading change</u> is large and in the same direction as that of the concurrent link orientation, and the <u>resemblance</u> (as computed in Rule 1) for the next few epochs is highest for that <u>concurrent link,</u> then it will be considered as the first identified link.

After determining the first link, and locating the vehicle on it, the algorithm goes into tracking mode. If the vehicle loses the track (which is determined by criteria discussed below), then the whole first fix procedure (discussed above) is repeated before resending the algorithm to tracking mode. The two steps involved in the tracking mode sub-algorithm of the map matching framework are:

1) Tracking the correct road link

2) Determining the position of the vehicle on the identified road link.
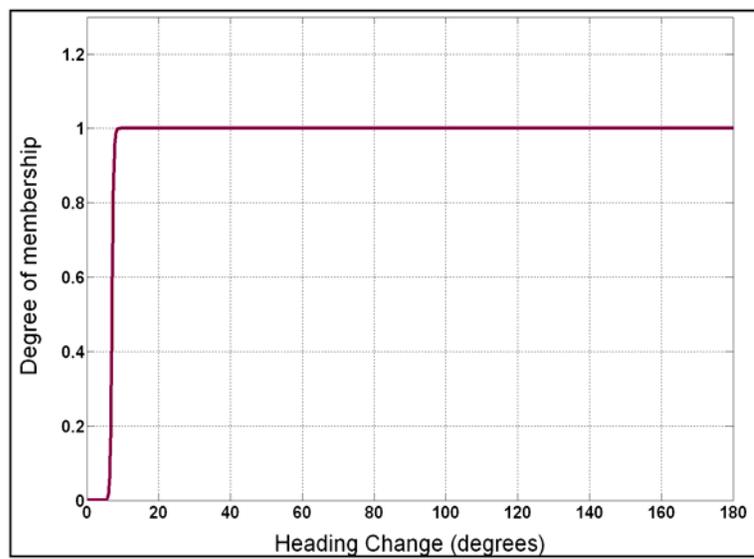
(a)
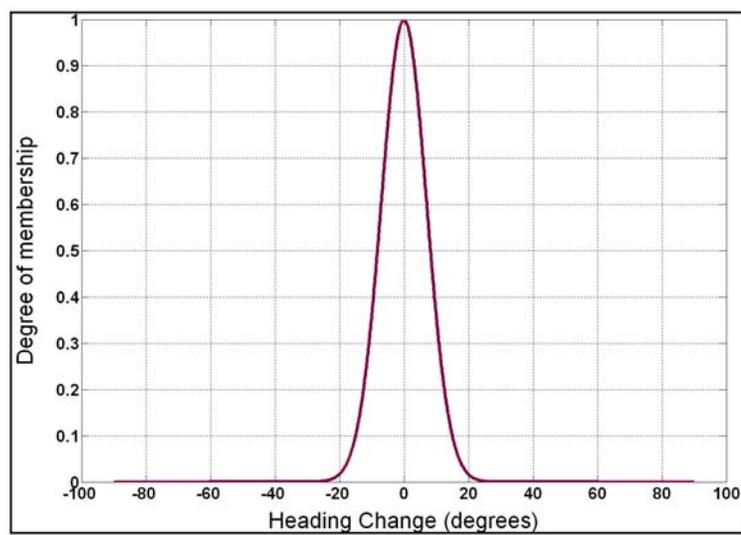
(b)
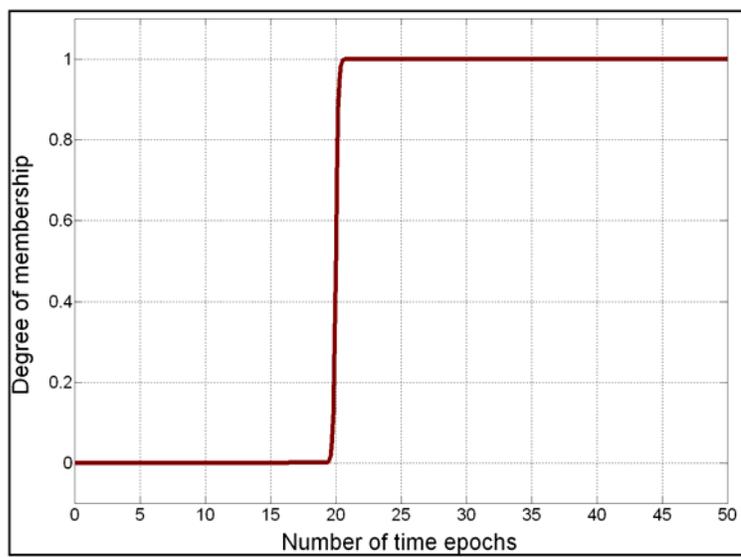
(c)
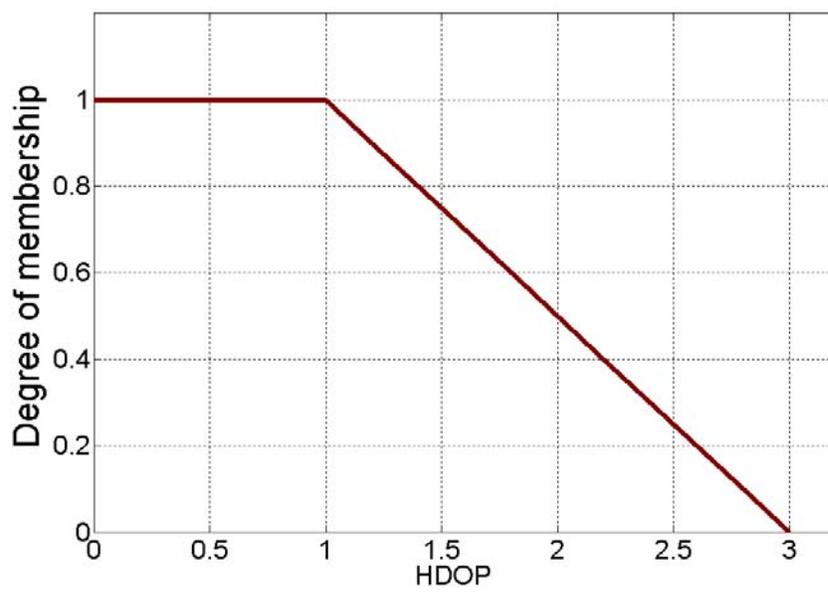
(d)
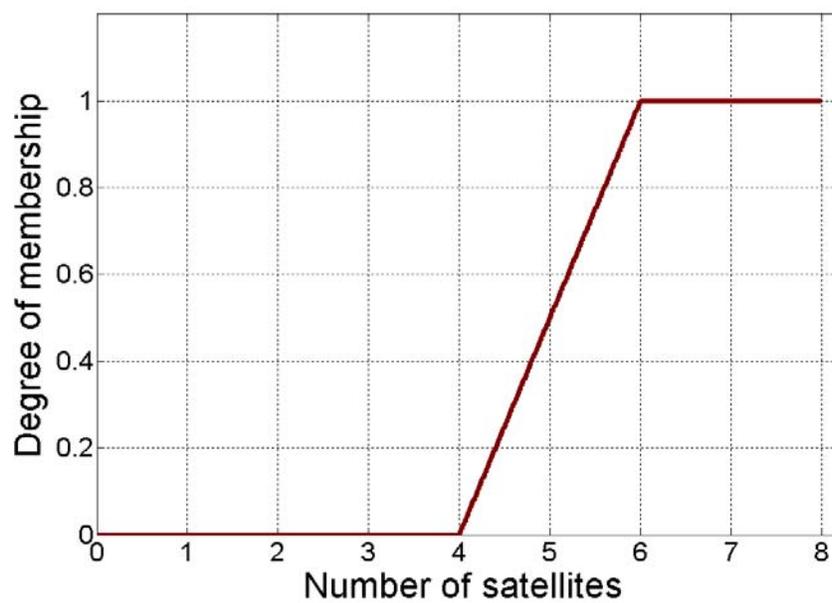
(e)
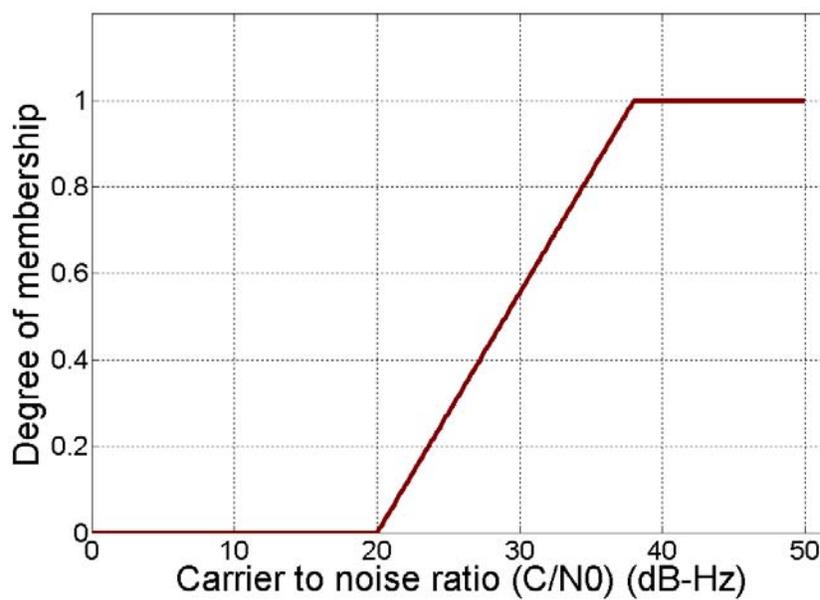
(f)
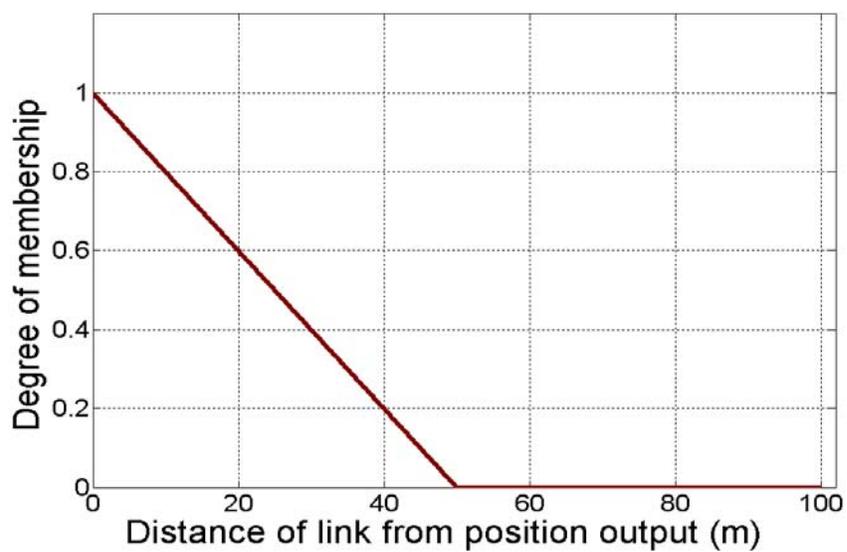
(g)
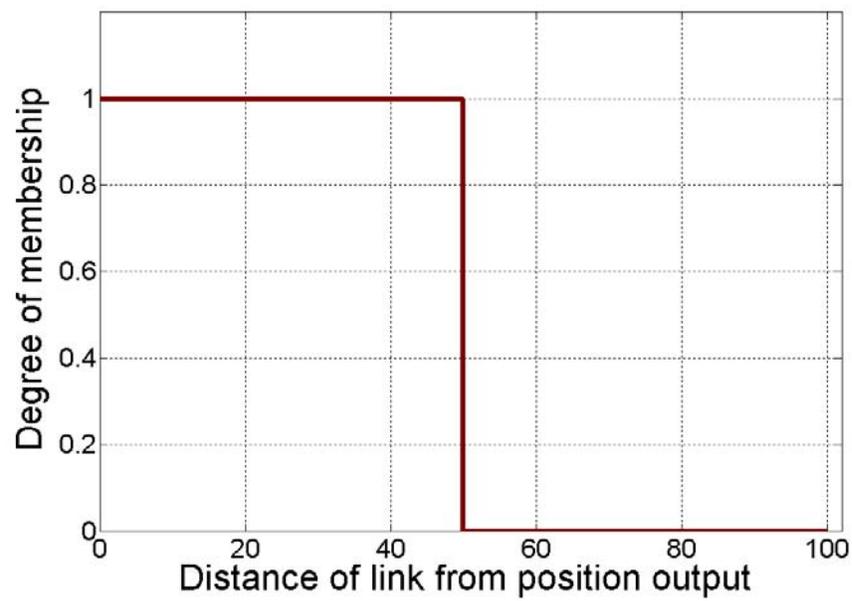
(h)
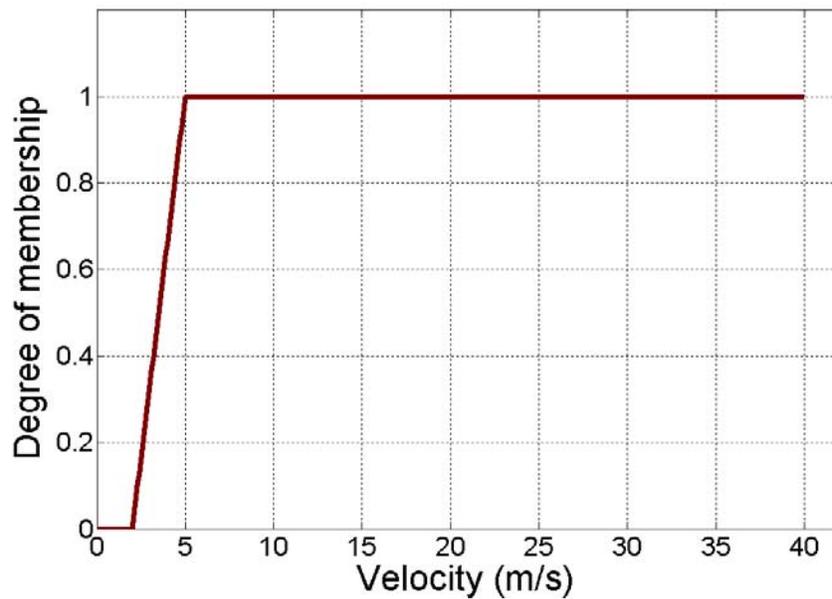
(i)

Figure 5.6: MF for a (a) Large Heading Change (b) Nominal Heading Change (c) Large Number of Epochs (d) Good HDOP (e) Large Number of Satellites (f) Good Signal Strength (g) Proximity of Position Solution from the Link (h) Close Link Set (i) Large Magnitude of Velocity

5.3.2 Tracking Mode Sub-Algorithm

The tracking mode involves the determination of the map matched solution by taking the history of motion into account. This road segment tracking is done using a modified Sugeno-type FIS.

The fuzzy inputs to this FIS are the same as that of the first fix FIS. The fuzzy sets in this case are:

1) Proximity of the position solution (to the link),

2) Small heading change,

3) Average distance traveled on the current link,

4) Large distance traveled on the current link, and

5) Small heading difference (which is defined as the difference between heading change and the angle between the current and concurrent link).

The MFs of the above mentioned fuzzy sets are shown in Figure 5.7. The fuzzy rules of the FIS are:

Rule 1: If the distance traveled on the current link is average and the <u>proximity of the position solution</u> to the current link is high and the <u>heading change</u> is small, then the <u>resemblance</u>, Z, of that link is high. The resemblance, Z, is computed empirically as

$$Z = MF1 \times \frac{1.5}{(1 + \frac{1}{1 + 0.1 \times MF2})} \times MF3 \tag{5.7a}$$

$$Z = MF1 \times MF2 \times MF3 \tag{5.7b}$$

where

MF1 is the DOM of the average distance traveled on the current link,

MF2 is the DOM of the proximity of the position solution to the current link, and

MF3 is the DOM of the small heading change.

The factor of 0.1 multiplied by MF2 in Equation 5.7a reduces the weight of position proximity. In the case of measurement domain approaches, Equation 5.7b

is used given that the distance of position from identified road segment is not as erratic as in the case of position domain approach. Rule 2 will be evaluated if the value of resemblance of the current link (obtained in Rule 1) falls below an empirically derived threshold value of 0.7.

Rule 2: If the <u>distance traveled on the current link</u> is large and the <u>heading difference</u> is small, then the <u>resemblance</u>, Z, of that link is high. The resemblance, Z, is computed empirically as

$$Z = MF_1 \times MF_2 \tag{5.8}$$

where

MF1　　is the DOM of the large distance traveled on the current link, and

MF2　　is the DOM of the small heading difference which is defined as the change in heading indicated by gyro and the angle between current link and concurrent link.
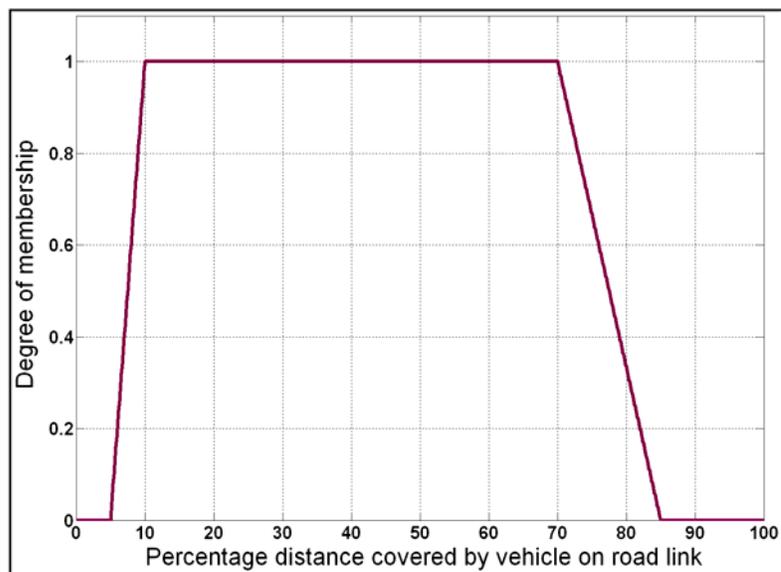
(a)
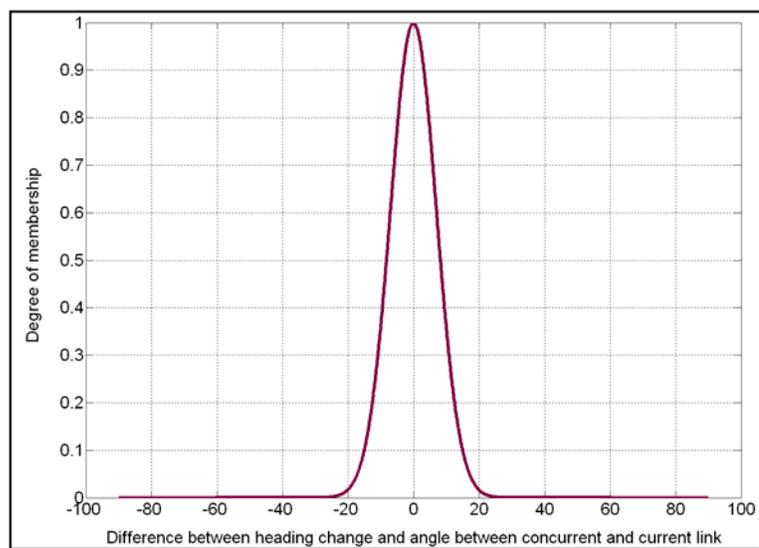
(b)
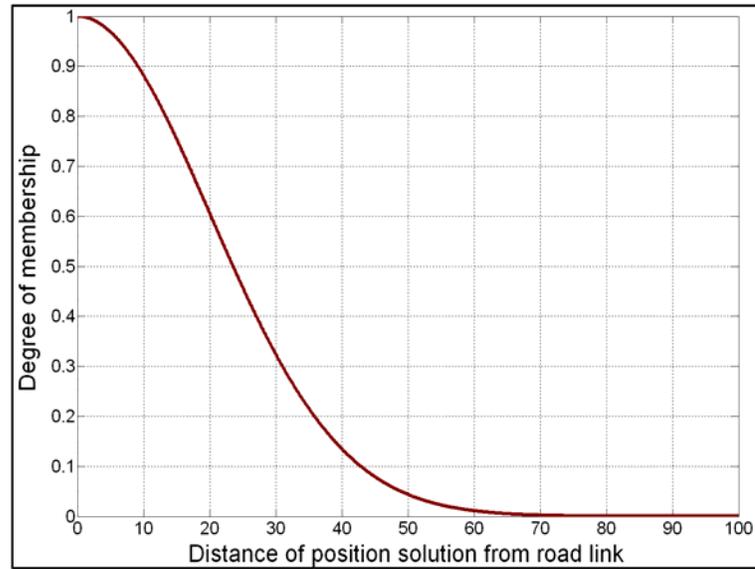
(c)
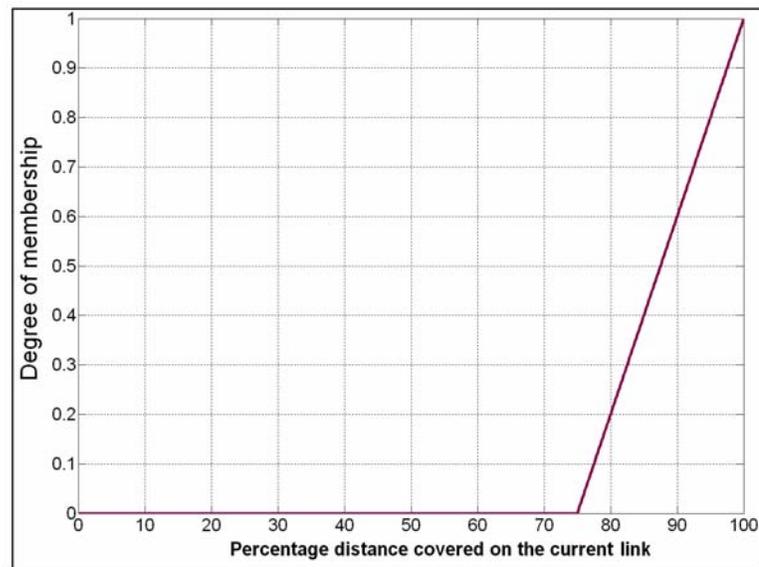
(d)

Figure 5.7: MF for an (a) Average Distance Traveled on Road Link (Percentage) (b) Small Heading Difference (c) Proximity of the Position Solution from the Link (d) Large Distance Traveled on Current Link (Percentage)
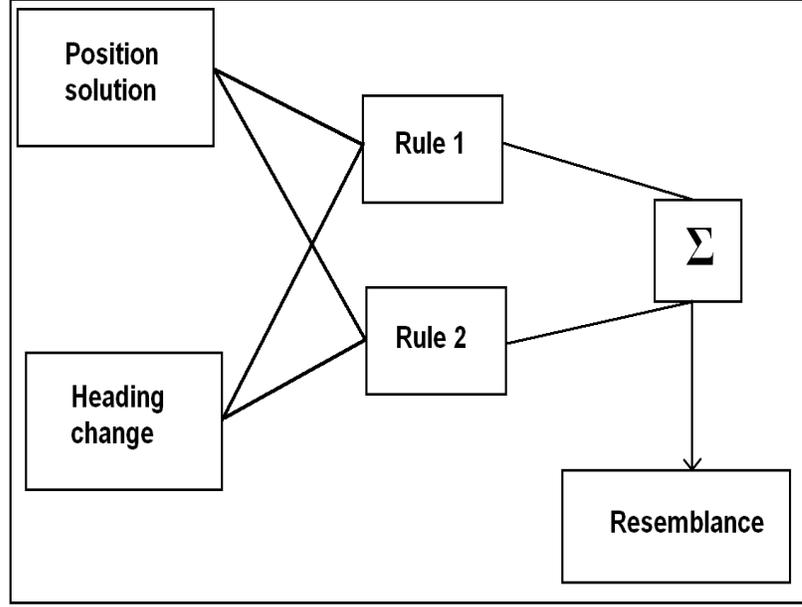
Figure 5.8: FIS for the Tracking Mode Sub-Algorithm

The position of the vehicle on the road segment, in the position domain approach, is computed by filtering the GPS-derived position with velocity (obtained from Doppler information) and directional aiding (obtained from the road link orientation) as given in Equation 5.9. The velocity propagated position component is underestimated by 2% to avoid along-track position overestimation. Similar position underestimation is employed in the MAGPS approach. Position determination in measurement domain approaches is discussed after the introduction of the MAGPS measurement model.

$$\vec{P}_{k,final} = (W \times pr(\vec{P}_{k,GPS})) + (1-W) \times (\vec{P}_{k-1,final} + 0.5 \times 0.98 \times (\vec{V}_k + \vec{V}_{k-1}))) \qquad (5.9)$$

$$W = \frac{0.5}{1+d} \qquad (5.10)$$

where

$\vec{P}_{k,final}$ is the map matched solution at the kth epoch,

$\vec{P}_{k,GPS}$ is the raw GPS position solution at the kth epoch,

$\vec{V}_k$ is the velocity component along the road link orientation at the kth epoch,

$pr(\vec{P}_{k,GPS})$ is the projection of $\vec{P}_{k,GPS}$ on the identified road segment,

W is the weight given to raw GPS position solution, and

d is the distance of $\vec{P}_{k,GPS}$ from the velocity-derived position along the identified road segment.

There is a mutual relationship between the identification of a road segment and the computation of the position solution. The identification of the correct link removes the error from the position output and helps to accurately determine the map-matched solution. This map matched solution, in turn helps to track the road segment in the next epoch. In case of measurement domain approaches, the identified road segment is extremely useful as it provides a constraint in the GPS measurement model. This will be discussed after the introduction of the MAGPS measurement model.

5.3.3 Loss of Vehicle Tracking

The system loses track of the vehicle position and goes to first fix mode when there are continuous outliers in the navigation solution and a turn is encountered amidst these

outliers. The system also loses track when it does not get outlier-free navigation output for 30 consecutive epochs (without any heading change). It can be seen from Figure 5.9 that continuous outliers restrict the optimality in computation of the map matched solution. This leads to an uncontrolled growth in the along-track position uncertainty. When this uncertainty grows to a level of 625 m^2, the algorithm cannot determine the destination point. This is because a vehicle can be off by one block along the road track due to this increased uncertainty. If a heading change is encountered amidst this situation the algorithm cannot distinguish the node as well as the conjugate road segment on which the vehicle has turned.
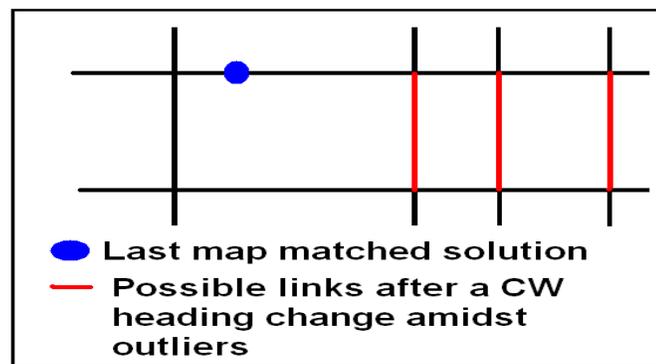
Figure 5.9: Loss of Track in the Proposed Algorithm

Loss of track in measurement domain approaches is based on the growth of uncertainty of the state vectors.

To summarize, the main characteristics of the proposed position domain algorithm are:

1) The time for the first fix on the road link depends upon the GPS initialization conditions.

2) A change in the road link is mainly identified by a heading change indicated by the gyro.

3) Heading information indirectly helps in position matching by identifying the correct road link. The link orientation along with the velocity magnitude is used for map matching the position output from GPS.

4) Long outages (or continuous outliers) lead to loss of track and the algorithm has to be reinitialized using the first fix mode.

5) The success of tracking a road link depends on the accuracy with which the map matched position is determined on the current link, and vice versa.

Some of the limitations of the proposed position domain approach are that:

1) Ambiguity in a road link selection at a "Y" intersection, since the heading measurement from gyro is not very accurate to identify the new road segment.

2) The algorithm takes a long time for initialization (typically about 1 minute), and requires the vehicle to be on one road segment during this time.

3) Consistent outliers lead to frequent loss of track.

To overcome some of these limitations, measurement domain algorithms are developed. These algorithms are more robust and have improved availability.

5.4 Map Aided Measurement Model

As discussed in Chapter 2, the road segments are assumed to be piecewise linear for map aiding. These linear segments are represented by the coordinates of end points. If (φ_1, λ_1) and (φ_2, λ_2) are the coordinates of the end point (as shown in Figure 5.10), then any point on the road segment (φ, λ) satisfies Equation 5.11. This constraint is used as an additional equation in the least squares model as shown in Equation 5.12. Outlier detection using standardized residual testing becomes very effective using this constraint as it is free of blunders.

$$(\lambda_1 - \lambda_2)\varphi + (\varphi_2 - \varphi_1)\lambda = (\lambda_1 - \lambda_2)\varphi_1 + (\varphi_2 - \varphi_1)\lambda_1 \qquad (5.11)$$

(φ1, Λ1)   (φ, Λ)   (φ2, Λ2)
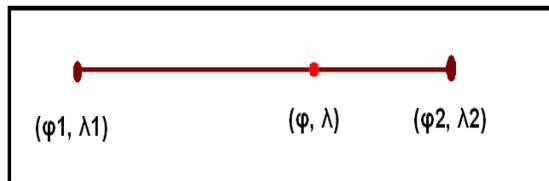
Figure 5.10: Piecewise Linear Representation of Road Segment

$$
\begin{bmatrix}
\Delta\rho_1 \\
\Delta\rho_2 \\
\cdot \\
\cdot \\
\cdot \\
(\lambda_1-\lambda_2)(\varphi_1-\varphi_{k,corr})+(\varphi_2-\varphi_1)(\lambda_1-\lambda_{k,corr})
\end{bmatrix}
=\mathbf{H}(\varphi_{k-1,corr},\lambda_{k-1,corr},h_{k-1,corr})
\begin{bmatrix}
\Delta\varphi_{k+1} \\
\Delta\lambda_{k+1} \\
\Delta h_{k+1} \\
\Delta^2 t_{k+1}
\end{bmatrix}
\qquad (5.12)
$$

where

$\Delta\rho_i$ is the pseudorange misclosure for i^{th} measurement corresponding to a given position and clock bias solution,

$\Delta\varphi_k$ is the correction to the latitude solution from k^{th} iteration,

$\Delta\lambda_k$ is the correction to the longitude solution from k^{th} iteration,

Δh_k is the correction to the height obtained from k^{th} iteration,

$\varphi_{k,corr}$ is the latitude solution obtained after applying corrections from k^{th} iteration,

$\lambda_{k,corr}$ is the longitude solution obtained after applying corrections from k^{th} iteration,

$h_{k,corr}$ is the latitude solution obtained after applying corrections from k^{th} iteration,

$\Delta^2 t_k$ is the correction to the receiver clock bias from k^{th} iteration, and

$\mathbf{H}(\varphi_k, \lambda_k, h_k)$ is the design matrix for GPS position computation after the kth iteration. This matrix is the Jacobian of the pseudorange measurement equation with last row given by Equation 5.11.

Additionally, if DEM information is used, then the model will have an additional constraint and the least squares model transforms to Equation 5.13.

$$
\begin{bmatrix}
\Delta\rho_1 \\
\Delta\rho_2 \\
\cdot \\
\cdot \\
(\lambda_1 - \lambda_2)(\varphi_1 - \varphi_{k,corr}) + (\varphi_2 - \varphi_1)(\lambda_1 - \lambda_{k,corr}) \\
f_{DEM}(\varphi_{k,corr}, \lambda_{k,corr}) - h_{k,corr}
\end{bmatrix}
= \mathbf{H}(\varphi_{k,corr}, \lambda_{k,corr}, h_{k,corr})
\begin{bmatrix}
\Delta\varphi_{k+1} \\
\Delta\lambda_{k+1} \\
\Delta h_{k+1} \\
\Delta^2 t_{k+1}
\end{bmatrix}
\quad (5.13)
$$

where $f_{DEM}(\varphi_k, \lambda_k)$ is the DEM mapping from the two dimensional coordinates to the height at that point.

If a constraint is imposed on the velocity to lie along a road segment direction, then the northing and easting components of the velocity should satisfy Equation 5.15. The resulting velocity measurement model is given by Equation 5.14.

$$
\begin{bmatrix}
\Delta\dot{\rho}_1 \\
\Delta\dot{\rho}_2 \\
\cdot \\
\cdot \\
\cdot \\
0 - \left(\dfrac{v_{n,k,corr}}{(\varphi_2 - \varphi_1)} - \dfrac{v_{e,k,corr}}{(\lambda_2 - \lambda_1)} \times k_{lat\,/\,long} \right) \\
0 - v_{u,k,corr}
\end{bmatrix}
=
\begin{bmatrix}
\mathbf{H}_{Doppler} \\
\overline{R}_1 \\
\overline{R}_2
\end{bmatrix}
\begin{bmatrix}
\Delta v_n \\
\Delta v_e \\
\Delta v_u \\
\Delta^2\dot{t}
\end{bmatrix}
\qquad (5.14)
$$

where

$\mathbf{H}_{Doppler}$ is the matrix relating pseudorange-rate misclosures to velocities and

   clock drift correction,

$\Delta\dot{\rho}_i$ is the pseudorange-rate misclosure for i^{th} measurement corresponding

   to a given velocity and clock drift solution,

Δv_n is the correction to velocity in the north direction,

Δv_e is the correction to velocity in the east direction,

Δv_u is the correction to velocity in the vertical direction,

$v_{n,k,corr}$ is the corrected north velocity after k^{th} iteration,

$v_{e,k,corr}$ is the corrected east velocity after k^{th} iteration,

$v_{u,k,corr}$ is the corrected vertical velocity after k^{th} iteration, and

$\Delta^2\dot{t}$ is the correction to receiver clock drift in m/s.

$\overline{R}_1$ and $\overline{R}_2$ are the condition equations which constrain the horizontal velocity

components along the road direction.

$$\overline{R}_1: \quad \frac{v_n}{(\varphi_2 - \varphi_1)} - \frac{v_e}{(\lambda_2 - \lambda_1)} \times k_{lat/long} = 0 \tag{5.15}$$

$$\overline{R}_2: \quad v_u = 0 \tag{5.16}$$

where $k_{lat/long}$ is the ratio of distance between unit change of longitude and unit change of latitude.

Each measurement/constraint used in the model has an associated variance, the details of which are given below:

1) The height measurement from DEM was given a variance of $10 \ m^2$.

2) The map constraint is given a variance of $2 \ m^2$.

3) The zero vertical velocity constraint was given a variance of $0.25 \ m^2/s^2$.

4) The variance of constraint $\overline{R}_1$ depends on the magnitude of vehicle velocity and is calculated by Equation (5.17). The relation is derived by assuming that the maximum difference between road orientation and velocity direction is 15 degrees.

$$\sigma^2 = (Max\{|\tan(\theta + 15) - \tan(\theta)|, |\tan(\theta - 15) - \tan(\theta)|\} \times |v|/3)^2 \tag{5.17}$$

where $Max(a, b)$ returns the maximum of a and b, and θ, is the orientation of the road segment.

5) The constraints and measurements are statistically independent of each other. Hence the cross-covariance values in the covariance matrix are zero.

6) The variance of pseudorange and Doppler measurements are computed by the model implemented in the C^3NAVG^{2TM} software, developed at University of Calgary (Petovello et al., 2000). The variance of XTrac's pseudorange measurements were magnified by a factor of 2 to account for the increased noise due to weak signal tracking.

The next two sections describe the MAGPS and MAGPS filtering approaches based on the measurement model discussed in this section.

5.5 MAGPS Approach: The Least Squares Algorithm

This algorithm uses the same map matching framework as described in Section 5.3. However, it differs in the computation of the navigation solution. The measurement models described in the previous section is used to compute the GPS navigation solution.

The basic steps in the computation of MAGPS navigation solution are as follows:

1) Solve for the position parameters using the GPS standard pseudorange model in first fix mode using least squares method. The standard pseudorange model is the measurement model discussed in Section 5.4 without the map/DEM constraints. In tracking mode however, the map (/DEM) constraint(s) are used in the position

computation. Outliers are detected using the separation of measurement approach discussed in Section 4.9.1. A key concept for multiple blunder detection, developed in this research, is the computation of *residual-in-abstentia*. The *residual-in-abstentia* for a PRN i, is defined as the sum of standardized residuals from all the other satellites, when PRN i is eliminated from the least squares computation. An example of outlier detection using separation of solution approach will be presented in the next chapter.

2) Obtain the velocity using a Kalman filter with:

    a) Constant velocity transition model given by Equation (5.18). The assumption is that the acceleration of the vehicle is band-limited white noise.

    b) The measurement model as discussed in Equation 5.14.

$$
\begin{bmatrix} v_n \\ v_e \\ v_u \\ \Delta \dot{t} \end{bmatrix}_{k+1} = \begin{bmatrix} v_n \\ v_e \\ v_u \\ \Delta \dot{t} \end{bmatrix}_{k} + \vec{\eta}_{k+1/k}
\tag{5.18}
$$

where $\vec{\eta}_{k+1/k}$ is the process noise for the transition of state vector from k to $(k+1)^{th}$ epoch

The process noise covariance is adapted using the innovation sequence method, as discussed in Section 4.7. The weight given to the innovation sequence in determining the

current process noise covariance in tracking mode (Equation 4.45, Section 4.6) depends on the distance of the previous position solution from the intersection. The higher the distance from the intersection, the higher the expected stationarity of the process, and higher the value of the weight w.

$$w = (x / |L_0|)$$ (5.19)

where

x is the distance from intersection, and

$|L_0|$ is the length of road segment.

The measurement noise variance from the sensors/constraint is as discussed in Section 5.4. The outliers are detected by the Chi-Square test discussed in Section 4.9.2. The resulting process noise covariance is increased by five times when a major heading change is reported by gyro (to reduce the weight of predicted state vector).

It should be noted that the constraints imposed by maps are never subjected to outlier testing as they are assumed to be "true" to the pre-stated level of uncertainty. Only the pseudorange and Doppler measurements are subjected to outlier testing.

Also, the outlier detection schemes for least squares computation and Kalman filtering are independent, in the sense that a satellite eliminated in the position computation may not be rejected in the velocity computation and this is often the case with the XTrac receiver. The Doppler measurements are fairly stable and have only a few outliers

compared to the pseudorange (code-phase) measurements. A possible explanation for this is that a Doppler measurement is less susceptible to multipath as compared to a pseudorange measurement.

The algorithm assigns suitable weights to the position solution and velocity propagated position solution depending on the variances of the computed solution. Also, since the position computation is more susceptible to magnification of errors due to the DOP and signal strength, the weight of the autonomous position solution is reduced suitably by these factors. This final position solution is computed as:

$$\vec{P}_{k+1,final} = W\vec{P}_{k+1,GPS} + (1-W)(\vec{P}_{k,final} + 0.5\Delta t_1 \times 0.98(\vec{V}_k + \vec{V}_{k+1})) \tag{5.20}$$

$$W = \left(\frac{\sigma_{GPS,vel}}{\sigma_{GPS,pos}}\right)^2 \times 10^{(C/N_0-35)/10} \times \frac{1}{(1+HDOP)^2} \quad \text{if } (C/N_0 < 35dB-Hz) \tag{5.21a}$$

$$= \left(\frac{\sigma_{GPS,vel}}{\sigma_{GPS,pos}}\right)^2 \times \frac{1}{(1+HDOP)^2} \quad \text{if } (C/N_0 > 35dB-Hz) \tag{5.21b}$$

where

$\vec{P}_{k,GPS}$ is the position solution vector obtained from pseudorange computation at k^{th} epoch,

$\vec{P}_{k,final}$ is the map matched position solution vector obtained at k^{th} epoch,

$\vec{V}_k$ is the Kalman filter derived GPS velocity,

C/N_0 is the average carrier to noise ratio of the outlier-free satellite measurements, and

Δt_1 is the sampling interval.

When an outlier-free position solution from the pseudorange is not computed (i.e. when the number of outlier-free pseudorange measurements is less than two with DEM/map information, or less than three with only map information), then the position is propagated solely by the Kalman filter-derived velocity solution.

5.6 MAGPS Filtering: A Centralized Kalman Filtering Approach

This section describes the last of the three approaches developed during this research. This approach is based on a centralized Kalman filtering concept (i.e. processing all the measurement and constraints in one single filter). The algorithm uses the same map matching framework as discussed in Section 5.3 and differs only in computation of navigation solution. The first fix sub-algorithm is identical to the MAGPS approach.

The measurement model is obtained by combining the position and velocity measurement models discussed in Section 5.4.

$$
\begin{bmatrix}
\Delta\rho_1 \\
\cdot \\
\Delta\rho_2 \\
\cdot \\
\cdot \\
\cdot \\
(\widehat{\lambda}_1 - \widehat{\lambda}_{k,corr})\widehat{\varphi}_1 + (\widehat{\varphi}_1 - \widehat{\varphi}_{k,corr})\widehat{\lambda}_1 \\
f_{DEM}(\varphi_k,\lambda_k) - h_{k,corr} \\
\Delta\dot{\rho}_1 \\
\Delta\dot{\rho}_2 \\
\cdot \\
\cdot \\
0 - \left(\dfrac{v_{n,k,corr}}{(\varphi_2 - \varphi_1)} - \dfrac{v_{e,k,corr}}{(\lambda_2 - \lambda_1)} \times k_{lat/long} \right) \\
0 - v_{u,k,corr}
\end{bmatrix}
=
\begin{bmatrix}
\mathbf{H}(\varphi_k,\lambda_k) & \overline{0} \\
\overline{0} & \mathbf{H}_{Doppler} \\
\overline{0} & \overline{R}_1 \\
\overline{0} & \overline{R}_2
\end{bmatrix}
\begin{bmatrix}
\Delta\varphi_{k+1} \\
\Delta\lambda_{k+1} \\
\Delta h_{k+1} \\
\Delta^2 t_{k+1} \\
\Delta v_{n,k+1} \\
\Delta v_{e,k+1} \\
\Delta v_{u,k+1} \\
\Delta^2 \dot{t}_{k+1}
\end{bmatrix}
+ \vec{\eta}_m
$$

(5.22)

where $\vec{\eta}_m$ is the measurement noise, and all the other terms have the same meaning as in Section 5.4.

A constant velocity transition model is used for this filter. This is based on the assumption that the acceleration is a band limited white noise. The measurement model is given by Equation 5.23.

$$
\begin{bmatrix} \varphi \\ \lambda \\ h \\ \Delta t \\ v_n \\ v_e \\ v_u \\ \Delta \dot{t} \end{bmatrix}_{t_{k+1}} = \begin{bmatrix} 1 & 0 & 0 & 0 & 1/R_M(\varphi_k,\lambda_k) & 0 & 0 & 0 \\ 0 & 1 & 0 & 0 & 0 & 1/R_T(\varphi_k,\lambda_k) & 0 & 0 \\ 0 & 0 & 1 & 0 & 0 & 0 & 1 & 0 \\ 0 & 0 & 0 & 1 & 0 & 0 & 0 & 1 \\ 0 & 0 & 0 & 0 & 1 & 0 & 0 & 0 \\ 0 & 0 & 0 & 0 & 0 & 1 & 0 & 0 \\ 0 & 0 & 0 & 0 & 0 & 0 & 1 & 0 \\ 0 & 0 & 0 & 0 & 0 & 0 & 0 & 1 \end{bmatrix} \begin{bmatrix} \varphi \\ \lambda \\ h \\ \Delta t \\ v_n \\ v_e \\ v_u \\ \Delta \dot{t} \end{bmatrix}_{t_k} + \vec{\eta}_t \qquad (5.23)
$$

where

$R_M(\varphi_k,\lambda_k)$ is the meridian radius of curvature of earth at (φ_k,λ_k),

$R_T(\varphi_k,\lambda_k)$ is the transverse radius of curvature of earth at (φ_k,λ_k), and

$\vec{\eta}_t$ is the transition noise.

The measurement noise covariance matrix is formed by the values discussed in Section 5.4. The process noise covariance is adapted using the innovation sequence as in the case of Kalman filter discussed in Section 5.5. The process noise covariance matrix is magnified by a factor of five when a major heading change is reported by the gyro.

During the first fix mode, the map constraint is not used in the MAGPS approaches, as a road segment is not identified. The constraints in the measurement model are imposed only in tracking mode for the computation of navigation solution.

5.7 Small Road Segments

All the above algorithms assume that the road segments are long enough to contain the vehicle position in the next epoch. If the road is curved then the piecewise representation of the map tries to define it by breaking it into a number of small linear segments. Some of these segments may be as short as 7 m. If a vehicle is moving with a speed of 20 m/s then this road segment gets crossed in one second and therefore should not be used in the measurement model. Although such situations are rare in downtown Calgary, the tracking algorithm is devised to handle such situations.

If the length of the road segment is smaller than the product of the velocity and time difference, then the algorithm searches for the next concurrent road segment. It then subtracts the length of the smaller segments from the velocity-derived distance in determining the next road link and vehicle location in the next epoch.

CHAPTER 6: RESULTS AND DISCUSSION

This chapter describes the results obtained from the three tests performed during this research to validate the proposed algorithms. Section 6.1 describes the test conditions and equipment set up. Section 6.2 describes the geometric algorithm followed by analysis of the first test. The objective of this is to compare the fuzzy logic-based position domain algorithm against the conventional type of geometric map matching. Section 6.3 describes the second test, which compares the results obtained using position domain algorithm and MAGPS approach. This section also discusses the effect of height aiding from a DEM in the least squares model and a simulation test to demonstrate the effectiveness of the proposed approach in identifying outliers. Section 6.4 compares MAGPS filtering with the MAGPS approach and position domain approach. In addition to the field test, this section describes a simulation test (zero velocity test) to validate the performance of the proposed filtering approach. The main reason for carrying out tests in simulation is to overcome the limitations of true reference solution. Section 6.5 concludes the chapter with remarks about the performances of different approaches.

6.1 Test Description

Three field trials were conducted in downtown Calgary in urban canyon conditions. The test trajectories were selected to have high rise buildings on the road side along with several turns. The duration of these tests varied from 20 to 25 minutes. Many of these

turns have underpasses which created severe signal availability problems for testing the system in harsh conditions. Figure 6.1 shows a picture of downtown Calgary. The downtown core has moderate to severely signal degraded conditions with a variety of tall buildings ranging from 40 m to 200 m. Figure 6.2 shows the C/N_0 values obtained from SiRF XTrac receiver in Test-1. This figure shows the high sensitivity of the XTrac receiver and the effect of attenuation and multipath on the signal strength which causes it to fluctuate. It also shows the tracking of echo only signal such as PRN 4. The across-track position error characteristics during the three tests are shown in Table 6.1.
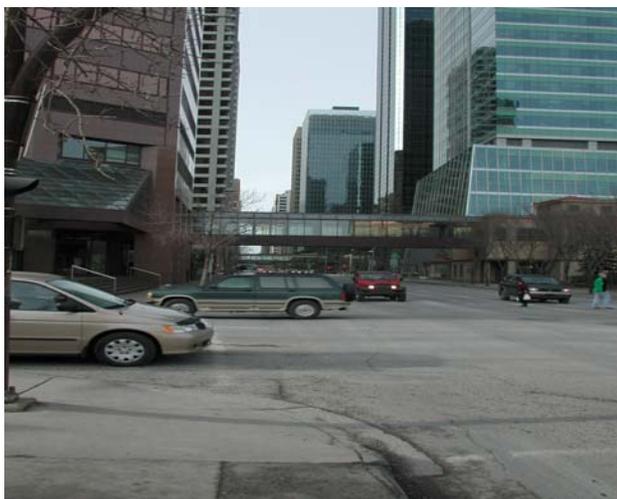
Figure 6.1: Urban Canyon Conditions for Field Tests

A GPS reference station was set up on the roof of the CCIT building at the University of Calgary for differential corrections. The equipment setup in the test van is as shown in Figure 6.3.

Two receivers (NovAtel OEM4 and SiRF XTrac) were used for data collection in order to make a comparison between their performances. NovAtel OEM4 is a geodetic grade receiver whereas the SiRF XTrac is an HS GPS receiver (Collin et al., 2003). The sensitivity of the XTrac receiver is observed to be 15 dB higher than the conventional OEM4 receiver (MacGougan, 2003). A NovAtel 600 antenna was placed on top of the van and connected to two receivers using a signal splitter. GPS data was logged at 1 Hz from both the receivers. A Murata gyro was mounted vertically with its sensitive axis pointing in the vertical direction to measure the heading changes. The maximum offset drift of the gyro is 9 deg/s (Murata, 1999). The data was sampled at 100 Hz from the Murata gyro using the LabView 7.0 software. The gyro output was passed through a third order low-pass Butterworth filter (with a cut off frequency of 0.25 Hz) to remove the noise due to vibrations and voltage fluctuations. Figure 6.4 shows the gyro output after using a low-pass filter. The spikes in the plot indicate a large change in heading and are used to detect the turns taken by the vehicle.

A two dimensional map supplied by the City of Calgary was used for the analysis. The centre line accuracy is about 5-10 m with 90% confidence. The DEM information was obtained from National Resources Canada (NRCAN) and has an accuracy of about 10 m for a contour interval of 10 m with a 90% confidence.
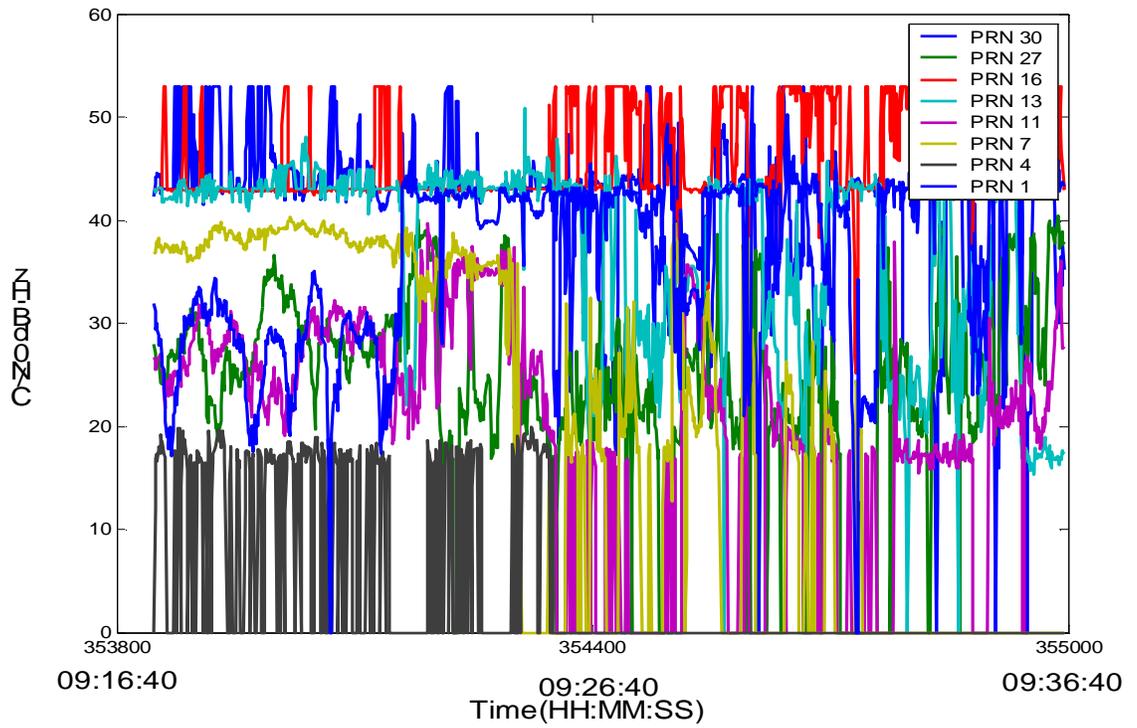
Figure 6.2: Carrier-to-Noise Ratio in Field Test-1
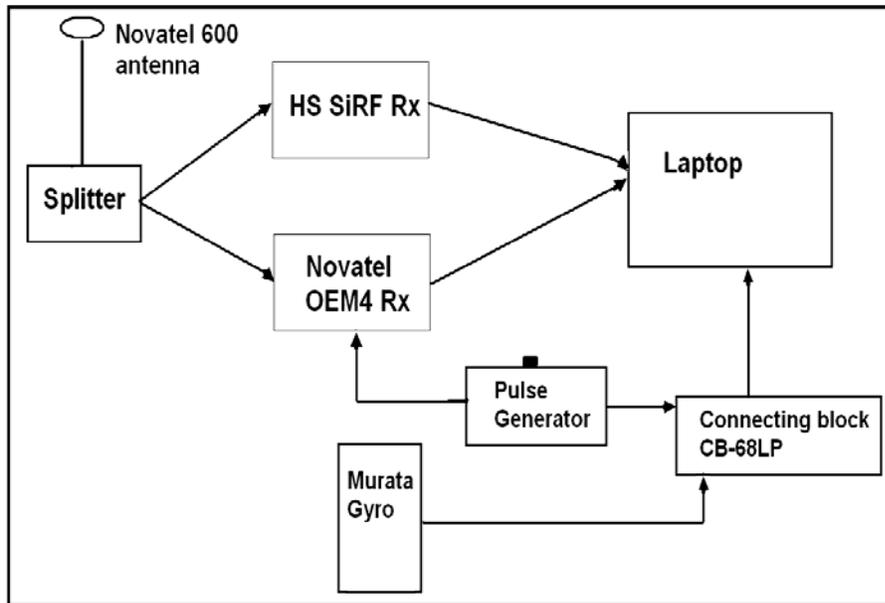
Figure 6.3: System Setup for the Test
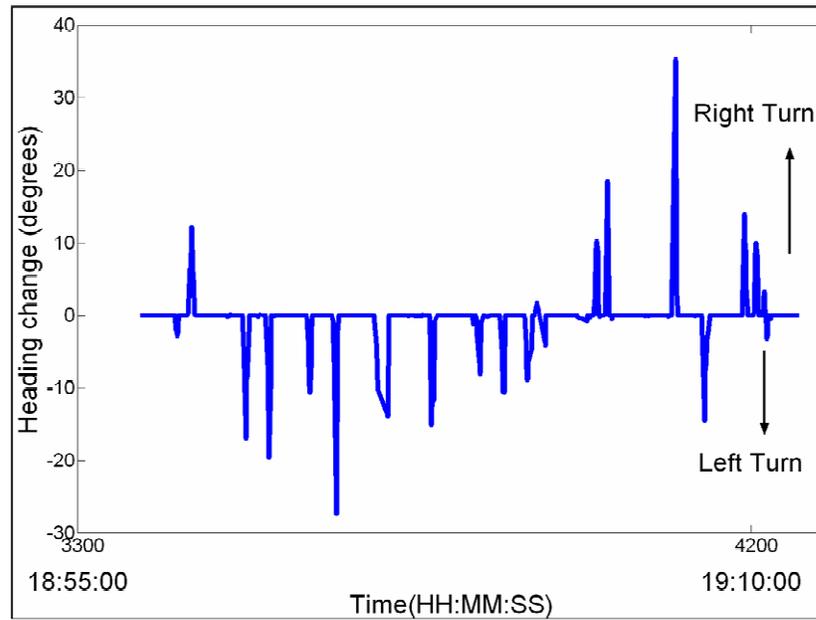
Figure 6.4: The Heading Output from Gyro after Filtering

Table 6.1: Across-Track Position Error Statistics

Receiver	Solution type	Maximum error(m)	Median error (m)
NovAtel OEM4	Internal	583.8	34.7
	LSQ	673.3	54.8
SiRF XTrac	Internal	189.3	23.8
	LSQ	520.4	56.1

6.2 Test-1: A Comparison Between the Fuzzy Logic-Based Position Domain Approach and Conventional Geometric Approach

This section describes the results obtained using the position domain algorithm and compares it with the conventional geometric approach. The navigation solution set used for analysis are (a) internal solution from the two receivers (XTrac and OEM4) and (b) the corresponding least squares solution obtained from C^3NAVG^{2TM} software (LSQ solution).

The geometric approach used in this analysis is based on pure geometric conditions. This type of technique works seamlessly with accurate navigation solution, and is representative of the conventional map matching techniques, although the full implementations of conventional techniques may be slightly advanced. This algorithm decides the road link on which the vehicle is travelling depending on the proximity of road link and the similarity in the direction of GPS velocity and the road link orientation. It does not take into account the history of motion and decides the road link depending on the information available from the instantaneous navigation solution. An unfixed solution in this case is obtained when the velocity direction does not match with any road segments which are close to the position solution.

6.2.1 GPS Solution Availability

This section describes the availability of the GPS solution from Test-1. The availability statistics of this test are similar for all the tests and will not be discussed in subsequent section for the sake of brevity. An average of 6 or 7 satellites were tracked by the XTrac receiver, whereas the average number of satellites tracked by the OEM4 was 4 to 5. The LSQ solution was obtained from the OEM4 and XTrac receivers in post-processed, differential mode using C^3NAVG^{2TM}, a software package developed at the University of Calgary. This software processes pseudorange and Doppler measurements using a Least Squares method (Petovello et al., 2000). The internal solutions from both the receivers were obtained in real-time without any differential corrections. The internal solution and the LSQ solution availability statistics from both receivers are shown in Table 6.2 and in Figure 6.5.

Table 6.2: Availability of Position Solution in Test-1 from NovAtel OEM4 and SiRF XTrac Receiver

Receiver	Internal solution availability (%)	LSQ solution availability (%)
NovAtel OEM4	78.0	46.8
SiRF XTrac	99.2	97.6
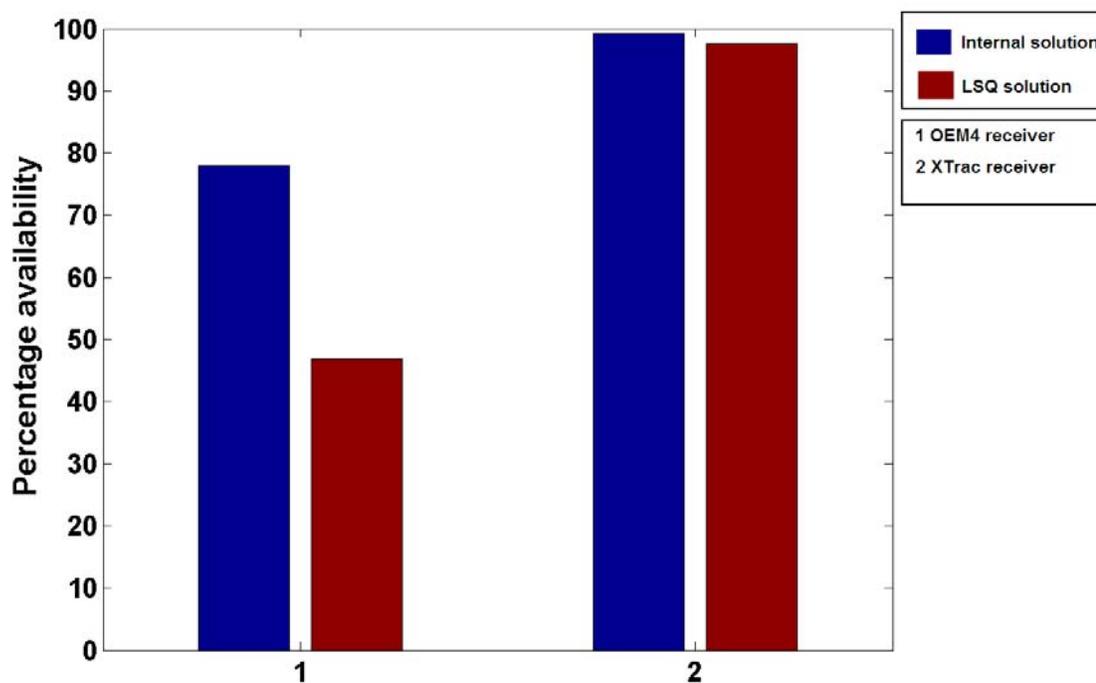
Figure 6.5: Graphical Representation of GPS Solution Availability in Test-1 from NovAtel OEM4 and SiRF XTrac Receivers

The following observations are made from Table 6.2 and Figure 6.5 about the availability of position solution:

1) In the case of the OEM4 receiver, the availability of the LSQ solution is significantly lower than the corresponding internal solution because C^3NAVG^{2TM} software imposes DOP constraint (of GDOP < 20) in the position computation. The number of satellites tracked by the OEM4 receiver is four for about 60% of the time. Also, since the test was conducted in urban canyon conditions which have visible satellites only at high elevations, the GDOP was above 20 for many epochs, leading to the rejection of solution.

2) The position errors in both the OEM4 solutions are large as compared to XTrac solutions as shown in Figure 6.6(a). This is due to the fewer number of satellites and poor geometry leading to magnification of range errors.

3) The availability of both the XTrac solutions is high due to its enhanced sensitivity which allows it to track a higher number of satellites. The XTrac's position outputs are shown in Figures 6.6(b) and 6.6(c) respectively.

4) XTrac's internal solution, which is obtained in single point mode (in real-time), is very smooth and has low errors for most of the time. However it has a continuous position drift for few epochs leading to large position errors during that interval.
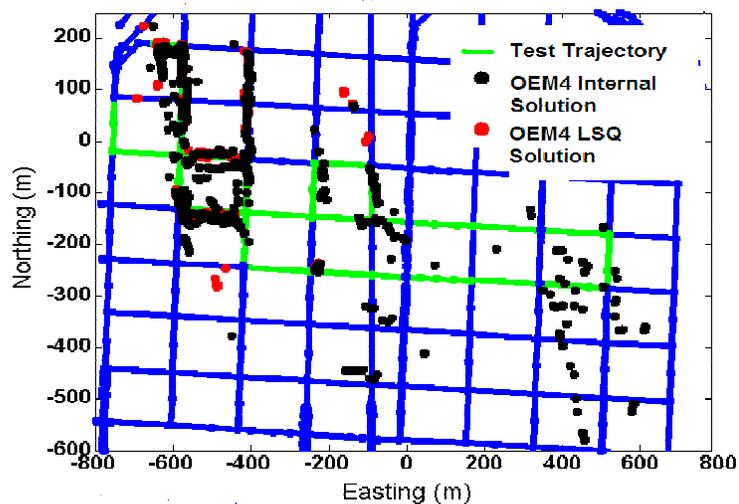
(a)
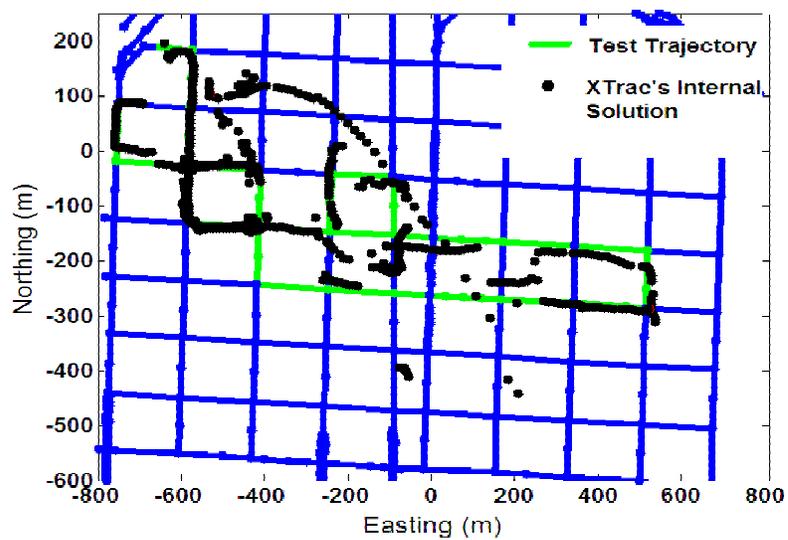
(b)
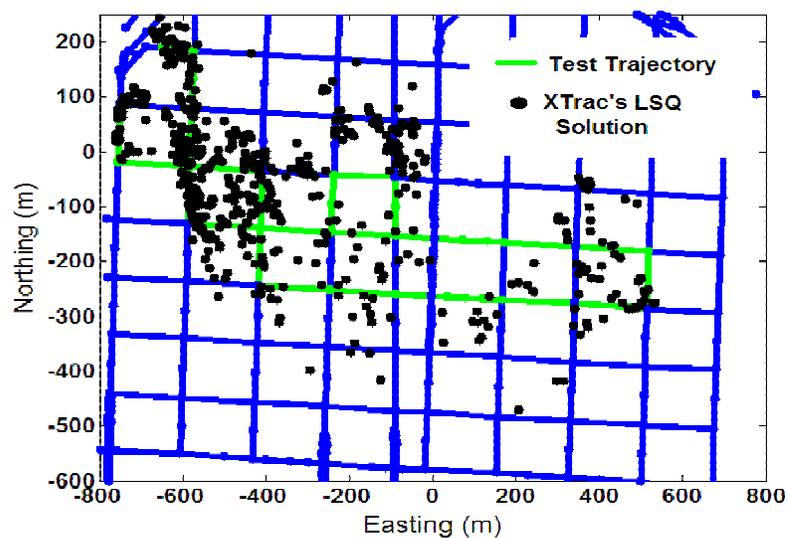
(c)

Figure 6.6 : The Position Output in Test-1 from (a) XTrac's Post-Processed LSQ DGPS Solution (b) XTrac's Real-Time Internal Solution (Without Differential Corrections) (c) OEM4's Real-Time Internal Solution (Without Differential Corrections) and Post-Processed DGPS LSQ Solution

6.2.2   Map Matching Results

XTrac's LSQ solution will be used in this section for illustrating the first fix sub-algorithm. The first fix is obtained using the fuzzy logic-based sub-algorithm discussed in Section 5.3.1. Figure 6.7 shows the close links set for the first 30 epochs after the heading output becomes steady. If the heading output is unsteady immediately after the start, then the vehicle is considered to be off the road. In this case, for all the initial epochs, the first correct link belongs to the set of close links. One of the assumptions in the position domain approach is that it assumes that the position errors decorrelate with time, and that the vehicle stays on the same link during the first fix mode.
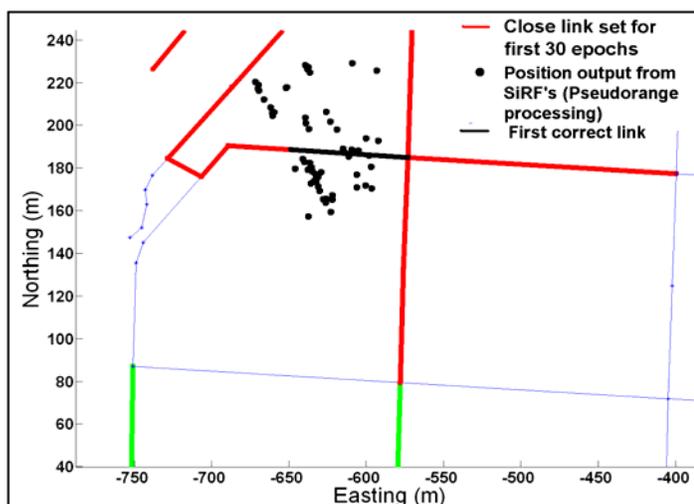
Figure 6.7: Close Links Set for the First 30 Epochs with XTrac's LSQ Solution in Test-1

The direction determined from velocity helps to identify the correct first link. Figure 6.8 shows the velocity direction for the first few epochs after the heading output becomes

steady. The first link is confirmed by the FIS when the change in velocity direction and heading corresponds to one of the concurrent links.
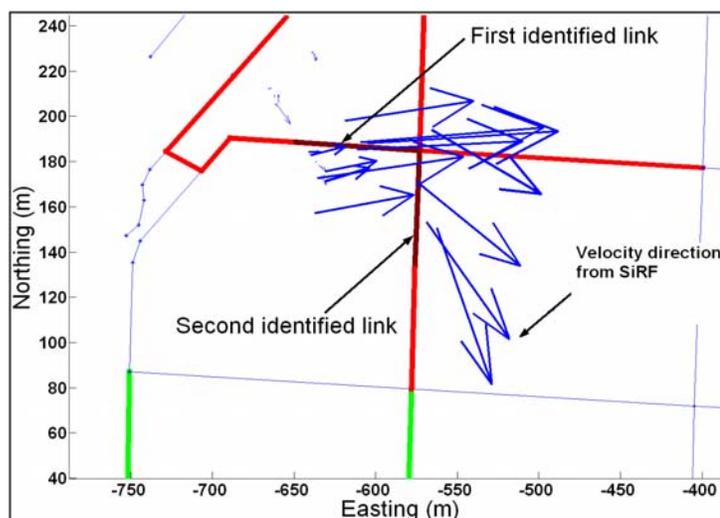
Figure 6.8: Velocity Direction for the First Few Epochs with XTrac's LSQ Solution in Test-1

Since the aim of a map matching algorithm is to locate the vehicle on the correct road, its performance can be assessed in terms of number of correct and false fixes on the road segment. The *percentage correct/false fixes* for a particular type of solution is defined as the number of correct/incorrect fixes on the road segment out of total number of test epochs for which the corresponding solution was available. An unfixed solution is when the algorithm does not match the position solution to any road segment. The percentage correct fix obtained from all the four solutions is shown in Table 6.3 and Figure 6.9. Figure 6.10 shows the map matched output obtained by using the proposed position domain algorithm. The percentage false fix is zero in all the cases.

Table 6.3: Performance of the Proposed Fuzzy Logic-Based Position Domain Algorithm in Test-1

Receiver	Internal solution		LSQ solution	
	Correct fix (%)	False fix (%)	Correct fix (%)	False fix (%)
NovAtel OEM4	23.7	0	11.1	0
SiRF XTrac	84.5	0	92.8	0
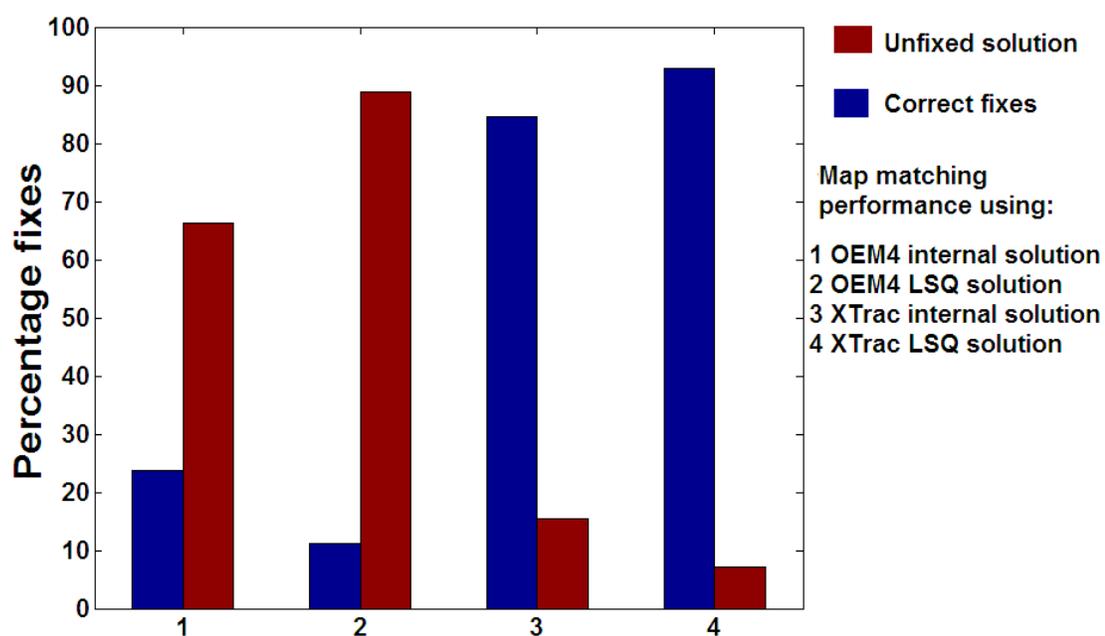
Figure 6.9: Graphical Representation of the Performances of the Proposed Fuzzy Logic-Based Position Domain Algorithm in Test-1

(a)

(b)

(c)
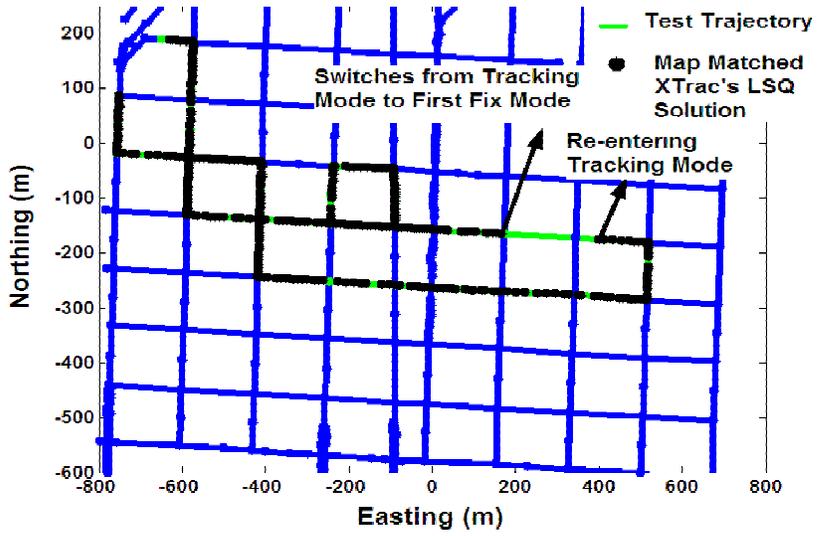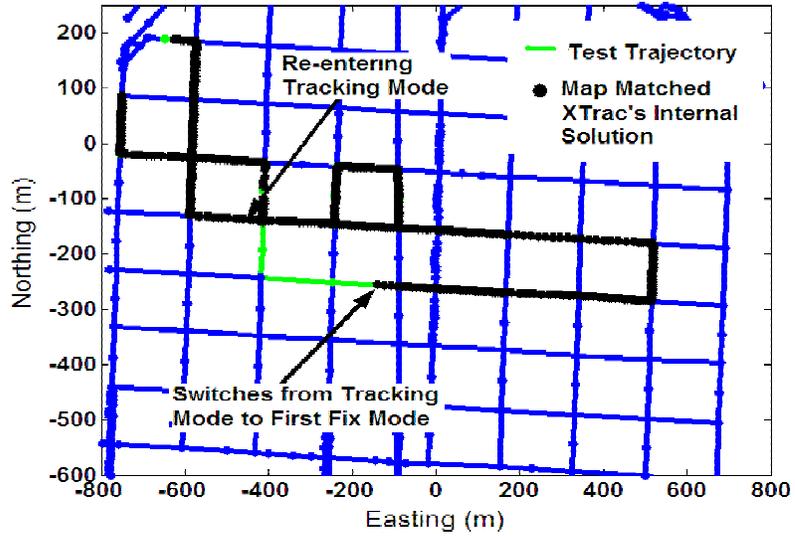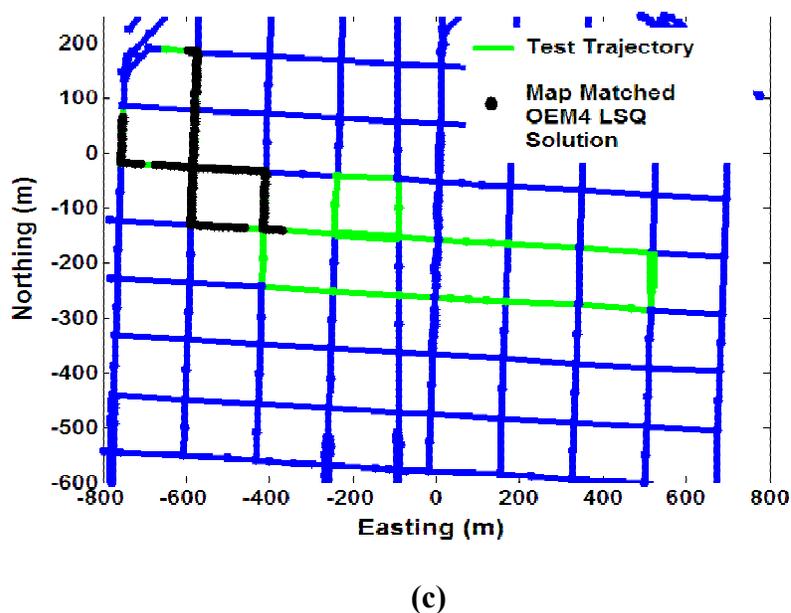
Figure 6.10: Map Matched Position Output in Test-1 Using the Proposed Fuzzy Logic-Based Position Domain Algorithm with (a) XTrac's LSQ Solution (b) XTrac's Internal Solution (c) OEM4's Solutions

The following observations are made from Table 6.3 and Figure 6.9 regarding the performance of the proposed map matching algorithm:

1) In the case of XTrac receiver, the internal solution has a lower percentage correct fix as compared to the LSQ solution because of the continuous position drift in the internal solution. The position drift is defined as the error in position propagation due to a change in the velocity direction. This is considered as an outlier by the proposed algorithm. The LSQ solution is noisy but does not have a continuous position drift problem as in the case of the internal solution. Figure 6.10(a) and 6.10(b) show the map matched outputs using the position domain algorithm with the XTrac's LSQ solution and internal solution, respectively.

There is a loss of track at one time in each case. While the loss of track with the XTrac's internal solution is due to a continuous position drift, the LSQ solution had the problem of continuous outliers which are not detected by the GPS least squares processing.

2) Unfixed solutions in the position domain algorithm arise when it loses track of the position and re-enters the first fix mode. Since the percentage false fix is zero using the proposed position domain algorithm, the unfixed solution percentage is obtained by subtracting the percentage correct fix from hundred.

3) In the case of OEM4 internal solution, the percentage correct fix is very low because of sporadic availability of the noisy internal solution which cannot be map matched using the position domain algorithm. The LSQ solution of the OEM4 is more sporadic and noisy to be map matched by the proposed algorithm and hence the percentage correct fix is the lowest of all. Figure 6.10(c) shows the map matching results obtained using the OEM4 internal solution. The algorithm in this case could map match the position only for a few epochs in good signal availability conditions.

Table 6.4 and Figure 6.11 shows a comparison between the results obtained from the proposed algorithm and a map matching algorithm based on a pure geometric approach. Figure 6.12 shows the map matched output obtained using the geometric map matching approach.

**Table 6.4: Performances of Proposed Fuzzy Logic-Based Position Domain
Algorithm and a Pure Geometric Map Matching Algorithm in Test-1**

Solution Mode	Proposed Position Domain algorithm			Geometric algorithm		
	Correct fix (%)	FalseFix (%)	Unfix (%)	Correct fix (%)	Falsefix (%)	Unfix (%)
XTrac internal	84.5	0	15.5	77.2	15.1	7.7
XTrac LSQ	92.8	0	7.2	27.1	29.8	43
OEM4 internal	23.7	0	76.3	56.1	21.3	22.6
OEM4 LSQ	11.1	0	88.9	13.3	16.7	70
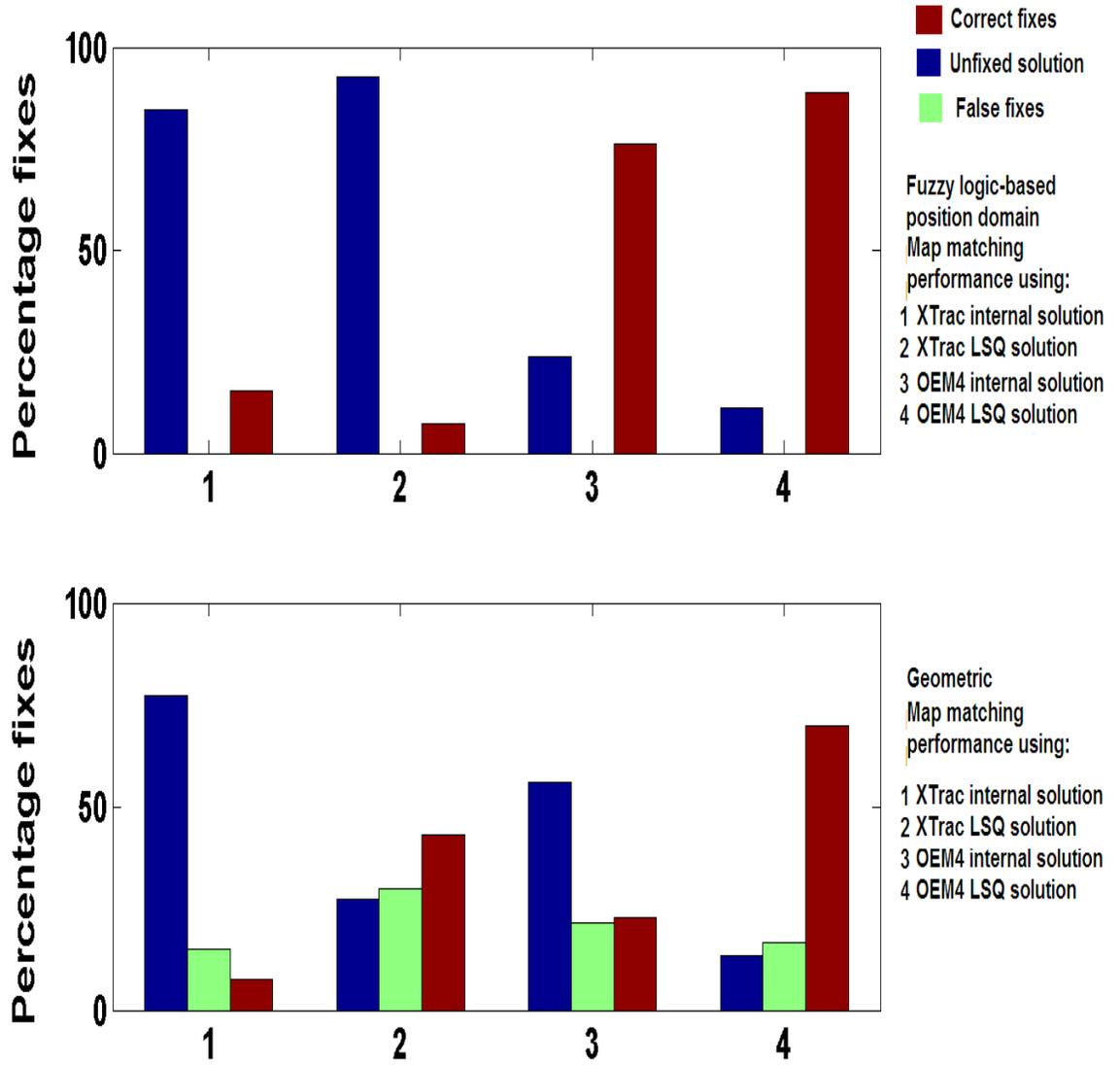
Figure 6.11: Graphical Representation of the Performance of Proposed Fuzzy Logic-Based Position Domain Algorithm and a Pure Geometric Map Matching Algorithm in Test-1
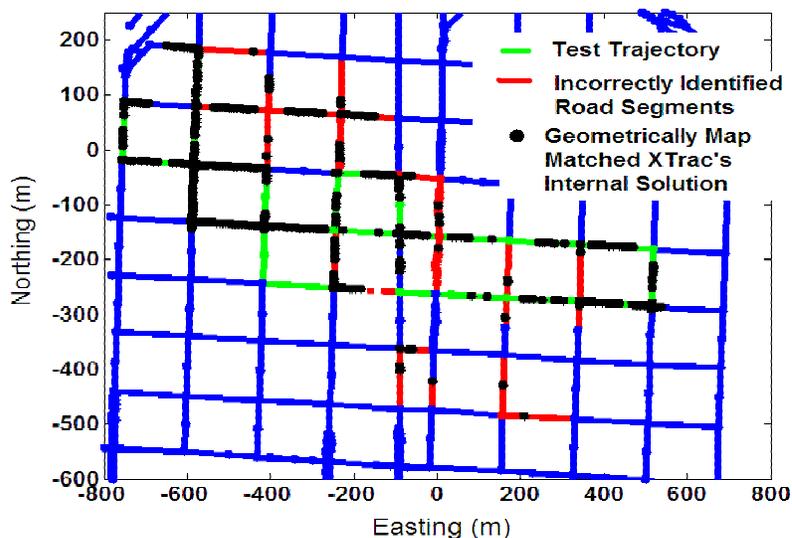
Figure 6.12: Map Matched XTrac's Internal Solution Obtained Using the Geometric Approach in Test-1

The following observations are made from Table 6.4 and Figure 6.11 about the performance of different map matching algorithms:

1) The XTrac's internal solution matches better than all of the other solution sets with the geometric map matching approach. This is because it has the least noise among all the available solutions. Less noise in the solution means a better match with the road segment if the solution is geometrically near to the identified road segment. With an increase in noise, the geometric approach identifies incorrect road segments, which in many cases are parallel to the true road segments. This is because the velocity direction remains fairly stable as compared to noisy pseudorange measurements. The continuous GPS solution drift in the XTrac's internal solution leads to a failure of the geometric algorithm in that area. Also,

the LSQ solutions are worse than the corresponding internal solutions for both the receivers because of the increased noise.

2) In case of both the OEM4 solutions, the percentage correct fix obtained by the geometric algorithm is higher as compared to that obtained by the proposed algorithm. This is because the proposed algorithm gives more weight to reliability as opposed to the geometric algorithm, which instantaneously decides the current road link. It should be noted that the percentage false fix from the proposed algorithm is zero, whereas it is significant in the case of geometric algorithm.

3) The results obtained from the proposed position domain algorithm are superior (in terms of availability of correct fixes) to those obtained by geometric matching with the XTrac's HS GPS receiver (which is the best among all the solution sets available for map matching using the geometric approach).

6.3 Test-2: A Comparison Between the Proposed Position Domain, MAGPS and Geometric Map Matching Approaches

This section discusses the map matching results obtained using the proposed MAGPS approach. The first part compares and discusses the results obtained using position domain map matching algorithm and the MAGPS approach. The second part discusses the effect of height aiding on MAGPS computations. The MAGPS algorithm is then compared against the geometric map matching algorithm in the third sub-section. The

aim of this section is to demonstrate the effectiveness of map matching in the measurement domain as compared to position domain approaches. The MAGPS algorithm uses the same fuzzy logic-based map matching framework. Thus the main difference in the results obtained from the two approaches is mainly due to the improvement in the navigation solution quality obtained by the elimination of outliers.

Table 6.5 and Figure 6.13 give the availability statistics for this test. Figure 6.14 shows the position output plots from different receivers.

Table 6.5: Availability of Position Solution in Test-2 from NovAtel OEM4 and SiRF XTrac Receiver

Receiver	Internal solution availability (%)	LSQ solution availability (%)
NovAtel OEM4	96.2	38.8
SiRF XTrac	98.9	74.6
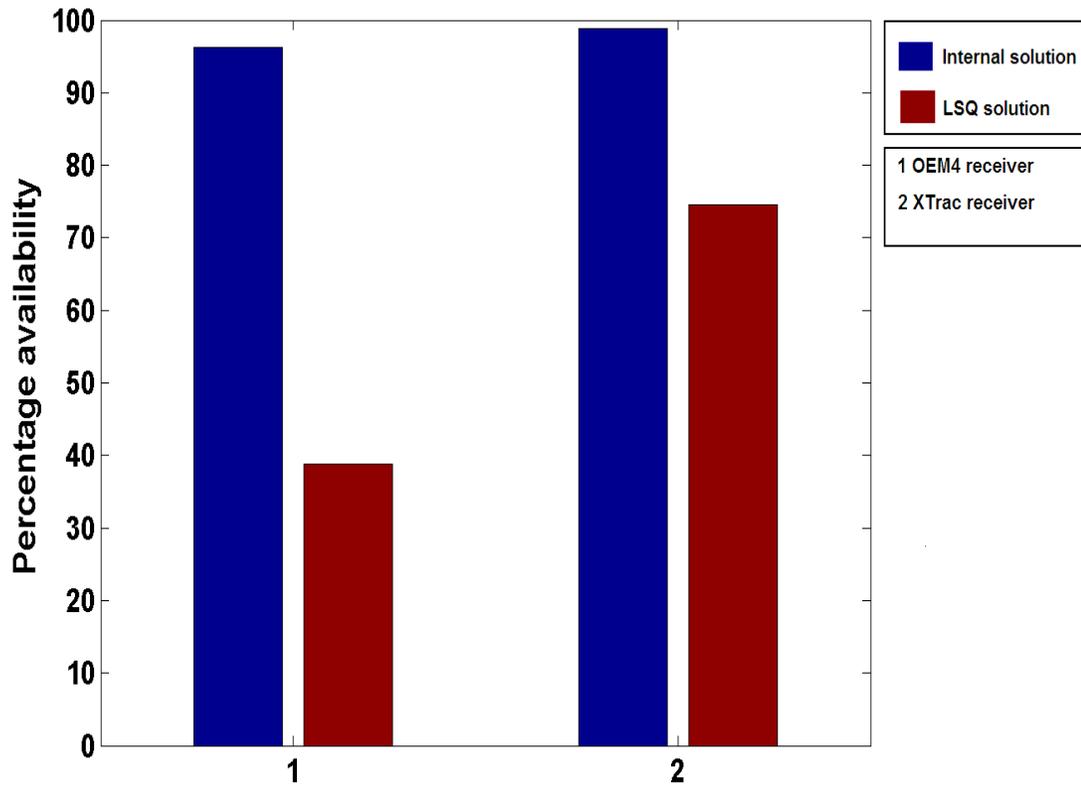
Figure 6.13: Graphical Representation of GPS Solution Availability in Test-2 from NovAtel OEM4 and SiRF XTrac Receivers
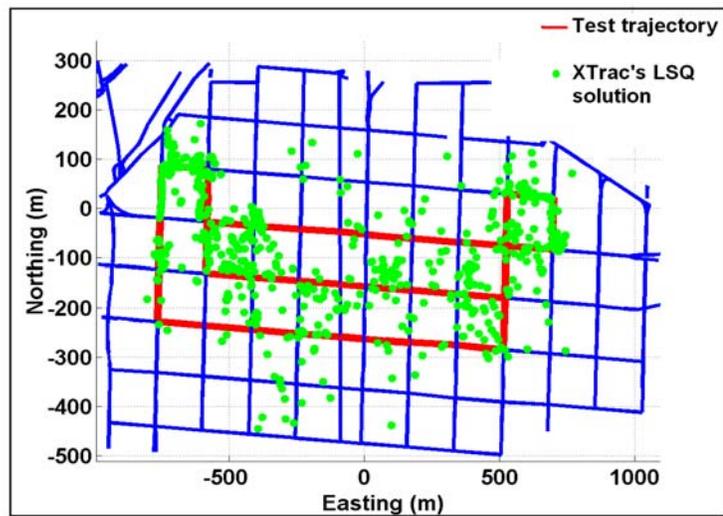
(a)
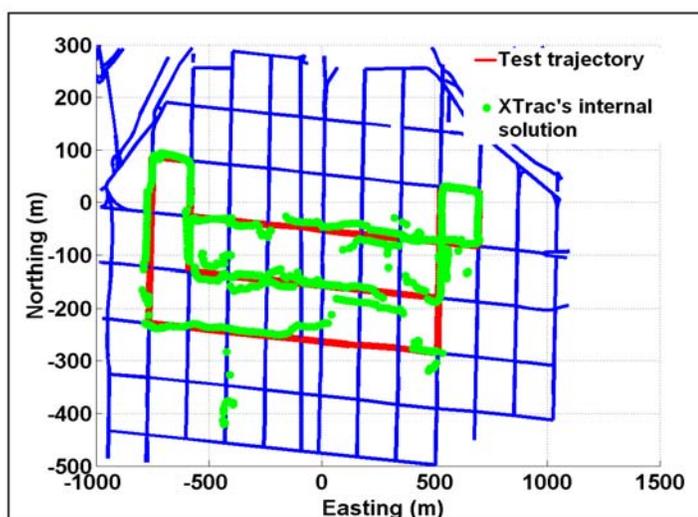
(b)
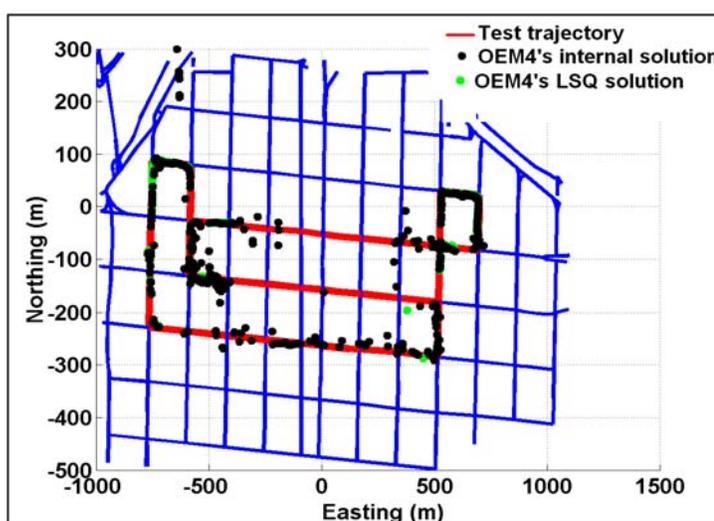
(c)

Figure 6.14: The Position Output in Test-2 from (a) XTrac's Post-Processed LSQ DGPS Solution (b) XTrac's Real-Time Internal Solution (without Differential Corrections) (c) OEM4's Real-Time Internal Solution (without Differential Corrections) and Post-Processed DGPS LSQ Solution

6.3.1 Proposed Outlier Detection Scheme

The next few tables demonstrate the separation of measurements approach used for outlier detection in simulation using Spirent STR6560 simulator. This scheme is tested in simulation and not in field Test-2 due to unavailability of true reference information in real world. A multipath delay of 70 m is introduced in pseudorange measurements from PRN 21 and 30. The other PRNs were simulated to have a multipath delay of 5 m. The available PRNs for the epochs are 6, 10, 16, 17, 21 and 30. The threshold for the outlier detection was selected to be 3.24 (with a 5% probability of Type-I error and 10% probability of Type-II errors). The global test fails when all the measurements are simultaneously used for computation.

The algorithm then removes one satellite at a time to check the standardized residual for each satellite (as shown in Table 6.6). It can be seen that none of the combination satisfies the condition that all standardized residuals are less than the threshold.

The algorithm then continues by eliminating two satellites at a time. The standardized residuals for successful combinations are given in Table 6.7. Table 6.8 gives the combination of satellite pairs which on simultaneous elimination gives standardized residuals less than the threshold for all the remaining satellites. The *residual-in-abstentia* for each satellite is shown in Table 6.9. The two satellites which have the lowest values of *residual-in-abstentia* (γ) are the one's which have outliers. The proposed approach successfully identifies the outliers. On the other hand, the sequential elimination

technique which permanently removes the measurement having highest standardized residual eliminates PRN 16 and 21.

Table 6.6: Standardized Range Residuals Obtained After Elimination of One Satellite at a Time

Eliminated satellite / range residual	6	10	16	17	21	29	30
6		0.30	-23.23	-1.03	23.31	21.88	-23.31
10	1.28		-21.94	-2.11	21.68	16.42	-22.77
16	7.84	-1.27		-5.24	-3.41	7.39	-8.01
17	0.63	-1.49	-22.47		21.71	14.36	-22.66
21	9.39	-3.62	-5.88	-4.09		9.21	-9.30
29	-16.55	7.97	-18.11	1.49	18.32		-18.36
30	-5.764	2.65	-5.67	2.08	5.78	-5.63	

Table 6.7: Standardized Range Residuals Obtained After Elimination of Two Satellites at a Time

PRNs rejected	6	10	16	17	21	29	30
6/16		1.97		-1.97	1.97	-1.97	-1.97
6/21		-0.22	-0.22	0.22		0.22	-0.22
6/30		0.54	0.54	-0.54	0.54	-0.54	
16/30	-1.14	1.14		-1.14	1.14	-1.14	
21/29	1.88	1.88	1.88	-1.88			-1.88
21/30	0.25	0.25	0.25	-0.25		-0.25	
29/30	-1.33	-1.33	-1.33	1.33	1.33		

Table 6.8: Combination of Satellite pairs which on Elimination Passes Standardized Residual Test

	PRN1	PRN2
1	6	16
2	6	21
3	6	30
4	16	30
5	21	29
6	21	30
7	29	30

Table 6.9: Residual-in-abstentia for all the Relevant Satellites

PRN1	Residual-in-abstentia
6	13.6
16	15.5
21	11.7
29	16.05
30	12.3

6.3.2 Map Matching Results

The map matched position output obtained from XTrac's pseudorange measurements with different algorithms are shown in Figure 6.15.
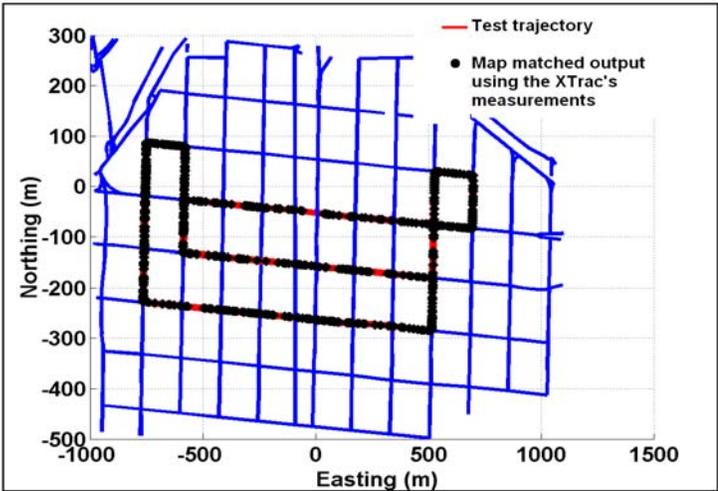
(a)
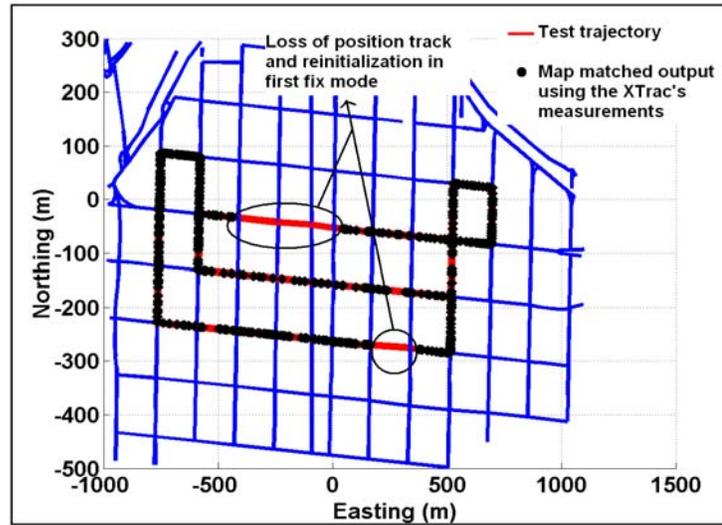
(b)
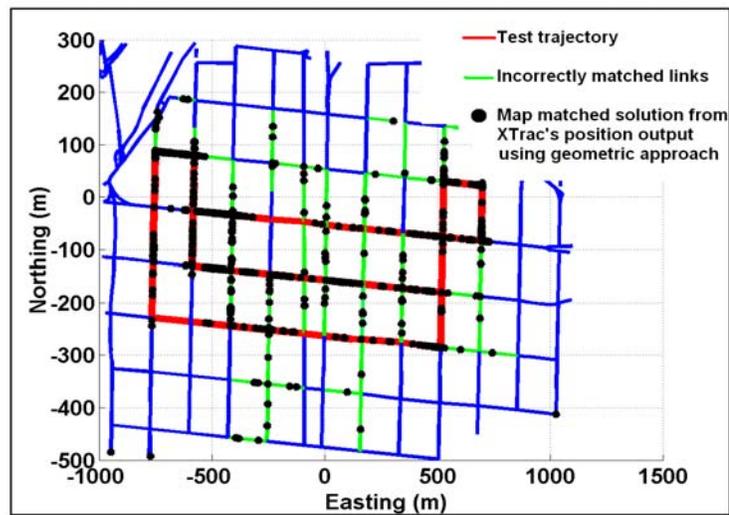
(c)

Figure 6.15: Map Matched Position Output in Test-2 Using XTrac's Measurements with: (a) The MAGPS Approach (b) The Fuzzy Logic-Based Position Domain Algorithm, and (c) The Pure Geometric Map Matching Algorithm

An unfixed solution in the MAGPS approach is when the algorithm is in first fix mode or when it loses track. Table 6.10 shows the percentage correct, false and unfixed solutions obtained using different map matching approaches. Figure 6.16 provides a graphical representation of the performances. Table 6.11 shows the effect of DEM aiding on map matching.
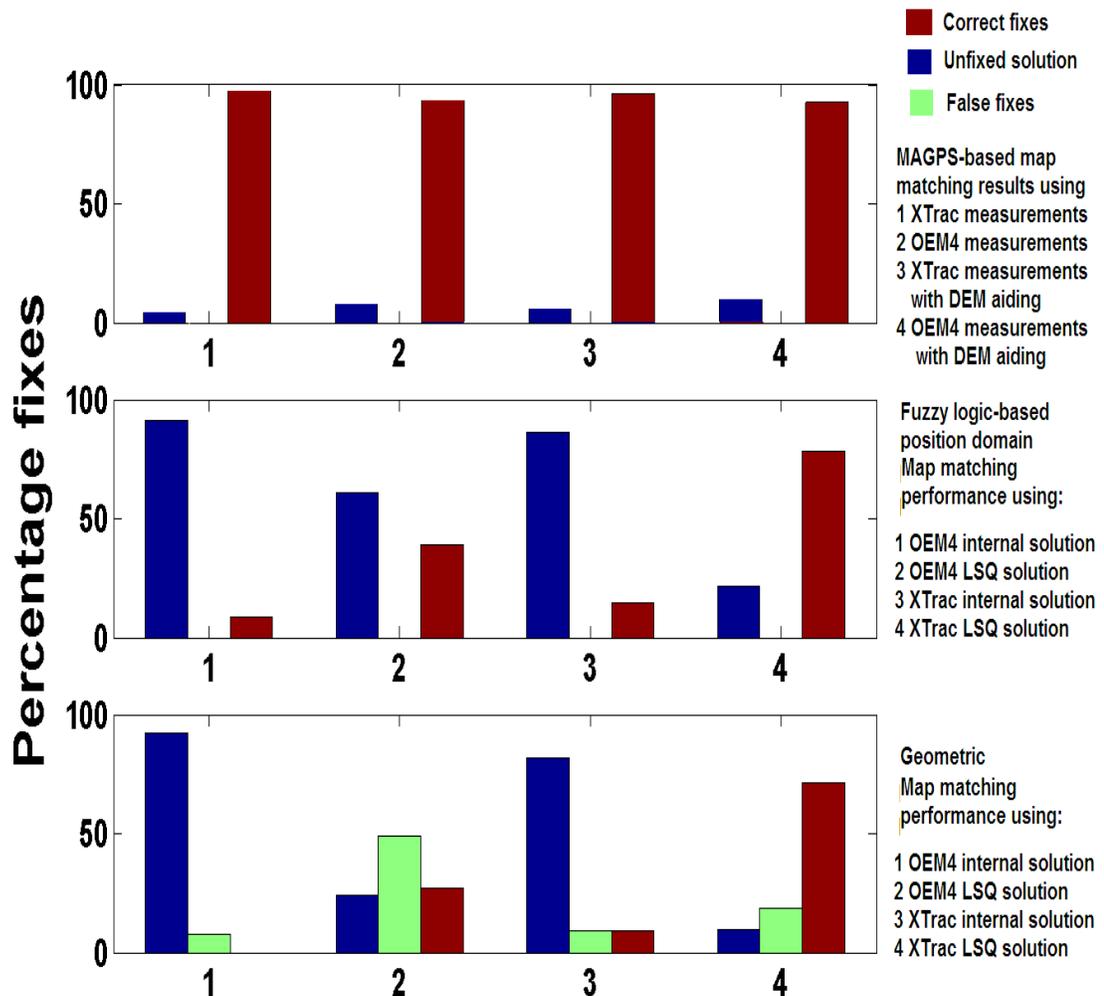
Figure 6.16: Graphical Representation of the Performances of Different Map Matching Approaches Using XTrac's Measurements in Test-2

Table 6.10: Performances of Different Map Matching Approaches in Test-2

Algorithm	GPS Soln. used	Correct fix (%)	False fix (%)	Un-fixed (%)	Ratio of false and correct fix, ratio of unfixed and correct fix	
MAGPS with DEM aiding	XTrac	97.3	0	2.7	0.00,	0.03
	OEM4	93.1	0	6.9	0.00,	0.08
MAGPS without DEM aiding	XTrac	96.9	0	3.1	0.00,	0.04
	OEM4	92.8	0	7.2	0.00,	0.08
Position-based fuzzy logic algorithm	XTrac LSQ	60.9	0	39.1	0.00,	0.22
	OEM4 LSQ	21.4	0	78.6	0.00,	3.71
	XTrac internal	91.1	0	8.9	0.00,	0.98
	OEM4 internal	86.1	0	14.9	0.00,	0.17
Geometric map matching algorithm	XTrac LSQ	24.3	48.8	26.9	2.08,	1.08
	OEM4 LSQ	9.6	18.8	71.6	1.92,	7.45
	XTrac internal	92.4	7.6	0	0.82,	0.00
	OEM4 internal	81.6	9.2	9.2	0.11,	0.11

Table 6.11: Performance of DEM Aided vs. Unaided MAGPS Approach

Aiding	Map matched solution availability (%)	Optimality (%)
DEM Aided	97.3	94.7
Unaided	96.9	79.2

The following inferences can be drawn about the performance of different map matching algorithms presented in Table 6.10 and Figure 6.16:

1) The performance of the XTrac GPS receiver is better than the OEM4 in terms of correct fix availability. This is observed by using both MAGPS and position domain algorithm (due to the reasons discussed in Test-1). The MAGPS has reduced availability using OEM4 solution (which can do position propagation based on the velocity output from Kalman filter) because of the increase in the uncertainty of the velocity solution causing the algorithm to lose track. Since OEM4 has fewer measurements, the uncertainty in the solution grows very rapidly.

2) The percentage false fix using both the proposed approaches is zero whereas the geometric approach gives many false fixes. This robustness of the proposed map matching framework was also observed in the results from Test-1.

3) The percentage correct fix increases by using the MAGPS algorithm as compared to using a position domain approach (with LSQ solution). This increase is about 33% in case of XTrac receiver and about 68% with OEM4 receiver. The main reason for this is that it takes longer time to obtain first fix in the fuzzy logic-based position domain algorithm (approximately a minute with 1 Hz GPS output) as compared to the proposed algorithm (which typically takes 5-10 seconds with 1 Hz GPS output). Also in position domain algorithm, it is not possible to separate erroneous pseudorange measurements from the GPS output solution as a result of which the fuzzy system detects failure and has to reinitialize itself frequently in harsh conditions leading to many unfixed solution epochs.

4) The increase in percentage correct fix by using the MAGPS algorithm instead of position domain algorithm is more significant in the case of OEM4 than XTrac. This is because of the more frequent loss of track in position domain algorithm due to less number of measurements.

5) The performance of the geometric algorithm worsens for LSQ solutions as compared to the corresponding internal solutions because of the increase in noise as discussed in Test-1.

6) The internal solutions from both the receivers gave higher percentage correct fixes using the proposed position domain algorithm as compared to the GPS LSQ solutions. This is because of the improvement in position quality by receiver's

internal filter. However filtering is not always desirable as sometimes it can lead to large position errors which go undetected (as seen in Test-1, with XTrac's internal solution).

7) The incorporation of DEM information led to an increase in the availability of *optimal solution*. Optimal solution is defined as the availability of both outlier-free position and velocity solution. This increase in optimality is because the number of satellites needed for getting a robust estimate of navigation solution reduces to 3. It should be noted that in many cases due to the harsh signal environment, the receiver could just track about 3-4 outlier-free pseudoranges. The presence of one extra constraint increases the number of epochs at which the optimal solution is computed by about 15%.

8) Incorporation of DEM information led to a slight increase in availability due to reliable initialization in a short time.

9) The proposed MAGPS algorithm has the highest percentage availability of correct fixes using both the receivers.

6.4   TEST-3: A Comparison Between MAGPS and MAGPS Filtering Approach

This section discusses the results obtained in Test-3. The algorithms analyzed include the MAGPS, MAGPS filtering approach, and position domain approach. For the sake of

brevity, Geometric approach and OEM4 solution are not discussed in this section as the inferences about them have already been stated in last two sections. This section aims at comparing the MAGPS filtering against MAGPS and proposed position domain approach. The first sub-section compares the performance of MAGPS filtering approach with the XTrac's algorithm and LSQ algorithm, in simulation. The second sub-section compares the overshooting problem in MAGPS filtering and XTrac's algorithm. The last sub-section makes a comparison between the three map matching approaches. Figure 6.17 shows the position output from XTrac receiver.
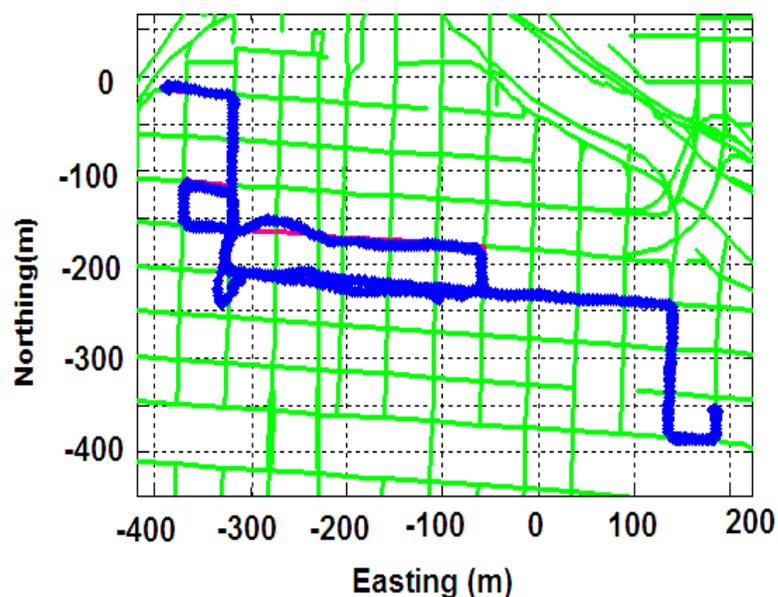
(a)
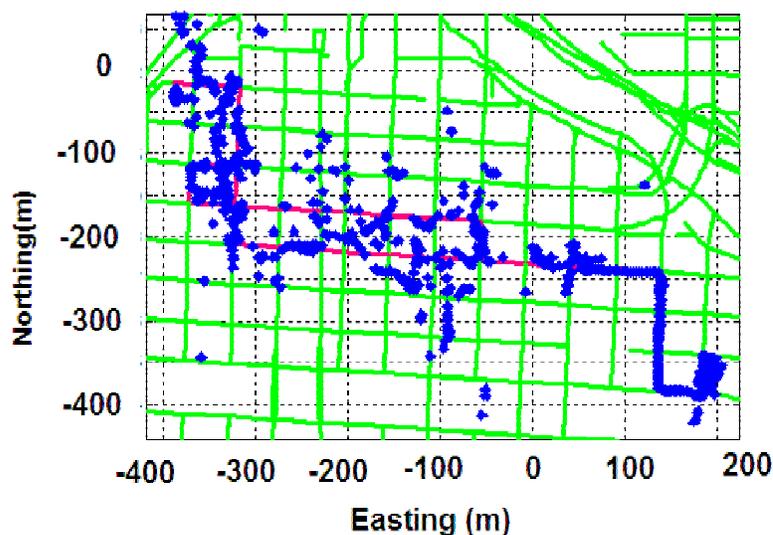
(b)

Figure 6.17: The Position Output in Test-3 from (a) XTrac's Real-Time Internal Solution (without Differential Corrections) (b) XTrac's Post-Processed LSQ DGPS Solution

6.4.1 Zero Velocity Test

This section describes the performance of XTrac's algorithm, proposed MAGPS filtering, and C^3NAVG^{2TM} algorithm. The vehicle was simulated to stay at rest in an urban canyon scenario created in Spirent STR6560 simulator. This test was conducted in simulation and not in field Test-3 due to unavailability of true reference information in real world. Table 6.12 and Table 6.13 give the RMS errors in velocity and position solution respectively. These tables show that the performance of MAGPS filtering and XTrac's algorithm is almost the same in urban canyon. The position domain performance of MAGPS filtering is slightly better than XTrac's algorithm because of the constraints imposed by the map.

Table 6.12: Velocity RMS Errors Obtained from Different Filtering Algorithms

RMS Velocity Error (m/s)	North	East	UP	Horizontal
MAGPS filter	0.7	0	0	0.7
XTrac's internal solution	0.9	0	0	0.9
C^3NAVG^{2TM}	2.6	3.7	1.8	4.9

Table 6.13: Position RMS Errors from Different Filtering Algorithms

RMS Position Error (m)	North	East	UP	Horizontal
MAGPS filter	1.1	0.3	0	1.1
XTrac's internal solution	2.3	0.2	0.2	2.3
C^3NAVG^{2TM}	23.8	28.7	19.3	42.0

6.4.2 Overshooting Issues

Overshooting is defined as the incorrect filtering of velocity on turns. This is mainly due to the fact that the filter continues to give the same weight to the predicted velocity on turns. The Kalman filter, on turnings, should give more weight to the solution obtained from measurements than the predicted solution. The MAGPS filtering with indirect

heading aid from gyro does not have this problem because of the prompt increase in the process noise variance. The indirect heading aid from gyro was discussed in Chapter 5.

Severe overshooting was observed on one of the turns using XTrac's algorithm. The proposed Kalman filter, without heading aid from gyro, mildly overshoots at about 6 turns. Overshooting causes problems in map matching as it leads to an incorrect road segment identification and subsequent loss of track due to incorrect tracking.

6.4.3 Map Matching Results

Table 6.15 and Figure 6.19 give the map matching performance of the proposed MAGPS algorithms with DEM aiding and proposed position domain algorithm. The proposed MAGPS algorithms behaved almost similar except for the fact that MAGPS approach had some minute discontinuities on turns. This is because of the velocity propagation effect in MAGPS, which leads to slight underestimation of position along the road segment. This underestimation in MAGPS is corrected when the vehicle turns at the end of road segment. MAGPS filtering approach however had one reset because of increase in uncertainty. This increase in uncertainty is because of the inclusion of position states (latitude/longitude/height) in state vector which often becomes unobservable. This problem is not there in velocity filter of MAGPS approach.

If the threshold uncertainty of state vector is raised by 2.25 times, then the filter never resets leading to a continuous navigation solution. Both MAGPS approaches have more availability of map matched solution than the position domain approach.

Table 6.14: Velocity Overshooting from Different Filtering Algorithms

	Total number of Epochs	Average magnitude of overshoot (m/s)
XTrac	5 (1 instance)	1.2
MAGPS without Heading aid	22 (6 instances)	1.8
MAGPS with heading aid	0	-

6.5 Summary

To summarize the chapter, following remarks can be made about the results obtained from the three test cases discussed above:

1) Position domain approach, which uses fuzzy logic-based framework, assumes that the errors in navigation solution decorrelate with time. The algorithm does not declare first fix until the errors get decorrelated as per the fuzzy rules. Hence it takes a long time for the algorithm to initialize robustly giving many unfixed solution epochs. Also, since outlier elimination is not possible in this algorithm, it

frequently loses track leading to increase in the number of unfixed solution epochs.

Table 6.15: Performances of Different Map Matching Approaches in Test-3

Algorithm	Availability	Correct fixes (%)	Incorrect fixes (%)
Position domain results with XTrac's internal solution	98.3	97.6	0
Position domain results with XTrac's LSQ solution	98	93.1	0
MAGPS	99.8	99.8	0
MAGPS filter	98.6	98.6	0

2) The measurement domain approaches on the other hand do not assume anything about the error correlation in determining the first fix. The assumptions made in this case are: (a) the number of "correct" measurements is greater than number of outliers, and (b) the errors are normally distributed. As a result, the initialization time and the number of unfixed solution epochs decreases by using the measurement domain approaches. In addition, the outlier elimination helps in preventing loss of track, thereby decreasing the number of unfixed solution epochs.
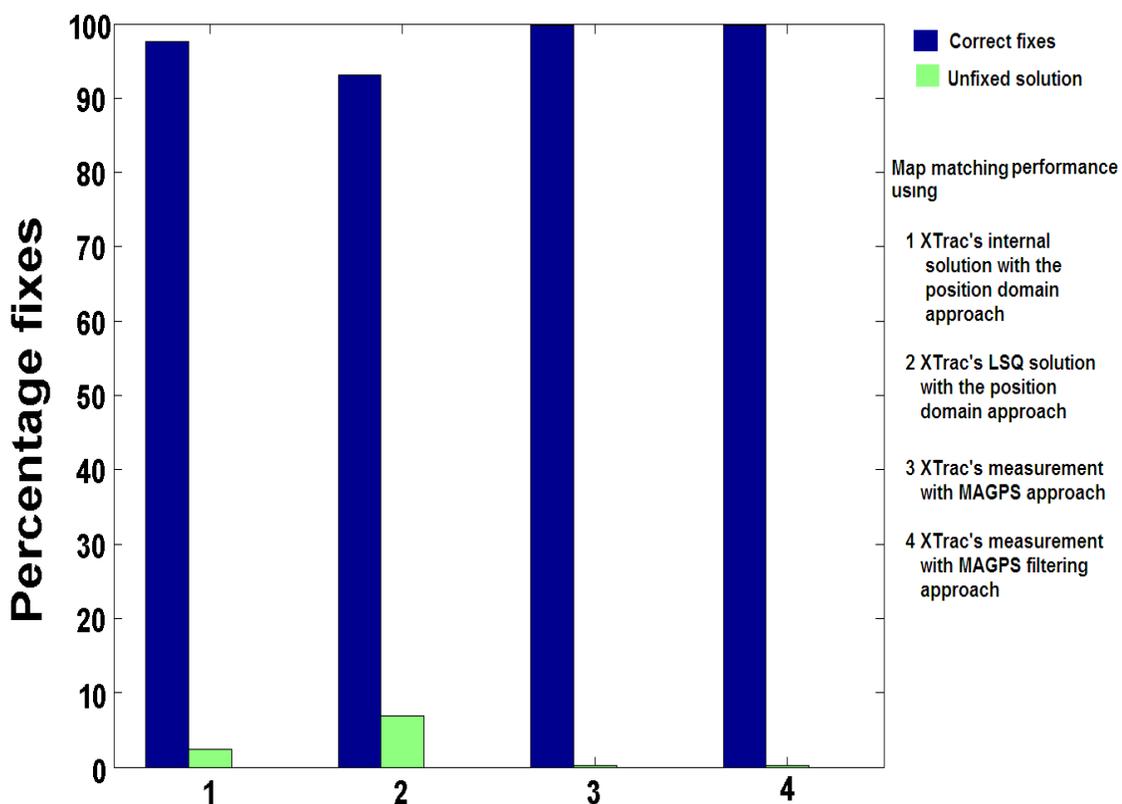
Figure 6.18: Graphical Representation of the Performances of Different Map Matching Approaches Using XTrac's Measurements in Test-3

3) Geometric approach does not incorporate the effective information theory resulting in many false fixes. The performance using this approach degrades with increase in noise and measurement errors. The geometric approach works well with a smooth and accurate navigation solution.

4) Among the proposed algorithms, MAGPS algorithms outperform the position domain approach whose accuracy and availability decreases with increase in severity of urban canyon conditions.

5) Centralized Kalman filter, used in MAGPS filtering approach, has almost the same performance as the MAGPS approach.

6) The effect of height aiding is significant in obtaining optimal solution in dense urban canyons. In addition, DEM aiding becomes crucial for quicker initialization amid reduced satellite availability.

CHAPTER 7: CONCLUSIONS AND RECOMMENDATIONS

The work presented in this thesis introduced and developed a new approach for vehicle navigation in urban canyon conditions using map aiding. The limitations of past research in this area were presented and a new map matching framework was developed. The motivation for this research comes from the fact that while HS GPS increases the availability, an algorithm is needed to monitor the integrity of measurement by detecting outliers. In this context, map and DEM provide useful constraints to detect and remove blunders.

The approaches developed during this research combine classical statistical theory with fuzzy logic techniques to tackle the vehicle navigation problem. Three approaches were developed and analyzed during the research. The effect of DEM as an extra constraint was also briefly discussed.

The position domain approach receives the input from an "external" GPS processing algorithm. The proposed approach then does the map matching using a robust fuzzy logic map matching framework. Measurement domain approaches (MAGPS and MAGPS filtering) on the other hand, use map information in the GPS measurement model. GPS measurements with map (and DEM) constraints are processed using either least squares method or a Kalman filter.

This novel concept of map matching in the measurement domain (instead of the position domain) is a first of its kind to tightly couple GPS with the map information. This approach is far more robust than conventional map matching which has many shortcomings in signal degraded environments. It is more effective than low cost GPS/DR integration because the extra conditions provided are not susceptible to large blunders, which may be present in the DR measurements. A fault detection methodology based on the separation of solution approach was developed based on the theory of outlier detection presented in Baarda (1968) and Teunissen (1998). This methodology has the capability of detecting and identifying multiple blunders in GPS measurements.

The performances of different map matching algorithms were then analyzed in terms of the number of correct and false fixes.

7.1 Conclusions

The following conclusions can be drawn from the work presented in this thesis:

1) Use of an HS GPS receiver increases availability and helps in effective vehicle navigation in urban canyon conditions. In the three tests discussed in the previous chapter, an average increase of 19% is observed in the availability of LSQ navigation solution by using an HS GPS receiver as compared to a conventional GPS receiver. The increase in availability depends on the severity of the urban canyon conditions. The increase is about 35% in Test-2.

2) At least one outlier was observed in 38% of epochs during the three urban canyon tests discussed above (with a 5% probability of Type-I error and 10% probability of Type-II errors). Thus, an integrity monitoring algorithm is needed to remove these outliers for effective navigation.

3) Tracking weak GPS signals lead to incorporation of additional outliers in GPS pseudorange measurements. Although the average availability increased by 19% using HS GPS, the number of epochs having at least one outlier increased by 21% as compared to conventional GPS receiver. Hence there is an increased requirement for integrity monitoring of HS GPS measurements.

4) Doppler measurements from XTrac receiver during the three tests were fairly stable. An average of 24% epochs had at least one outlier in Doppler measurements (with a 5% probability of Type-I error and 10% probability of Type-II errors).

5) The proposed fuzzy logic-based map matching framework is very robust as it did not give any false fixes during the three tests.

6) The conventional map matching algorithm based on geometric conditions is prone to increased noise and outliers. The performance is further degraded by using the weak signals. The geometric map matching algorithm gave an average of 27% false fixes during the Test-1 and Test-2 using XTrac's LSQ solution.

7) Although outlier detection is possible using fuzzy logic technique, it is not possible to identify and isolate the outlier from the solution. The outlier elimination is only possible by using classical statistics with special rules.

8) Map and DEM provide effective constraints for detecting outliers in GPS measurements as these constraints are accurate to the specified level of accuracy. The separation of measurements approach discussed in Chapter 5 may not work properly in the absence of such rigorous constraints.

9) Map and DEM constraints also reduce the satellite availability requirement for the computation of navigation solution. The LSQ solution availability increased by 23% in second test by using the map information.

10) The number of unfixed solution epochs decreased by 35% by using measurement domain approaches (MAGPS and MAGPS filtering) as compared to the position domain approach.

11) The DEM helped in obtaining a faster first fix and in the computation of optimal solution. An increase of 15% is observed in the computation of optimal solution.

12) The proposed MAGPS and MAGPS filtering approaches are ideal for vehicle navigation in urban canyons because of the increase in reliability and availability.

The average availability of correct fixes using the XTrac HS GPS receiver with MAGPS approach in Calgary downtown was about 98%.

13) A significant performance difference is not observed by using a centralized Kalman filter in MAGPS filtering approach as compared to the MAGPS approach. The possible explanation for this is that the significant contribution for computation of final navigation solution comes from the map aiding and velocity solution (which in principle is identical for both the approaches).

7.2 Recommendations

The following enhancements can be made to the map matching approaches developed during this research:

1) The work presented here uses a low cost gyro to detect change in road segments. Accurate characterization of the gyro should be done and the effect of using it directly in the measurement model should be analyzed. This will be effective in determining the road segment at Y-intersections, where the proposed algorithm may have a potential failure.

2) Further analysis on MAGPS filtering is needed in terms of filter adaptation and covariance analysis which are not thoroughly dealt with in this thesis.

3) The concept of virtual differential corrections proposed by Taylor and Blewitt (1999) should be used to determine corrections for the next epoch instead of using differential corrections from a reference station. This will make the system autonomous.

4) The benefits of adding a speedometer or odometer which give independent distance measurements should be analyzed.

5) Driving constraints should be incorporated in the FIS to reduce the search space of the road segments.

6) The effect of using additional measurements from the new GPS L2C signal and Galileo on vehicle navigation should be studied in simulation to determine their feasibility in vehicle safety applications.

7) The map matching work discussed in this thesis should be implemented in a Relational Database Management Systems (RDBMS) like Oracle which has highly sophisticated inbuilt querying algorithms instead of a flat-file search system. This will make the computation less cumbersome.

REFERENCES

Automated Collision Notification (ACN) Report (2001), National Highway Traffic Safety Administration, US Department of Transportation, Washington, D.C., USA, pp.7-8.

Aloi, D.N. and F. Van Graas (2004), Ground-Multipath Mitigation via Polarization Steering of GPS signal, IEEE Transactions on Aerospace and Electronic Systems, Volume 40, No. 2, pp. 536 - 552.

Ashjaee, J. (1985), GPS Doppler Processing for Precise Positioning in Dynamic Applications, IEEE OCEANS, 15-19 November, Volume 17 , pp. 195 – 203.

Astroth, J. (2001), Knowledge Sharing and Communication the Hallmark of the New Economy, GEO INFOMATICS, Volume 4, pp.37-46.

Audenino, P., L. Rognant, J.M. Chassery and J.G. Planes (2001), Fusion Strategies for High Resolution Urban DEM Remote Sensing and Data Fusion over Urban Areas, Proceedings of IEEE/ISPRS Joint Workshop, 8-9 November, pp. 90 – 94.

Axelrad, P. and R.G. Brown (1994), GPS Navigation Algorithms, Global Positioning System: Theory and Applications, American Institute of Aeronautics and Astronautics Publications, Washington, DC, USA, Volume 1, No. 9, pp. 409-433.

Baarda, W. (1967), Statistical Concepts in Geodesy, Netherlands Geodetic Commission, Volume 4, No. 2, pp. 76-83,

Baarda, W. (1968), A Testing Procedure For Use in Geodetic Networks, Netherlands Geodetic Commission, Volume 5, No. 2, pp. 107-113.

Bandemer, H.Y. and W. Näther (1992), Fuzzy Data Analysis, Kluwer Academic Press, Dordretch, Netherlands.

Beck, J.V. and K.J. Arnold (1976), Parameter Estimation in Engineering and Science, John Wiley and Sons Publication, New York, NY, USA.

Bernstein, D. and A. Kornhauser (1996), An Introduction to Map Matching for Personal Navigation Assistants, Technical Report, New Jersey TIDE Center, New Jersey Institute of Technology, New Jersey, NY, USA. http://www.njtide.org/reports/mapmatchintro.pdf

Biacs, Z., G. Marshall, M. Moeglein and W. Riley (2002), The Qualcomm/SnapTrack Wireless-Assisted GPS Hybrid Positioning System and Results from Initial Commercial

Deployments, SnapTrack, A Qualcomm Company, Proceedings of ION GPS, 24-27 September, Portland, OR, USA, pp. 378-384.

Borenstein, J. (1994), Internal Correction of Dead-Reckoning Errors with the Smart Encoder Trailer, Proceedings of the IEEE/RSJ/GI International Conference on Intelligent Robots and Systems, 12-16 September, Volume 1, pp. 127 - 134.

Braasch, M.S. (1996), GPS Multipath Model Validation, Proceedings of IEEE PLANS, 22-26 April, Volume 1, pp. 672-678.

Braasch, M.S. (2001), Performance Comparison of Multipath Mitigating Receiver Architectures, Proceedings of IEEE Aerospace Conference and Electronic Systems, Volume 3, pp. 1309-1315.

Brown, R.G. (1993), Receiver Autonomous Integrity Monitoring, Global Positioning System: Theory and Applications, American Institute of Aeronautics and Astronautics Publications, Washington, DC, USA, Volume 2, pp. 143-165.

Brown, R.G. and P.W. McBurney (1987), Self-Contained GPS Integrity Check Using Maximum Solution Separation as the Test Statistics, Proceedings of the satellite division First technical meeting, The Institute of Navigation, 21-25 September, Colorado Spring, CO, USA, pp. 263-268.

Brown, R. G. and P.Y.C. Hwang (1992), Introduction to Random Signals and Applied Kalman Filtering, Second Edition, John Wiley and Sons Publication, New York, NY, USA.

Bullock, J.B. (1995), A Prototype Portable Navigation System Utilizing Map Aided GPS, M.Sc. Thesis, UCGE Report 20081, University of Calgary, Calgary, AB, Canada.

Cannon, M.E. (2001), GPS Modernization and the Emergence of New GNSS Systems and Applications, Keynote Address, Proceedings of the Japanese GPS Conference, 15 -16 November, Tokyo, Japan, pp. 9-14.

Cannon, M.E., G. Lachapelle, R. Nayak, O. Salychev and V. Voronov (2001), Low Cost INS/GPS Integration: Concepts and Testing, Journal of Navigation, Royal Institute of Navigation, Volume 54, No. 1, pp. 119-134.

Cardstensen, Jr, L.W. (1998), GPS and GIS: Enhanced Accuracy in Map Matching Through Effective filtering of Autonomous GPS points, Cartography and Geo Info System, Volume 25, No. 1, pp. 51-62.

Chansarkar, M. and L. J. Garin (2000), Acquisition of GPS Signals at Very Low Signal to Noise Ratio, Proceedings of the ION NTM, 26-28 January, Anaheim, CA, USA, pp. 730–737.

Chen, S.J. and C.L. Hwang (1992), Fuzzy Multiple Attribute Decision Making, Springer-Verlag Publications, London, UK.

Choi, W.J. and S. Tekinay (1992), Location Based Services for Next Generation Wireless Mobile Networks, Proceedings of the 57th IEEE Semi-annual Conference on Vehicular Technology, 22-25 April, Volume 3, pp. 1988 - 1992.

Collier, W.C. (1990), In-Vehicle Route Guidance Systems Using Map Matched Dead Reckoning, Proceedings of IEEE-PLAN Symposium, 'The 1990's - A Decade of Excellence in the Navigation Sciences', 20-23 March, pp. 359-363.

Collin, J., H. Kuusniemi, O. Mezentsev, G. MacGougan and G. Lachapelle (2003), HS GPS Under Heavy Signal Masking: Accuracy and Availability Analysis, Proceeding of NORNA 03 Conference: Navigation in the 21st Century, 2-4 December, Stockholm, Netherlands, pp. 478-487.

Dote, Y. (1995), Introduction to fuzzy logic, Proceedings of the 1995 IEEE IECON 21st International Conference on Industrial Electronics, Control, and Instrumentation, 6-10 November, Volume 1, pp. 50 – 56.

Dubois, D. and H. Prade (1979), Fuzzy Real Algebra: Some Results, Journal of Fuzzy Sets and Systems, Volume 2, pp. 327-348.

El-Sheimy, N., K. P. Schwarz, M. Wei and M. Lavigne (1995), VISAT: A Mobile City Survey System of High Accuracy, Proceedings of ION GPS, Palm Spring, CA, USA, pp. 1307–1315.

Endreny, T.A., E.F. Wood and A. Hsu (2000), Correction of Errors in SPOT-Derived DEM's Using GTOPO30 Data, IEEE Transactions on Geoscience and Remote Sensing, Volume 38, No. 3, pp. 1234 – 1241.

Etak (2000), Etak Real-Time Traffic Information Delivery System

http://www.etak.com/traffic/present1.html

Farrell, J. A., T. D. Givargis and M. J. Barth (2000), Real-Time Differential Carrier Phase GPS-Aided INS. IEEE Transactions on Control Systems Technology, Volume 8, No. 4, pp. 709–720.

FCC (2000), Federal Communications Commision, USA, OET BULLETIN No. 71, Guidelines for Testing and Verifying the Accuracy of Wireless E911 Location Systems, www.fcc.gov/Bureaus/Engineering Technology/Documents/bulletins/oet71/oet71.pdf

Feng. S and C. Law (2002), Assisted GPS and its Impact on Navigation in Intelligent Transportation Systems, Proceedings of 5th IEEE International Conference on Intelligent Transportation Systems, pp. 926 – 931.

French, R.L. (1997), Land Vehicle Navigation and Tracking, Global Positioning System: Theory and Applications, American Institute of Aeronautics and Astronautics Publications, Washington, DC, USA, Volume 2, pp. 275 – 301.

Gao, Y. (1993), Reliability Assurance for GPS Integrity Test, Proceedings of ION GPS, 22-24 September, Salt Lake City, Utah, USA, pp. 567-574.

Gao, Y., Z. Liu and Z.Z. Liu (2002), Internet-Based Real-Time Kinematic Positioning, GPS Solutions, Volume 5, No.3, pp. 61-69.

Garin, L. J., M. Chansarkar, S. Miocinovic, C. Norman and D. Hilgenberg (1999), Wireless Assisted GPS-SiRF Architecture and Field Test Results, Proceedings of the ION GPS, 14-17 September, Nashville, TN, USA, pp. 489–497.

Garin, L. J., F. Van Diggelen and J. Rousseau (1996), Strobe & Edge Correlator Multipath Mitigation for Code, Proceedings of ION GPS, 17-20 September, Kansas City, MI, USA, pp. 657-664.

Gelb, A. (1974), Applied Optimal Estimation, M.I.T. Press Publication, Cambridge, MA, USA.

GPS SPS Performance Standard (2001), October Issue, US DOD, Washington, DC, USA.

Greenfeld, J.S. (2002), Matching GPS Observations to Locations on a Digital Map, Proceedings of the 81st Annual Meeting of the Transportation Research Board, 22-27 May, Washington, DC, USA, pp. 376-384.

Grejner-Brzezinska, D. A., R. Da and C. Toth (1998), GPS Error Modeling and OTF Ambiguity Resolution for High-Accuracy GPS/INS Integrated System, Journal of Geodesy, Volume 72, No. 1, pp. 626–638.

Grim, P. (1993), Self-Reference and Chaos in Fuzzy Logic, IEEE Transactions on Fuzzy Systems, Volume 1, No. 4, pp. 237-253.

Greenspan, R.L. (1996), GPS and Inertial Integration, Global Positioning System: Theory and Applications, American Institute of Aeronautics and Astronautics Publications, Washington, DC, USA, Volume 2, pp. 432- 439.

Grewal, M. S. and A. P. Andrews (1993), Kalman Filtering Theory and Practice, Prentice Hall Publication, New York, NY, USA.

Grewal, M.S., R. Lawrence, A.P. Andrews (2001), Global Positioning Systems, Inertial Navigation, and Integration, John Wiley and Sons Publications, New York, NY, USA.

Hampel, F.R., E.M. Ronchetti, P.J. Rousseuw and W.A. Stahel (1986), Robust Statistics, John Wiley and Sons Publication, New York, NY, USA.

Han, S. and C. Rizos (1997), Comparing GPS Ambiguity Resolution Techniques. GPS World, Volume 8, No. 10, pp. 54–61.

Harvey, R. (1998), Development of a Precision Pointing System Using an Integrated Multi-Sensor Approach, M.Sc. Thesis, UCGE Report 20117, University of Calgary, Calgary, AB, Canada.

Hewitson, S. (2003), GNSS Receiver Autonomous Integrity Monitoring: A Separability Analysis, Proceedings of ION GPS, 9-12 September, Portland, OR, USA, pp.1502-1509.

Hofmann-Wellenhof, B., H. Lichtenegger and J. Collins (1994), Global Positioning System Theory and Practice, Third Revised Edition, Springer-Verlag, New York, NY, USA.

Hu, C., W. Chen, Y. Chen and D. Liu (2003), Adaptive Kalman Filtering for Vehicle Navigation, Journal of Global Positioning Systems, Volume 2, No. 1, pp. 42-47.

Huber, P.J. (1964), Robust Estimation of Location Parameters, Annals of Mathematical Statistics, Volume 36, pp. 1753-1758.

ICD200C (2000), GPS Interface Control Document, ARINC Research Corporation, NAVSTAR GPS Space Segment/Navigation User Interfaces, IRN-200C-004, Annapolis, MD, USA.

Iwaki, F., M. Kakihari and M. Sasaki (1989), Recognition of Vehicle's Location for Navigation, Proceedings of the Vehicle Navigation and Information Systems Conference, 11-13 September, Toronto, ON, Canada, pp. 131-138.

Jacobs, O.L.R. (1993), Introduction to Control Theory, Second Edition, Oxford University Press, London, UK.

Jang, J. S. R. and C. T. Sun (1997), Neuro-Fuzzy and Soft Computing: A Computational Approach to Learning and Machine Intelligence, Prentice Hall Publications, New York, NY, USA.

Jekeli, C. (2000), Inertial Navigation Systems with Geodetic Applications, Walter de Gruyter Publications, New York, NY, USA.

Joshi, R. (2001), A New Approach to Map Matching for In-Vehicle Navigation Systems: The Rotational Variation Metric, IEEE PLAN Transactions on Intelligent Transportation Systems, 25-29 August, pp. 33 -38.

Kalman, R. E. (1960), A New Approach to Linear Filtering and Prediction Problems, Transaction of the ASME, Journal of Basic Engineering, Volume 12, No. 1, pp. 35-45.

Kaplan, E. (1996), Understanding GPS Signal Characteristics, Artech House Publication, Boston, MA, USA.

Karunanayake, D., M.E. Cannon, G. Lachapelle and G. Cox (2004), Evaluation of AGPS in Weak Signal Environments Using a Hardware Simulator, Proceedings CD of ION GNSS, 21-24 September, Long Beach, CA, USA.

Kaufmann, A. and M.M. Gupta (1985), Introduction to Fuzzy Arithmetic, Van Nostrand Reinhold Publications, New York, NY, USA.

Kevin, L. and M. Chansarkar (1996), Enhanced GPS Usage in Urban Environments, Proceedings of the 9th International Technical Meeting of the Satellite Division, The Institute of Navigation, 17-20 September, Kansas City, MI, USA, pp. 505-508.

Kickert, W.J.M. (1978), Fuzzy Theories on Decision Making: A Critical review, Martinus Nijhoff Publications, Dordretch, Netherlands.

Koch, K.R. (1999), Parameter Estimation and Hypothesis Testing in Linear Node, Second Edition, Springer Verlag, New York, NY, USA.

Kohli, S. (1992), Application of Massively Parallel Signal Processing Architectures to GPS/Inertial Systems, Proceedings of IEEE PLAN Symposium, 23-27 March, pp. 345-351.

Kok, J.J. (1984), Data Snooping and Multiple Outlier Testing, NOAA Technical Report, Rockville, MD, USA, NOS-NGS 30.

Konno, M. and S. Sugawara (1987), Equivalent Circuits of a Piezoelectric Vibratory Gyro, Proceedings of IEEE Ultrasonics Ferroelectric & Frequency Control Society, 14-16 May, Volume 1, pp. 539-542.

Kim, J.S., J.H. Lee, T.H. Kang, W.Y. Lee and Y.G. Kim (1996), Node Based Map Matching Algorithm for Car Navigation System, Proceedings of the 29th ISATA Symposium, Florence, Italy, Volume 10, pp. 121 – 126.

Kim, J., and S. Kim (1999), Q-Factor Map Matching Method Using Adaptive Fuzzy Network, Proceedings of IEEE Fuzzy Systems, 22-25 August, pp. 628 -633.

King, R.W., E.G. Masters, C.Rizos, A. Stolz and J. Collins (1987), Surveying with GPS, Dümmler-Bonn, pp. 128.

Krakiwsky, E.J., C. B. Harris and R.V.Wong (1988), A Kalman Filter for Integrating Dead Reckoning, Map Matching and GPS Positioning, Proceedings of IEEE PLAN symposium, 29th November-2ndDecember, pp. 39-46.

Kyriazakos, S., D. Draikoilis and G. Karetsos (2000), Optimization of Hand over Algorithm Based on Position of Mobile Terminal, Proceedings IEEE PLAN symposium, 21-24 October, pp. 76-81.

Lachapelle, G. (1995), Far Reaching Recommendations on GPS Made by High Level U.S. Study, Invited Contribution, Geomatics Info Magazine, International Journal for Geomatics, Volume 9, No. 8, pp. 48-49.

Lachapelle, G., H. Kuusniemi, D. Dao, G. MacGougan and M.E. Cannon (2003), HS GPS Signal Analysis and Performance Under Various Indoor Conditions, Proceedings of ION GPS, 7-9 September, Portland, OR, USA, pp. 237-245.

Lamb, P. and S. Threbaux (1999), Avoiding Explicit Map-Matching in Vehicle Location, Proceedings of 6th World ITS Conference, Toronto, ON, Canada, pp. 73 -85.

Langley, R.B. (1991), The GPS receiver - An Introduction, GPS World, Volume 2, No. 1, pp. 50-53.

Langley, R.B. (1993), The GPS observables, GPS World, Volume 4, No. 4, pp. 52-59.

Laplin, T. (1999), The New Road Rage. Wired, Condé Nast Publications Inc., London, UK.

Leick, A. (1995), GPS Satellite Surveying, Second Edition, John Wiley & Sons Publication, New York, NY, USA.

Lewis, R. (1986), Optimal Estimation with an Introduction to Stochastic Control Theory, John Wiley and Sons Publication, New York, NY, USA

Lin, D.M. and J.B.Y. Tsui (2001), A Software GPS Receiver for Weak Signals, Microwave Symposium Digest, Proceedings of IEEE MTT-S International, 20-25 May, Volume 3, pp. 2139 - 2142.

Lipp, A. and X. Gu (1994), Cycle-Slip Detection and Repair in Integrated Navigation Systems, Proceedings of IEEE PLAN Symposium, 11-15 April, pp. 681 - 688.

Liu, Z. (2000), A Java-Based Wireless Framework for Location-Based Services Applications, M.Sc thesis, UCGE Report 20161, University of Calgary, Calgary, AB, Canada.

MacGougan, G., G. Lachapelle, R. Klukas, K. Siu, L. Garin, J. Shewfelt and G. Cox (2002), Performance Analysis of a Stand-Alone High Sensitivity Receiver, GPS Solutions, Volume 6, No. 3, pp. 179-195

MacGougan, G. (2003), High Sensitivity GPS Performance analysis in Degraded Signal Environment, M.Sc Thesis, UCGE Report No. 20176, University of Calgary, Calgary, AB, Canada.

Ma, C., G. Jee, G. MacGougan, G. Lachapelle, S. Bloebaum, G. Cox, L. Garin and J. Shewfelt (2001), GPS Signal Degradation Modeling, Proceedings of the ION GPS, 11-14 September, Salt Lake, UT, USA, pp. 882–893.

Mamdani, E.H. and S. Assilian (1975), An Experiment in Linguistic Synthesis with a Fuzzy Logic Controller, International Journal of Man-Machine Studies, Volume. 7, No. 1, pp. 1-13.

Mathwork's Help Documents (2002), User Guide for Fuzzy Logic Tool Box, Mathwork Inc., Release 13, version 2.1.2, 9 July, Natick, MA, USA
 http://www.mathworks.com/access/helpdesk/help/pdf_doc/fuzzy/fuzzy_tb.pdf

Maybeck, P.S. (1982), Stochastic Models, Estimation and Control, Volume 1, Navtech Book and Software Store, Arlington, TX, USA.

Mehra, R.K. (1970), On the Identification of Variance and Adaptive Kalman Filtering, IEEE Transaction on Automatic Control, Volume 15, No. 2, pp. 175-184.

Mehra, R.K. (1972), Approaches to Adaptive Filtering, IEEE Transaction on Automatic Control, Volume 16, No. 1, pp. 127-139.

Mendel, J.M. (1995), Fuzzy Logic Systems for Engineering: A Tutorial, Proceedings of the IEEE, 23-25 March, Volume 83, No. 3, pp. 345–377

Misra, P. and P. Enge (2001), Global Positioning System Signals, Measurements, and Performance, Ganga-Jamuna Press, Lincoln, MA, USA.

Moeglein, M. and N. Krasner (1998), An Introduction to SnapTrack Server-Aided GPS Technology, Proceedings of the ION GPS, 15-18 September, Nashville, TN, USA, pp. 333–342.

Mohamed, A. H. (1999), Optimizing the Estimation Procedure in INS/GPS Integration for Kinematic Applications, Ph.D. Thesis, UCGE Report 20127, University of Calgary, Calgary, AB, Canada.

Murata (1999), Piezoelectric Vibrating Gyroscope ENC Series, Catalog S42E-2, Murata, Kyoto, Japan. http://www.murata.com/catalog/s42e3.pdf

Nayak, R. (2000), Reliable and Continuous Urban Navigation Using Multiple GPS Antennas and a Low Cost IMU, M.Sc. Thesis, UCGE Report No. 20144, University of Calgary, Calgary, AB, Canada

Peterson, B., D. Bruckner and S. Heye (1997), Measuring GPS Signals Indoors, Proceedings of ION GPS, 16-19 September, Kansas City, MI, USA, pp. 389-395.

Petovello, M. (2003), Real-time Integration of a Tactical-Grade IMU and GPS for High-Accuracy Positioning and Navigation, Ph.D. Thesis, UCGE Report No. 20173, University of Calgary, Calgary, AB, Canada.

Petovello, M., M.E. Cannon and G. Lachapelle (2000), C^3NAVG^{2TM} Operating Manual, Version 3, University of Calgary, Calgary, AB, Canada.

Phatak, M., M. Chansarkar and S. Kohli (1999), Position Fix From Three GPS Satellites and Altitude: a Direct Method, IEEE Transactions on Aerospace and Electronic Systems, Volume 35, No. 1, pp. 350-354.

Quddus, M.A., W. Y. Ochieng, Z. Lin and R.B. Noland (2003), A General Map-Matching Algorithm for Transport Telematics Applications, GPS solutions, Volume 7, No. 3, pp. 157-167.

Ray, J.K. (2000), Mitigation of GPS Code and Carrier Phase Multipath Effects Using a Multi-Antenna System, Ph.D. Thesis, UCGE Report No. 20136, University of Calgary, Calgary, AB, Canada.

Ray, J.K., M.E. Cannon and P. Fenton (2001), Code and Carrier Multipath Mitigation Using a Multi-Antenna System, IEEE Transactions on Aerospace and Electronic Systems, Volume 37, No. 1, pp. 183-195.

Romay, M.M., A. Alarcón, I. J. Villares and E. H. Monseco (2001), An Integrated GNSS Concept, Galileo and GPS, Benefits in Terms of Accuracy, Integrity, Availability and Continuity, Proceedings of ION GPS, 11-14 September, Salt Lake City, UT, USA, pp. 2114-2124.

Ross, T.J. (2004), Fuzzy Logic with Engineering Applications, Second Edition, John Wiley and Sons Publishers, New York, NY, USA.

Ryan, S. J. (2002), Augmentation of DGPS for Marine Navigation. Ph.D. Thesis, UCGE Report 20164, University of Calgary, Calgary, AB, Canada.

Salychev, O. (1998), Inertial Systems in Navigation and Geophysics, Bauman MSTU Press, Moscow, Russia.

Savage, P. (1978), Strapdown Sensors, NATO AGAARD Lecture Series No. 95, Linthicum Heights, MD, USA.

Schaffrin, B. (1997), Reliability Measures for Correlated Observations, Journal of Surveying Engineering, Volume 123, pp. 126-137.

Scott, C. (1994), Improved GPS Positioning for Motor Vehicles Through Map Matching, Proceedings of ION GPS, 20-23 September, Salt Lake City, UT, USA, pp. 172- 1979.

Scott-Young S., A. Kealy and P. Collier (2001), Intelligent Land Vehicle Navigation: Integrating Spatial Information into the Navigation Solution, Proceeding CD of the 3rd International Symposium on Mobile Mapping Technology, 3-5 January, Cairo, Egypt.

Shewfelt, J. L., R. Nishikawa, C. Norman and G. F. Cox (2001), Enhanced Sensitivity for Acquisition in Weak Signal Environments through the Use of Extended Dwell Times, Proceedings of ION GPS, 11-14 September, Salt Lake, UT, USA, pp. 155–162.

Spilker, J. J. (1996b). Signal Structure and Theoretical Performance, Global Positioning System: Theory and Applications, American Institute of Aeronautics and Astronautics, Washington, DC, Volume 1, pp. 89-121.

Spilker, J.J. Jr. and B.W. Parkinson (1994), Overview of GPS Operation and Design, Global Positioning System: Theory and Applications, American Institute of Aeronautics and Astronautics, Washington, DC, Volume 1, pp. 29-56.

Sorenson, H. W. (1970), Least-Squares estimation: from Gauss to Kalman, IEEE Spectrum, Volume 7, pp. 63-68.

Srikantan, K.S. (1961), Testing For a Single Outlier in a Regression Model, Sankhya Series, A23, Kolkata, India, pp. 251-260.

Stephen, J. (2000), Development of a Multi-Sensor GNSS Based Vehicle Navigation System, M.Sc. Thesis, UCGE Report No. 20140, University of Calgary, Calgary, AB, Canada.

Sugeno M. (1985), Industrial Applications of Fuzzy Control, Elsevier Science Publications, Amsterdam, Netherlands.

Syed, S. and M.N. Kulkarni (2002), Development of Web-based Automated GPS Processing Engine, Proceedings of Map India International Conference, New Delhi, India, 6-8 February, pp. 107-110

Tanka, K. and T. Niimura (1996), An Introduction to Fuzzy Logic for Practical Applications, Springer-Verlag Publications, New York, NY, USA.

Taylor, G. and G. Blewitt (1999), Virtual Differential GPS and Reduction Filtering by Map Matching, Proceedings of ION GPS, 20-23 September, Salt Lake City, UT, USA, pp. 591-598.

Taylor, G., J. Uff, and A. Hamdani (2001), GPS Positioning Using Map Matching, Drive Restriction Information and Road Network Connectivity, Proceedings of 9th Annual Conference on GIS Research UK, 7-9 November, Glamorgan, UK, pp. 114-119.

Teunissen, P.J. (1990), Quality Control in Integrated Navigation Systems, Proceedings of IEEE Symposium on PLAN, 20-23 March, pp. 158-165.

Thomas, H. (1991), Map Projections and Airborne Moving Map Displays, Proceedings of the Digital Avionics Systems Conference, 14-17 October, pp. 493-498

Tong, R.M. and P.P. Bonissone (1984), Linguistics Solutions to Fuzzy Decision Problems, Fuzzy Sets and Decision Analysis, North-Holland Publication, New York, NY, USA, pp. 323-334.

Tsakiri, M. (1996), Integrated GPS and DR for Land Vehicle Navigation, Proceedings of the Western Australia Land Information System Forum, 17-22 February, Adelaide, Australia, pp. 529-534.

Van Diggelen, F. (2001), Indoor GPS, Wireless Aiding and Low SNR Detection, Navtech Seminars Course Notes, Course 218, 9-12 September, Salt Lake City, UT, USA.

Virrantus, K., J. Veijalinen, J. Markkula, G. Artern, E. Vagan, K. Artem and T. Henry (2001), Developing GIS Supported Location-Based Services, Computer Society, Proceedings of the 2nd International Conference on WEB Information Systems Engineering, 3-6 December, Kyoto, pp. 423-432.

Wang J., and C. Baigen (2003), A Low-Cost Integrated GPS/INS Navigation System for the Land Vehicle, Proceedings of IEEE symposium on Intelligent Transportation Systems, 12-15 October, Volume 2, pp. 1022 - 1026.

Ward, P.W. (1996), GPS Receiver Search Techniques, Proceedings of IEEE PLAN Symposium, 22-26 April, pp. 604 - 611.

Wieser, A. (2002), Robust and Fuzzy Techniques for Parameter Estimation and Quality Assessment in GPS, Ph.D. Thesis, ISBN 3826598075, TU Graz, Graz, Germany.

Wells, D.E., N. Beck, D. Delikaraoglou, A. Kleusberg, E.J. Krawkisky, G. Lachapelle, R.B. Langley, M. Nakiboglu, K.P. Schwarz, J.M. Tranquilla and P. Vanicek (1987), Guide to GPS Positioning, Second Edition, Canadian GPS Associates, Fredericton, New Brunswick, Canada.

Yang, J.S. (1998), Some Analytical Results on Piezoelectric Gyroscopes, Proceedings of the IEEE International Frequency Control Symposium, 27-29 May, pp. 733 - 741.

Zadeh, L.A.(1965), Fuzzy Sets, Journal of Information and Control, Volume 8, pp.338-353

Zadeh, L. (1995), Preface to Mathwork's User Guide to Fuzzy Logic Toolbox, Mathwork Inc., Release 9, version 2, January, Natick, MA, USA

http://www.mathworks.com/access/helpdesk/help/pdf_doc/fuzzy/fuzzy_tb.pdf

Zhao, Y. (1997), Vehicle Location and Navigation Systems: Intelligent Transportation Systems, Artech House Publication, Boston, MA, USA.

Zhao, L., W.Y. Ochieng, M.A. Quddus and R.B. Noland (2002), An Extended Kalman Filter Algorithm for Integrating GPS and Low Cost Dead Reckoning System Data for Vehicle Performance and Emissions Monitoring, Journal of Navigation, Royal Institute of Navigation, Volume 56, No. 2, pp. 257-275.

Ziedan, N.I. and J.L. Garrison (2004), Unaided Acquisition of Weak GPS Signals Using Circular Correlation or Double-Block Zero Padding, Proceedings of IEEE PLAN Symposium, 26-29 April, pp. 461-470.

APPENDIX A: RANDOM PROCESSES, VARIABLES AND THEIR

CHARACTERISTICS

The foundation of estimation theory is based on the concept of random variables. Random variables are the outcomes of random experiments (Maybeck, 1982). They can take a value at random and are characterized by a distribution which determines the probability of the variable taking a value less than a fixed number. Thus a key concept associated with random variables is the probability distribution function. If X is a random variable, then the occurrence of X which is less than a fixed number x is a random event. The *probability distribution function* of X, $F(X)$, is defined as

$$F(x) = P(X < x)$$
(A.1)

where $P(X < x)$ represents the probability that a random variable X is less than a specific value x.

The essential characteristic of distribution function is their non-decreasing monotone nature (Mohammed, 1999). The other function used in the context of random variable is *probability density function* $f(x)$ defined as

$$f(x) = \frac{dF(x)}{dx}$$
(A.2)

The simultaneous consideration of more than one random variable is often necessary and useful. The probability of occurrence of a combination of values is described by the nth order joint probability distribution function.

$$F_n(x, y, z, ...) = P(X < x, Y < y, Z < z.......)$$ (A.3)

The corresponding n^{th} order joint probability density function is given by

$$f_n(x, y, z, ...) = \frac{\partial^n F_n(x, y, z, ...)}{\partial x \partial y \partial z.....}$$ (A.4)

It is intuitive that any k^{th} order probability distribution, where $k < n$, can be determined if the nth order joint probability distribution function is known.

The expected value of a random variable, often referred to as *expectation,* is defined as the sum of all the possible values a random variable can take weighted by the corresponding probability with which the value is taken (Gelb, 1974). This expectation is often referred to as the *mean* value or *first moment* of the random variable.

$$E[x] = \int_{-\infty}^{\infty} x f(x) dx$$ (A.5)

The *second moment* of the random variable gives the *mean square value*. The variance of the random variable is the mean squared deviation from the mean.

$$\sigma^2 = \int_{-\infty}^{\infty} (x - E[x])^2 f(x) dx = E[x^2] - (E[x])^2 \tag{A.6}$$

Another interesting concept is the statistical correlation between two or more random variables. The *covariance* gives the degree of correlation between the random variables. The covariance between two random variables is given by

$$E[(X - E[X])(Y - E[Y])] = \int_{-\infty}^{\infty} dx \int_{-\infty}^{\infty} dy (x - E[X])(y - E[Y]) f_2(x, y) = E[XY] - E[X][Y] \tag{A.7}$$

The covariance, normalized by the standard deviations of the random variables is called the correlation coefficient and is given by

$$\rho_{XY} = \frac{E[XY] - E[X]E[Y]}{\sigma_X \sigma_Y} \tag{A.8}$$

The other important property describing a random variable is the *characteristic function*. Characteristic function is the Fourier transformation of the probability density function with a reversal of sign on ω.

$$\psi_X(\omega) = \int_{-\infty}^{\infty} f(x) e^{j\omega x} dx \tag{A.9}$$

Given the characteristic function, it is easy to derive the moments of the random variable by taking the derivates of the characteristic function about $\omega = 0$.

$$E[X^n] = \int_{-\infty}^{\infty} x^n f(x)dx = \frac{1}{j^n}\left[\frac{d^n\psi_X}{d\omega^n}\right]_{\omega=0} \tag{A.10}$$

The most common distribution observed by many random variables in the real world is the *normal* or *Gaussian* distribution. The central limit theorem states that a random variable obtained by the superposition of many random processes tends towards a normal distribution. This is the reason for its common occurrence in nature. The normal probability distribution shown in Figure A.1 has the analytical form

$$f(x) = \frac{1}{\sqrt{2\pi}\sigma}\exp\left[-\frac{(x-m)^2}{2\sigma^2}\right] \tag{A.11}$$

A normal distribution is described by two parameters, i.e. the mean and standard deviation. The area within $\pm\sigma$ bounds centered about a mean 0.68 and within $\pm 2\sigma$ is approximately 0.95 of the total area under the Gaussian curve.
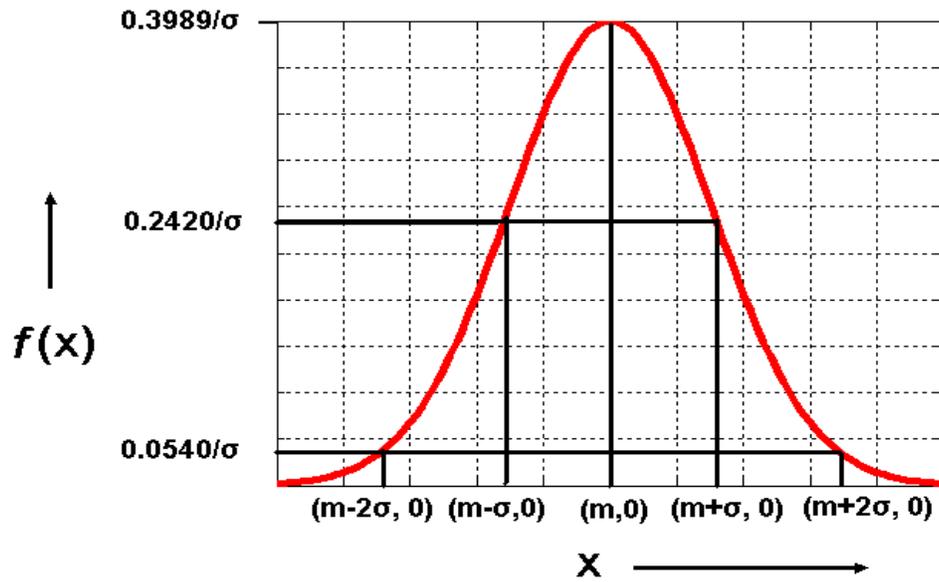
Figure A.1: Gaussian Distribution

Random processes are key in statistical computations due to the fact that chance or randomness is encountered more or less in almost every computation model and observation (Jekeli, 2000). A random process maybe thought of as a collection, or an ensemble of functions of time, any of which might be observed on any trial of an experiment (ibid). The exact outcome from a random process is not known beforehand and can only be described in terms of probability. The value of the observed member of the ensemble at a particular time is a random variable. The notion of probability distribution (density) function for random process is analogous to the corresponding random variable except for the dependency on the time of observation.

$$F(x_1, t_1) = P(x(t_1) \leq x_1) \tag{A.12}$$

The probability of the occurrence of a collection of values in certain range is given by higher order probability distribution (density) functions.

$$F_n(x_1,t_1;x_2,t_2;...x_n,t_n) = P(x(t_1) < x_1, x(t_2) < x_2..., x(t_n) < x_n)$$ (A.13)

If two or more random processes are under consideration, a joint distribution and density function is needed to describe the correlation.

$$F_2(x,t_1;y,t_2) = P(x(t_1) < x, y(t_2) < y)$$ (A.14)

The *autocorrelation* and *cross-correlation functions* measure the first moment of the distributions of the random processes and is defined as

$$\varphi_{xx}(t_1,t_2) = E[x(t_1)x(t_2)] = \int_{-\infty}^{\infty} dx_1 \int_{-\infty}^{\infty} dx_2 \ x_1 x_2 \ f_2(x_1,t_1;x_2,t_2)$$ (A.15)

$$\varphi_{xy}(t_1,t_2) = E[x(t_1)y(t_2)] = \int_{-\infty}^{\infty} dx \int_{-\infty}^{\infty} dy \ xy \ f_2(x,t_1;y,t_2)$$ (A.16)

The frequency characteristics of the random process are given by the *power spectral density* function. Power Spectral Density and Cross Power Spectral Density are obtained by taking the Fourier transformation of the autocorrelation and cross-correlation function respectively.

$$\phi_{xx} = \int_{-\infty}^{\infty} \varphi_{xx}(\tau) \ \exp(-j\omega\tau) \ d\tau \tag{A.17}$$

$$\phi_{xy} = \int_{-\infty}^{\infty} \varphi_{xy}(\tau) \ \exp(-j\omega\tau) \ d\tau \tag{A.18}$$

A *stationary random process* is one whose statistical properties are invariant in time. This implies that first order probability density function is independent of time. In this case, the second order probability density function is not dependent on the absolute times of the observation, but it still depends on the difference between them. Another concept associated with random processes is the property of *ergodicity*. This hypothesis claims that any statistics calculated by averaging over all the members of an ergodic ensemble at a fixed time can also be calculated by averaging over all times on a single representative member of the ensemble. In practice, almost all empirical results for a stationary process are derived from tests on a single member of ensemble, under the assumption that the ergodic hypothesis holds. A Student's T-test or F-test can be performed to test the ergodicity.

The most commonly encountered random process in nature is the Gaussian process. A Gaussian process is one characterized by the property that its joint probability distribution functions of all higher orders follow a multidimensional normal distribution. An important characteristic of this random process is that it is completely described by mean and standard deviation. The joint multivariate distribution of such process is given by

$$f(\bar{X}) = \frac{1}{\sqrt{2\pi}|\mathbf{C}_X|} \exp\left[-\frac{1}{2}(\bar{X}-\bar{m})^T \mathbf{C}_X^{-1}(\bar{X}-\bar{m})\right] \qquad (\text{A.19})$$

where

$\bar{X}$ is the vector of random variable,

$\bar{m}$ is the mean values of the $\bar{X}$, and

$\mathbf{C}_X$ is the covariance matrix of $\bar{X}$.